

Late Cenozoic Paleoceanographic Changes in the
Northwest Pacific Using Radiolarian Biostratigraphy
of ODP Site 1179 and others

Warna Susanne Downey

Submitted in Partial Fulfillment of the Requirements for the Degree of
Bachelor of Science
Department of Earth Sciences
Dalhousie University, Halifax, Nova Scotia
April, 2001

Abstract

The radiolarian zonation of ODP Site 1179 was accessed using core-catcher samples. The data indicate that the soft sediments analyzed range from late Miocene to Recent. The radiolaria biostratigraphy of ODP Site 1179 yielded reliable results even though only core-catcher samples were studied, as seen by the comparison of the radiolarian and magnetostratigraphy based sedimentation rates.

Sedimentation rates at DSDP/ODP sites (578, 579, 580, 581, 881, 1149 and 1179) range from 23.1 m/Ma in the north to 3.4 m/Ma in the south during the late Miocene. The sedimentation rates during the Pliocene range from 58.4 m/Ma in the north to 14.0 m/Ma in the south site and during the Quaternary they range from 65.4 m/Ma in the north to 27.7 m/Ma in the south.

The initiation of Miocene biosiliceous sedimentation in the Northwest Pacific Ocean, as recorded at DSDP Sites 578 and 581 and ODP Site 1179, indicates that this event was diachronous. The onset of biosiliceous sedimentation began in the middle Miocene at DSDP Site 581 and moved southward during the late Miocene. Since this time the Kuroshio/Oyashio transition zone has been migrated north and south. The current path does not move straight to the east, instead its path is curved.

The position of the Kuroshio/Oyashio transition zone during the late Quaternary as indicated by radiolarian data occurs between 39 to 41⁰N; this is not consistent with Koizumi (1985). There is a slight drift in the apparent latitude of the Kuroshio/Oyashio convergence boundary based on paleoceanographic sea surface currents and sedimentation indicators.

Acknowledgements

First and foremost, I would like to thank the Canadian Secretariat of the Ocean Drilling Program for giving me the opportunity to participate in the Under Graduate Student Trainee Program. This unique project allowed me collect and analyze the sample for my thesis from start to finish. I would also like to thank Dr. Dave Scott, Dr. Martin Gibling, Dr. Marcos Zentilli and Dr. Francine McCarthy for their insightful input and advice. I would like to thank Eugene MacDonald for all of his expertise in the proper processing and slide mounting procedures, and for always being there when I needed to borrow that crucial paper on radiolaria. I would like to thank Aaron Dondale for letting me hog all the counter space in his office so I could learn how to keep the randomness. Finally I would like to thank my family and friends for always being supportive and listening to me ramble.

Table of contents

Abstract.....	i
Acknowledgements.....	ii
Table of contents.....	iii
Table of figures.....	v
Table of tables.....	vi
1.0 Introduction	
1.1 General Statement.....	1
1.2 Objective of Project.....	1
1.3 Scope of Project.....	1
1.4 Radiolaria	2
1.4.1 History of Study.....	4
1.4.2 Geologic Range and Diversity.....	5
1.5 Previous work in the Northwest Pacific Basin	5
1.6 Organization.....	6
2.0 Geologic Background	
2.1 General Geologic and Physical Setting of the North West Pacific.....	7
2.2 Leg 191 Objectives.....	11
2.3 Site Geophysics.....	12
2.4 Core Analysis.....	14
2.5 Lithological Setting.....	15
2.6 Paleomagnetism.....	20
2.7 Biostratigraphy.....	20
3.0 Methods	
3.1 Introduction.....	24
3.2 Radiolarian Processing.....	24
3.3 Slide Mounting Procedure.....	25
3.4 Radiolarian Examination.....	26
3.5 Biostratigraphic Framework.....	28
4.0 Results	
4.1 General Statement.....	29
4.2 ODP Site 1179 Core Catcher Samples.....	29
4.3 ODP Site 1179 In Core Other Samples.....	37
5.0 Pacific Zonal Definitions for the Middle Latitudes.....	38
6.0 Discussion	
6.1 General Statement.....	43
6.2 Radiolarian Biostratigraphy.....	43
6.2.1 Biostratigraphy of Leg 191, Site 1179, Hole D.....	44
6.2.2 Biostratigraphy of Leg 191, Site 1179, Hole C.....	44

6.2.3 Biostratigraphy of Leg 191, Site 1179, Hole B.....	46
6.3 Sedimentation Rate based on Radiolarian Zones and Magnetostratigraphy at ODP site 1179.....	46
6.4 Comparison of ODP Site 1179 with DSDP and ODP Sites in the Northwest Pacific.....	47
6.4.1 DSDP and ODP sites of interest.....	50
6.4.2 Sedimentation rates of comparable DSDP and ODP Sites in the Northwest Pacific.....	65
6.4.3 Late Miocene to Recent Paleoceanographic Changes in the Northwest Pacific Basin.....	67
 7.0 Conclusions.....	 78
 Systematic Taxonomy.....	 80
 References.....	 85
 Appendix 1: Visual Core Description Barrel Sheets	 91

Table of Figures

1.1	Radiolaria from the order Spumellaria and Nassellaria showing spherical and bilateral symmetry, respectively.	3
2.1	General location of ION Site WP-2 (ODP Site 1179) showing the seismic station coverage in the Northwest Pacific.	8
2.2	Magnetic anomalies near ODP Site 1179.	9
2.3	Stratigraphy of DSDP/ODP sites on the abyssal seafloor in the Northwest Pacific Basin.	10
2.4	Seismic stratigraphic profile of ODP Site 1179 including lithologic column.	13
2.5	Position of holes at site 1179 relative to each other.	16
2.6	General lithology, magnetostratigraphy, and ranges of radiolarians, dinoflagellate cysts, calcareous nannofossil and foraminifer observed in core-catchers at ODP Site 1179	22
3.1	Setup of apparatus used in the slide mounting procedure.	
4.1	General lithology, magnetostratigraphy, and ranges of radiolarians observed from core-catchers at ODP Site 1179.	
6.1	Sedimentation rate diagram based on radiolaria and paleomagnetic data.	48
6.2	Map showing location of DSDP/ODP sites drilled on the abyssal seafloor in the Northwest Pacific Basin and the location of the modern Kuroshio and Oyashio Currents.	49
6.3	Biostratigraphic zonation of DSDP/ODP sites South of Site 1179	52
6.4	Biostratigraphic zonation of DSDP/ODP sites West and North of Site 1179	53
6.5	Biostratigraphic zonation of comparable DSDP/ODP sites	66
6.6	Map showing relative location of Kuroshio and Oyashio during the late Miocene.	71
6.7	Map showing the relative location of the Kuroshio and Oyashio Current convergence during the Pliocene.	73
6.8	Map showing the relative location of the Kuroshio and Oyashio Current convergence during the early Quaternary.	75
6.9	Map showing the relative location of the Kuroshio and Oyashio Current convergence during the middle Quaternary.	76
6.10	Map showing the relative location of the Kuroshio and Oyashio Current convergence during the late Quaternary.	77

Table of Tables

2.1	Summary of latitude, longitude and water depths of holes drilled at ODP Site 1179.	17
2.2	Summary of holes, cores, total depth below seafloor and recovery	18
2.3	An overview of the Lithological Units of ODP Site 1179	21
4.1	Summary of radiolarian examined in core-catcher samples.	31
4.2	Summary of core samples processed.	35
6.1	Summary of location and water depth of DSDP and ODP Sites in the Northwest Pacific Basin	51
6.2	Summary of lithology of DSDP and ODP Sites in the Northwest Pacific Basin.	54
6.3	Sedimentation rates in the Northwest Pacific Basin.	70

Chapter One - Introduction

1.1 General Statement

This thesis focuses on radiolarian data produced from samples taken aboard the *Joides Resolution* as part of the Ocean Drilling Program (ODP) Leg 191 in the Northwest Pacific off the coast of Japan, from July 17 to September 11, 2000. The radiolarian samples were collected, processed and analyzed, solely, by this author. These data also appear in the Ocean Drilling Program Initial Reports Volume: Leg 191, where the author participated as part of the shipboard scientific party as one of the first undergraduate student trainees. Subsequent analysis allowed these new data to be put in the framework of Northwest Pacific Cenozoic evolution.

1.2 Objective of Project

The objective of this thesis is to examine the radiolarians collected from samples taken at the International Ocean Network (ION) seismic installation Site WP-2a (ODP Site 1179) for the purpose of constructing a general biostratigraphic zonation. All specimens observed were examined to the species level. Additionally, comparisons are made with findings from previous Deep Sea Drilling Project (DSDP) and Ocean Drilling Program (ODP) cruises in the Northwest Pacific Basin to ascertain the movement of the Kuroshio/Oyashio convergence boundary since the late Miocene.

1.3 Scope of Project

The study is confined to the cores recovered at ODP Site 1179, the ION seismic installation Site WP-2a. Samples were taken from the core catchers, approximately every

9.25m from core 191-1179B-1H to 191-1179C-27X. In particular, samples were taken approximately every 0.75m from core 191-1179B-1H (0-7.43 mbsf) through to core 191-1179C-3H (58.30 – 67.70 mbsf). The section that is being studied corresponds to the topmost layer in the Northwest Pacific stratigraphy, a radiolarian and diatomaceous ooze with numerous ash layers and zeolitic clays.

The samples taken for this thesis were used to construct a radiolaria zonation for ODP Site 1179 and are compared with data from DSDP and ODP sites drilled on the abyssal sea floor in the Northwest Pacific Basin.

1.4 Radiolaria

Radiolarians are of particular importance in the Pacific where the Carbonate Compensation Depth (CCD) is at 4000 m. Deep sea sediments in the Pacific Ocean are virtually carbonate free due to the positioning of the CCD; the only microfossils left for observation are siliceous (radiolarians, diatoms and silicoflagellates) or organic (palynomorphs) which have well understood distribution and stratigraphic ranges.

Radiolaria are defined as marine, holoplanktic protozoa belonging to the class Actinopodea of the phylum Sarcodina (Anderson, 1983). Only one order of the subclass Radiolaria is preserved in the geologic record, the order Polycystinea. Polycystinea or Polycystine radiolaria contain three suborders: Spumellaria, Nassellaria and Phaeodaria (Casey, 1993). Spumellarians and nassellarians have amorphous opaline silica skeletal tests and Phaeodarians have smooth tests that are a mixture of silica and organic matter (Casey, 1993). Spumellarian skeletons (Figure 1.1) exhibit spherical symmetry where as nassellarian skeletons (Figure 1.1) exhibit bilateral symmetry (Casey, 1993).

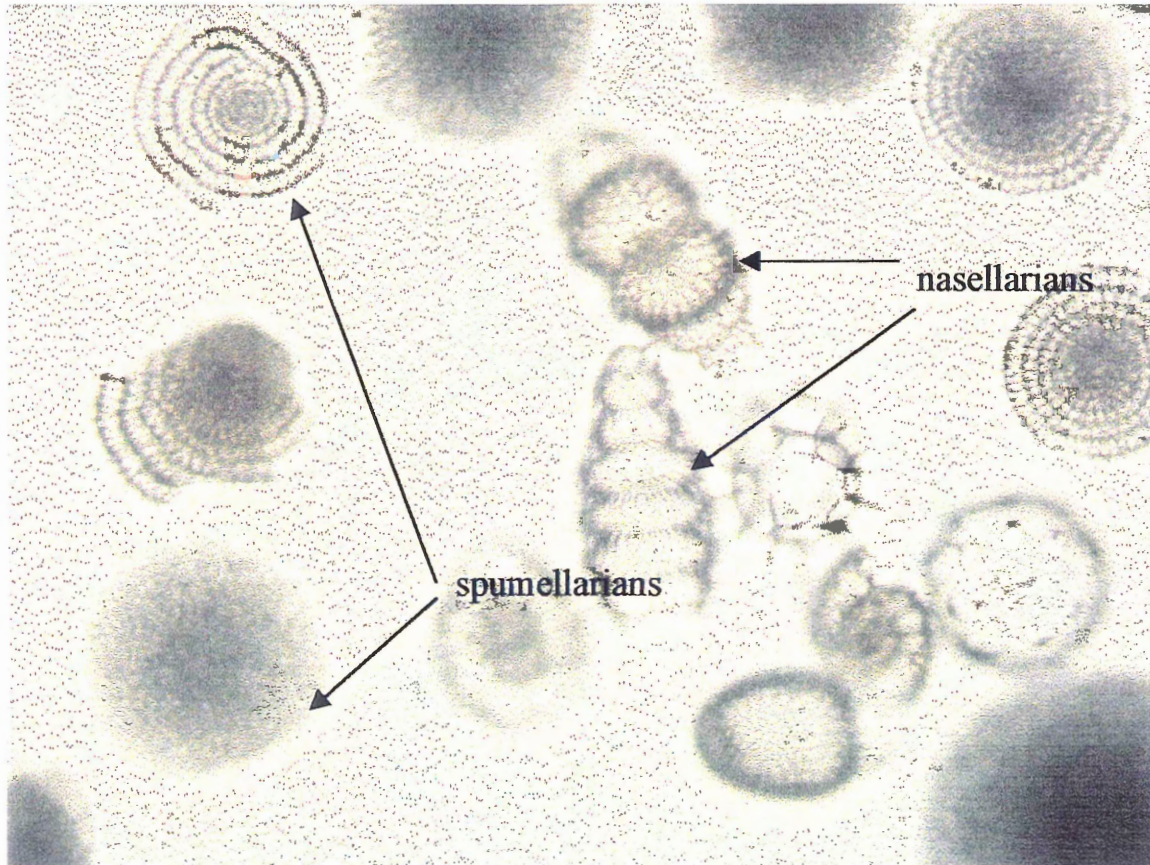


Figure 1.1 - Radiolaria from the order Spumellaria and Nassellaria showing spherical and bilateral symmetry, respectively.

1.4.1 History of Study

Radiolarians, living and fossil forms, were first described in the mid-nineteenth century by Ehrenburg (1847). He presented a classification scheme for the class Polycystinea. Ernest Haeckel presented the first comprehensive report on radiolaria (Haeckel, 1887) based on work done on the *HMS Challenger* Expedition (1873-1876). It took Haeckel over 10 years to examine the material from the *Challenger* Expedition and he identified over 3000 new species (Anderson, 1983). A second resurgence in work on radiolaria began with the creation of the Deep Sea Drilling Project (DSDP). William Riedel began developing a Tertiary tropical radiolarian biostratigraphic zonation (Riedel, 1953) using deep-sea cores recovered on DSDP cruises. Hays (1970), Nigrini and Sanfilippo (1992, 2001) and others have done further work on the biostratigraphy and classification of radiolaria.

Work done by Casey (1971) discusses radiolaria as past and present water-mass indicators. His studies of plankton and sediments indicated that species diversity varies with water-mass. He found that certain species of radiolaria were endemic to specific water-masses (e.g., high latitude species such as *Cycladophora davidsoni davidson* are endemic to Arctic water masses). Based on this type of work paleotemperature calculations have been worked out. The initial paleotemperature analyses were done by generalized curves (Hay, 1965). Modified curves were made based on work that was been done with diatoms in the North Pacific by Nigrini (1970). The relative abundance

of radiolaria in the Northwest Pacific sediments is directly tied to the oceanographic properties in the surface and near surface waters (Robertson, 1975; Hays and Morley, 1985) allowing for paleotemperatures to be reconstructed using Q-mode factor analysis (Heusser and Morley, 1996).

1.4.2 Geologic Range and Diversity

Radiolaria first appear during the Cambrian and have persisted to recent times (Anderson, 1983). The diversity and relative abundance through time is difficult to assess because of dissolution of some species and their loss through the fossil record (Tappan and Loeblich, 1973). During the Cambrian spumellarians were the dominant order (Anderson, 1983). However, by the Carboniferous nassellarians began to greatly diversify (Anderson, 1983). Through the Tertiary there is little diversity amongst radiolaria species, but in the Quaternary it is expanding (Casey, 1993).

1.5 Previous Work in the Northwest Pacific Basin

Several DSDP and ODP Legs (6, 20, 32, 86, 145, and 185) have penetrated that abyssal seafloor of the Northwest Pacific Basin. Radiolarian biostratigraphy of these sites has determined that the olive green to gray siliceous clay and ooze with numerous ash layers are of Miocene to Pleistocene age (Kanazawa, Sager et al, submitted). Thickness greater than 200m have been observed resulting from high productivity in waters of the western boundary currents (Kanazawa, Sager et al, submitted). A radiolarian barren zone of red pelagic clays overlies a sequence of chert and chalk, this

sequence contains radiolarian assemblages from the early to late Cretaceous (Kanazawa, Sager et al, submitted).

The Miocene to Pleistocene unit contains eight mid-latitude radiolarian zones of significance. These zones are not observed in all the sites drilled because many were not drilled continuously. The sites that were drilled continuously, however, show varying thicknesses of the mid-latitude zones.

1.6 Organization

This paper is organized in the following manner. Chapter two provides a background of the work accomplished by the shipboard scientific party aboard Leg 191; chapter three provides a detailed outline of the methodology used in sample collection, sample processing and sample analysis; chapter four shows the results from radiolarian sample analysis for the study; chapter five contains Pacific Zonal Definitions for the Middle Latitudes; chapter six contains the discussion, and is followed by conclusions in chapter seven. The pages immediately following the conclusion contain the Systematic Taxonomy of Radiolaria. Appendix One contains the visual core description barrel sheets of the sediments and sedimentary rock recovered at ODP Site 1179.

Chapter Two – ODP Site 1179 Background Information

2.1 General Geological and Tectonic Setting of the Northwest Pacific

ION Site WP-2a (ODP Site 1179) is located to the northwest of Shatsky Rise in the Pacific Ocean (Fig 2.1). It is 1650km east of Japan on the abyssal seafloor (Kanazawa, Sager et al., submitted). This part of the Pacific plate was formed during the early Cretaceous, specifically during the Hauterivian stage (Gradstein et al., 1994) according to the M-8 magnetic anomaly (Nakanishi et al., 1999) near which ODP Site 1179 is centered (Fig 2.2). This area of the Pacific plate was formed at 10°N latitude according to paleomagnetic data and has drifted northward 30° since the early Cretaceous (Sager and Pringle, 1988; Larson et al., 1992). If the Pacific plate continues northward at its present rate the lithosphere along with the sediment at ODP Site 1179 will be subducted beneath the southern Kuril Trench in 7-8Ma (Kanazawa, Sager et al., submitted).

Over the past 30 years work done in the Northwest Pacific Basin by the Deep Sea Drilling Project (Legs 6, 20, 32 and 86) and ODP (Legs 145, 185 and 191) shows that there is similar stratigraphy in the Northwest Pacific (Figure 2.3), mainly three primary layers (Hazen et al., 1971; 1973; Larson et al., 1975; Plank et al., 2000). Unit C, the bottom unit is composed of calcareous oozes, chalk or marl deposits (Figure 2.3). These poorly recovered layers were deposited soon after the crust was formed while it was still at a depth well above the CCD (Kanazawa, Sager et al., submitted). Unit B, the second unit synonymous to the Northwest Pacific, is a barren brown to reddish clay layer of largely undetermined age (Figure 2.3). At some Sites (51, 194, 195) the age of this unit

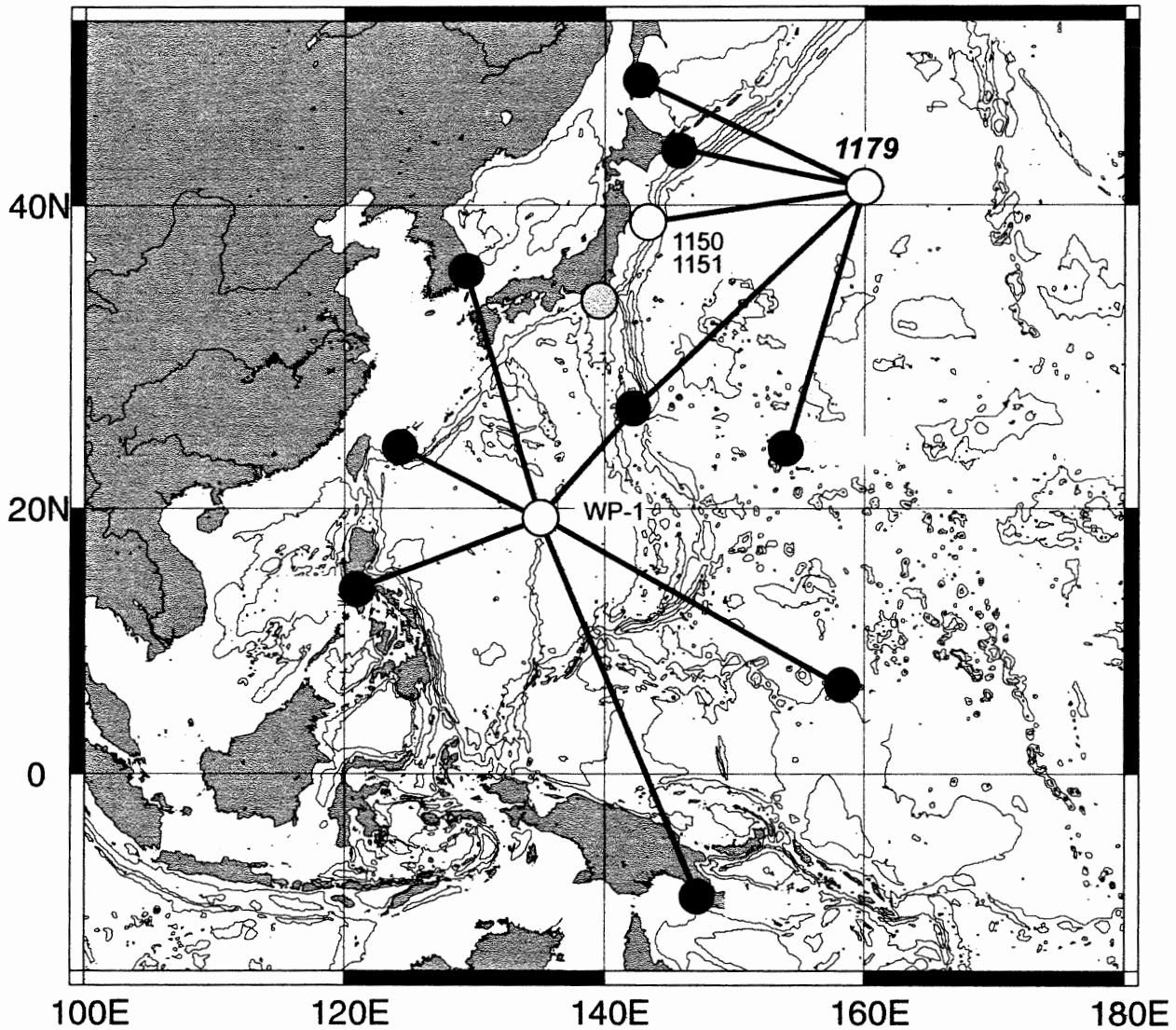


Figure 2.1 - General location of ION Site WP-2 (ODP Site 1179) showing the seismic station coverage in the Northwest Pacific. Open circle indicate borehole observatories, filled circles indicate land stations (after Kanazawa, Sager, et al., submitted).

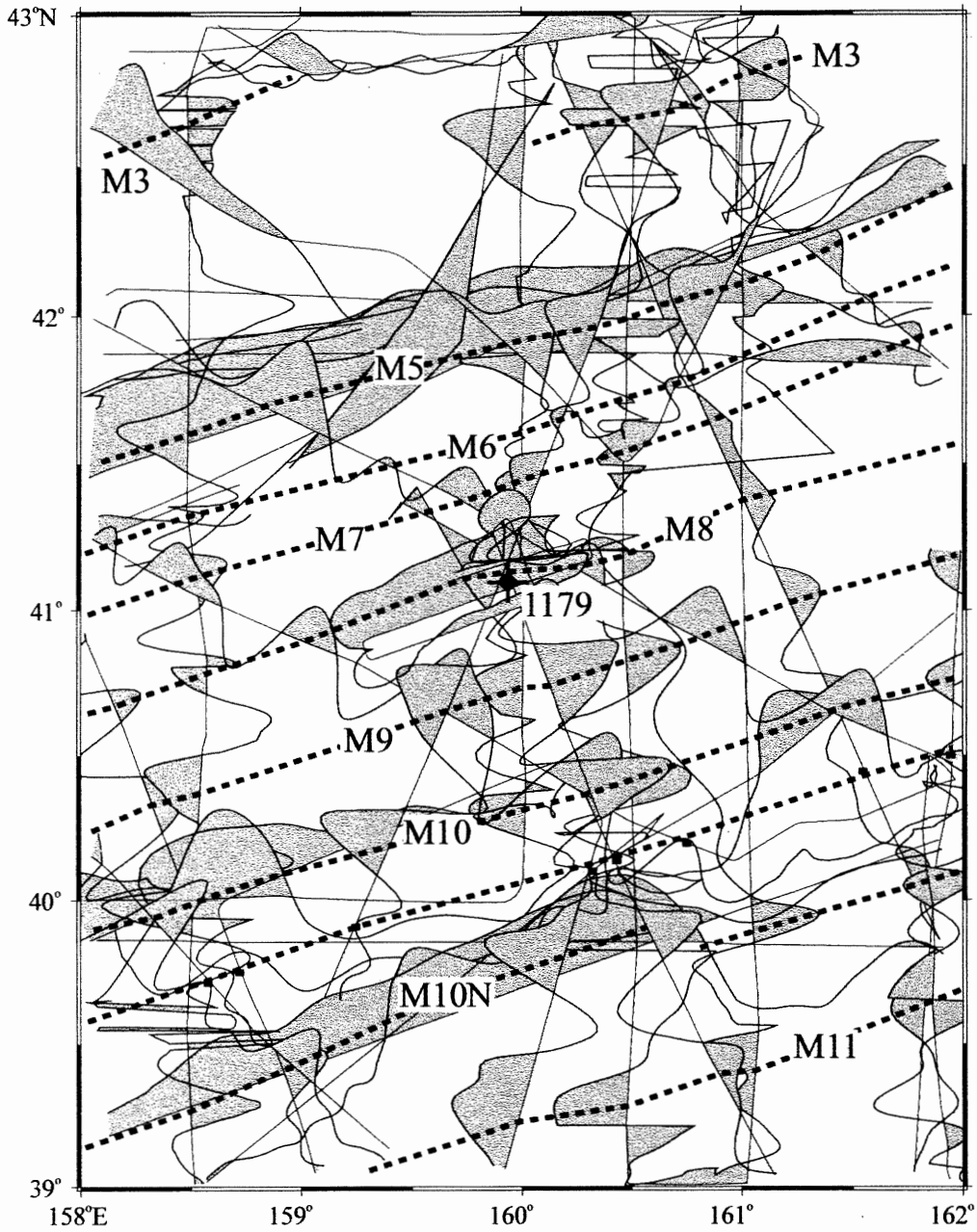


Figure 2.2 - Magnetic anomalies near ODP Site 1179. Thin, curved lines represent magnetic anomalies, shaded where positive (after Kanazawa, Sager, et. al., submitted).

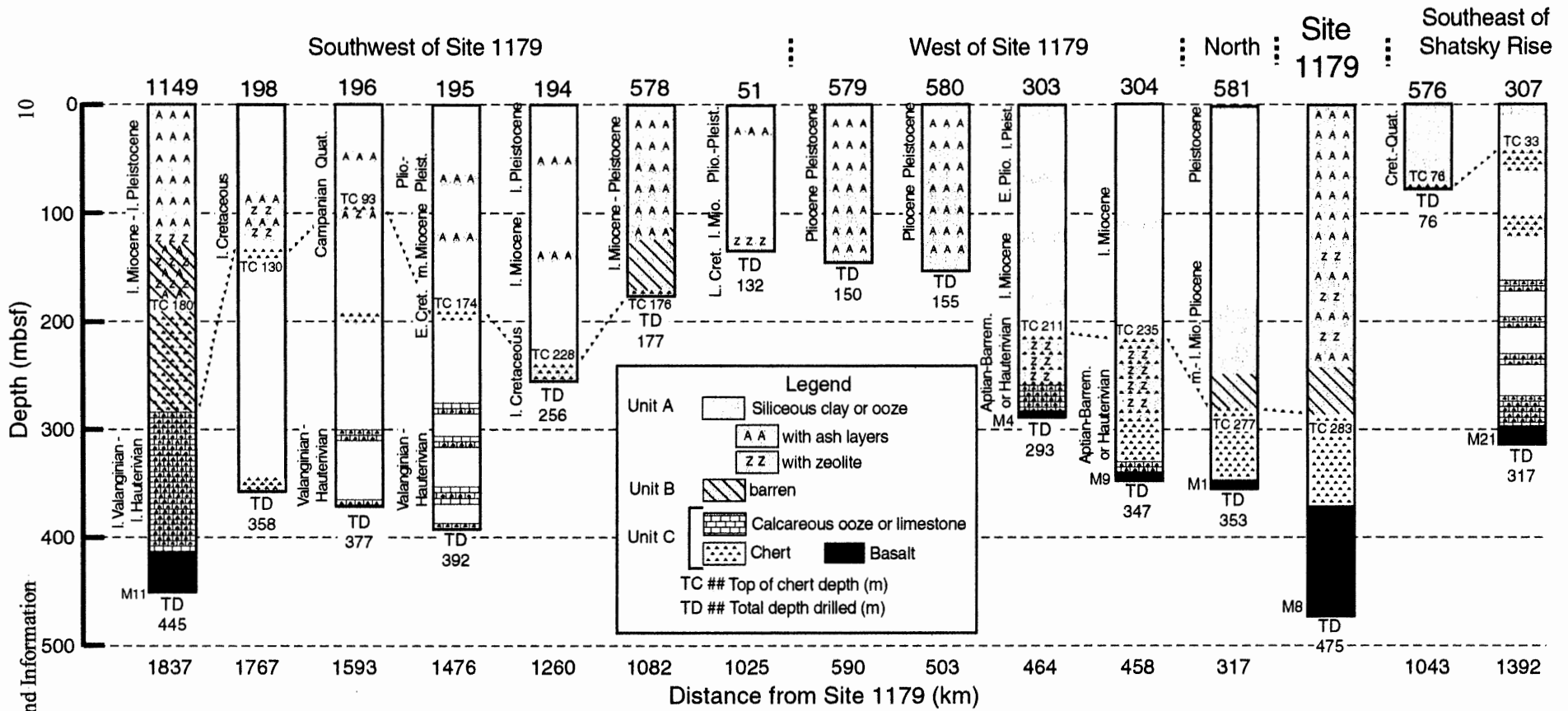


Figure 2.3- Stratigraphy of DSDP/ODP sites on the abyssal seafloor in the Northwest Pacific Basin (after Kanazawa, Sager, et al, submitted)

belongs to the mid- to late- Cretaceous. This unit may also contain a highly condensed section of the Tertiary (Site 576) (Kanazawa, Sager et al., submitted).

Unit A, the topmost unit, is a Miocene to Pleistocene olive green to gray siliceous clay and ooze with numerous ash layers (Figure 2.3). This unit contains common to abundant radiolaria and diatoms, but few calcareous microfossils are found. The lack of calcareous microfossils is due to the fact that this part of the Pacific Ocean has been well below the Carbonate Compensation Depth (CCD) for millions of years. This Neogene layer also contains zeolites in its lower parts. This layer has been observed to be greater than 200m in thickness as a result of high productivity in waters of the western boundary currents, mainly in the region of convergence between the Kuroshio and Oyashio currents (Kanazawa, Sager et al., submitted).

2.2 Leg 191 Objectives

ODP Site 1179 was selected as the ION WP- 2 installation Site (Figure 2.1) to help provide earthquake coverage of the subduction zone beneath the southern Kuril trench near Japan in conjunction with ION Site WP-1 (Figure 2.1). A seismometer at this location will record seismic rays passing through parts of the mantle that would not otherwise be imaged. This site was ideal for installation because it has a thin package of overlying sediments, which can be easily drilled through to reach basaltic crust. Installing the seismometer in basalt is essential because it has an increased signal to noise ratio (Kanazawa, Sager et al., submitted). Like all ODP legs, the secondary objective is to collect data of geologic nature for scientific analysis there by adding to the general knowledge of the world's oceans.

2.3 Site Geophysics

Seismic surveys of this area were conducted prior to Leg 191 during cruise KH96-3-1 of the R/V *Hakuho Maru*, from the University of Tokyo Ocean Research Institute. The vessel was navigated by satellite GPS and collected standard underway geophysical data, including magnetic field measurements and 3.5 kHz echo-sounder profiles (Kanazawa, Sager et al., submitted). Seismic reflection data were collected using a 24-multichannel seismic streamer. The seismic data were then stacked, filtered and migrated for final interpretation (Kanazawa, Sager et al., submitted).

The seismic stratigraphy from profiles (Figure 2.4) show that ODP Site 1179 has a stratigraphy similar to typical sections in this area of the Northwest Pacific Ocean. Previous DSDP and ODP legs (6, 20, 32, 86, 185) in the region have conducted seismic surveys that show a transparent layer consisting of late Cretaceous to early Tertiary siliceous ooze unit having several ash layers and highly condensed barren clay unit (Ewing et al., 1968; Kanazawa, Sager et al., submitted). The top of the transparent interval at Site 1179 occurs at a depth of 6.93 seconds two-way travel time and is 0.32 seconds thick (Figure 2.4), this roughly corresponds to findings from previous studies. There is a reverberant layer directly below the barren clay unit that corresponds to a pervasive chert layer with soft sediment intervals that are washed away during drilling (Ewing et al., 1968; Plank et al., 2000). The top of the cherty interval occurs at 7.24 seconds two-way travel time and is 0.13 seconds thick (Figure 2.3). The acoustic basement is a high-amplitude reflector that occurs at a depth of 7.33 seconds two-way travel time (Figure 2.4).

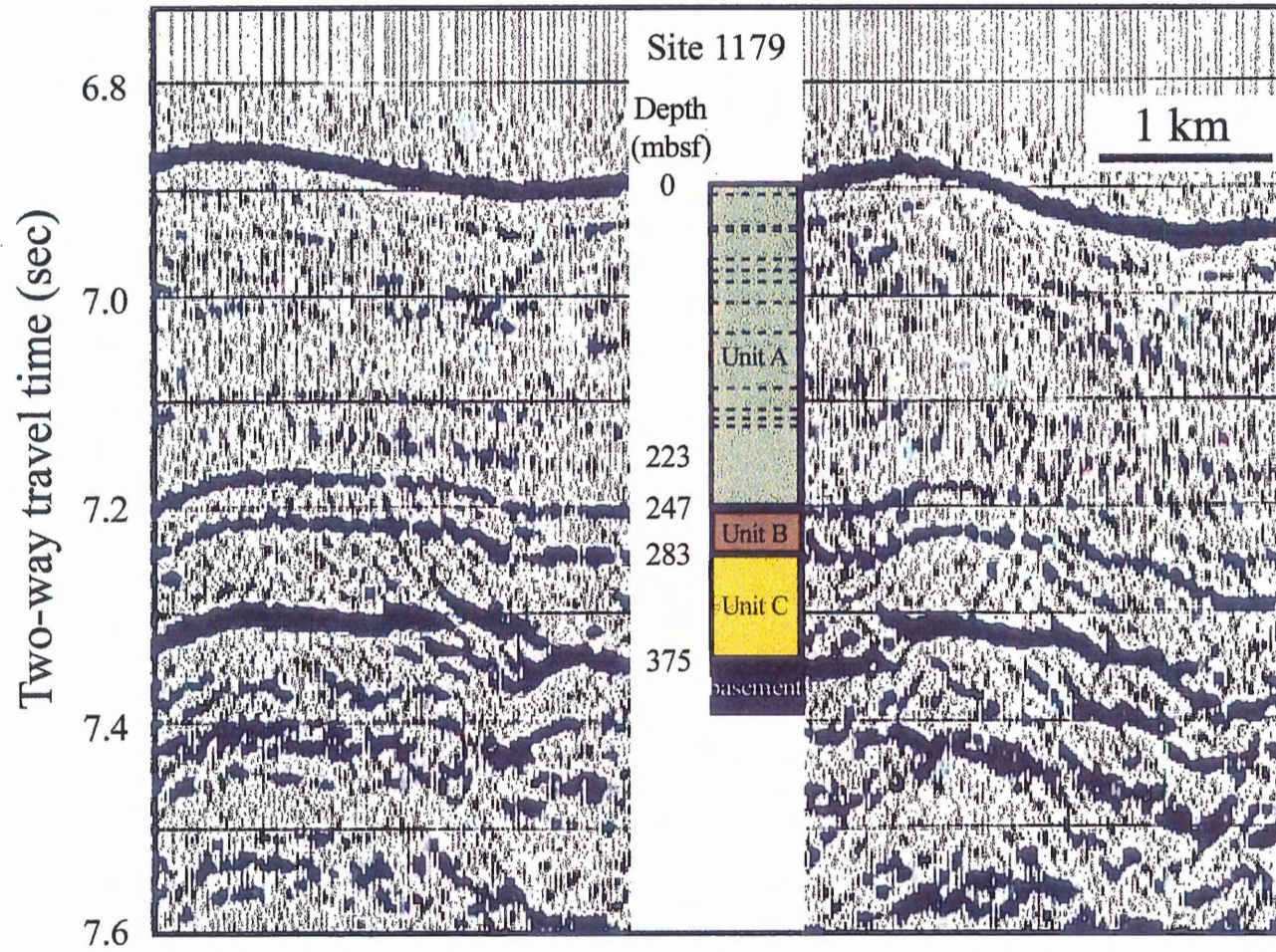


Figure 2.4 - Seismic stratigraphic profile of ODP Site 1179 including lithologic column (after Kanazawa, Sager, et al., submitted).

Seismic profiles of ODP Site 1179 show layers that conformably overlies each other, therefore seafloor topography represents undulations in the crystalline basement (Figure 2.4). These observations imply that sedimentation has been uniform and pelagically sourced (Kanazawa, Sager et al., submitted). Figure 2.4 has the lithologic data and predicted depths of unit boundaries incorporated in the seismic profile. There is a strong seafloor reflector and the Unit A/B and B/C boundaries line up with two parallel reflectors at 7.21 and 7.26 seconds two-way travel time, having depths of ~ 247 mbsf and ~ 283 mbsf, respectively. The Unit C/basement boundary appears as a sharp reflector at 7.33 seconds two-way travel time, a depth of 375 mbsf (Kanazawa, Sager et al., submitted).

2.4 Core Analysis

The cores average 9.5 m and are divided up into 1.5 m intervals, with the interval being measured in meters below seafloor (mbsf). A conventional system is used to catalogue core samples and contains the following information: leg, site, hole, and core number, core type, section number, and interval in centimeters from top of section. For example, a sample identification of “191-1179B-2H-1W, 78-80 cm” represents a sample taken from the interval between 78-80 cm of section 1 of core 2, which was taken during hydraulic piston coring of Hole B at Site 1179 during Leg 191. Similarly, a sample identification of “191-1179C-5H-CC” denotes a sample taken from the core-catcher of core 5, which was taken during hydraulic piston coring of Hole B at Site 1179 during Leg 191. A description of sedimentary units recovered during Leg 191 includes estimates of sediment composition based on smear slides, thin sections, carbonate measurement, X-

ray diffraction, documentation of sedimentary and deformational structures, drilling disturbance, presence and type of fossils, bioturbation intensity, diagenetic alteration and colour (Kanazawa, Sager *et al.*, submitted). A visual core barrel description was also included in the analysis of the core recovered, this can be viewed in Appendix One.

2.5 Lithological Setting

There were 377 m of sediments and sedimentary rock recovered during the ION seismic station installation as ODP Site 1179. The five holes drilled at this site: 1179A, 1179B, 1179C, 1179D and 1179E provided 1, 2, 27, and 11 cores, respectively. Hole 1179E was drilled strictly to install the ION seismic station, therefore no core was recovered. The configuration of the holes drilled at Site 1179 can be found in Figure 2.5 and the precise location of the holes can be found in Table 2.1 (Kanazawa, Sager *et al.*, submitted).

Soft sediments make up Lithologic Units I-III and Lithological Unit IV is composed of sedimentary rock. Units I-III average 98.8% recovery (Table 2.2) and reach a depth of ~ 293 mbsf. Lithological Unit I (late Miocene to Recent) is 223.5 m thick and comprises a clay- and radiolarian-bearing diatom ooze with frequent ash layers. Unit I is found in 191-1179A-1H, 0-120 cm, 191-1179B-1H, 0 cm through to 6H-CC and 191-1179C-1H, 0 cm through to 20H-4, 80 cm. Lithological Unit II (early late Miocene to late Miocene) is 22.5 m thick and comprises a clay- and diatom- bearing radiolarian ooze with frequent ash layers. Unit II is found in 191-1179C-20H-4, 80 cm through to 22H-5, 125 cm. Lithological Unit III (late Miocene and older) is 37.53 m thick and comprises pelagic clays. Unit III is found in 191-1179C-22H-5, 125 cm through to 26X-CC. Unit IV has a 2 – 11% recovery rate (Table 2.2) and is found from ~ 293 – 377 mbsf.

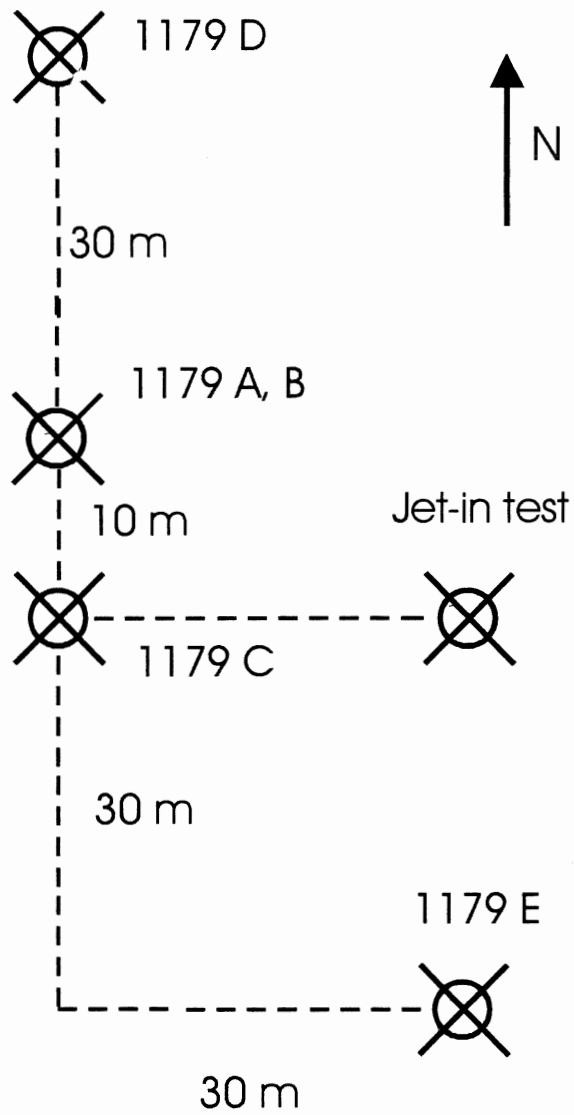


Figure 2.6 - Position of holes at site 1179 relative to each other (after Kanazawa, Sager, *et al.*, submitted)

HOLE	LATITUDE	LONGITUDE	WATER DEPTH
1179 A	41 ⁰ 4.7884' North	159 ⁰ 57.7877' East	5565.6 m
1179 B	41 ⁰ 4.7887' North	159 ⁰ 57.7879' East	5563.90 m
1179 C	41 ⁰ 4.7871' North	159 ⁰ 57.7856' East	5563.90 m
1179 D	41 ⁰ 4.8122' North	159 ⁰ 57.7862' East	5566.00 m
1179 E	41 ⁰ 4.7729' North	159 ⁰ 57.7973' East	5577.00 m

Table 2.1 - Summary of latitude, longitude and water depth of holes drilled at site 1179 (modified from Kanazawa, Sager, et al., submitted)

Hole 1179A

Core No.	Top Depth (mbsf)	Bottom Depth (mbsf)	Length Cored (m)	Length	
				Recovered (m)	Recovery (%)
1H	0.0	10.0	10.0	10.02	100.2
Total			10.0	10.02	100.2

Hole 1179B

Core No.	Top Depth (mbsf)	Bottom Depth (mbsf)	Length Cored (m)	Length	
				Recovered (m)	Recovery (%)
1H	0.0	7.6	7.6	7.53	99.1
2H	7.6	17.1	9.5	9.14	96.2
3H	17.1	26.6	9.5	10.04	105.7
4H	26.6	36.1	9.5	9.46	99.6
5H	36.1	45.6	9.5	10.07	106.0
6H	45.6	55.1	9.5	9.65	101.6
Total			55.1	55.89	101.4

Hole 1179C

Core No.	Top Depth (mbsf)	Bottom Depth (mbsf)	Length Cored (m)	Length	
				Recovered (m)	Recovery (%)
1H	0.0	5.8	5.8	5.83	100.5
Drilled	5.8	48.8			
2H	48.8	58.3	9.5	10.02	105.5
3H	58.3	67.8	9.5	9.56	100.6
4H	67.8	77.3	9.5	10.11	106.4
5H	77.3	86.8	9.5	9.78	103.0
6H	86.8	96.3	9.5	10.06	105.9
7H	96.3	105.8	9.5	9.62	101.3
8H	105.8	115.3	9.5	10.01	105.4
9H	115.3	124.8	9.5	9.25	97.4
10H	124.8	134.3	9.5	9.84	103.6
11H	134.3	143.8	9.5	9.62	101.3
12H	143.8	153.3	9.5	10.17	107.1
13H	153.3	162.8	9.5	9.65	101.6
14H	162.8	172.3	9.5	10.12	106.5
15H	172.3	181.8	9.5	9.66	101.7
16H	181.8	191.3	9.5	10.04	105.7

Table 2.2 - Summary of holes, cores, total depth below sea floor and recovery (modified from Kanazawa, Sager, et al., submitted)

Hole 1179C

Core No.	Top Depth (mbsf)	Bottom Depth (mbsf)	Length Cored (m)	Length	
				Recovered (m)	Recovery (%)
17H	191.3	200.8	9.5	9.82	103.4
18H	200.8	210.3	9.5	9.96	104.8
19H	210.3	219.8	9.5	9.60	101.1
20H	219.8	229.3	9.5	9.97	105.0
21H	229.3	238.8	9.5	9.71	102.2
22H	238.8	248.3	9.5	10.12	106.5
23H	248.3	257.8	9.5	8.73	91.9
24H	257.8	266.8	9.0	9.17	101.9
25X	266.8	273.7	6.9	6.44	93.3
26X	273.7	283.3	9.6	9.83	102.4
27X	283.3	292.9	9.6	0.20	2.1
Cored			249.9	246.89	98.8
Drilled			43		
Total			292.9		

Hole 1179D

Core No.	Top Depth (mbsf)	Bottom Depth (mbsf)	Length Cored (m)	Length	
				Recovered (m)	Recovery (%)
Drilled	0	281.0			
1R	281.0	290.6	9.6	0.98	10.2
2R	290.6	300.2	9.6	0.19	2.0
3R	300.2	309.8	9.6	0.26	2.7
4R	309.8	319.4	9.6	0.99	10.3
5R	319.4	329.0	9.6	0.57	5.9
6R	329.0	338.6	9.6	0.82	8.5
7R	338.6	348.2	9.6	1.10	11.5
8R	348.2	357.9	9.7	0.25	2.6
9R	357.9	367.5	9.6	0.65	6.8
10R	367.5	377.1	9.6	1.09	11.4
11R	377.1	386.7	9.6	2.53	26.4
12R	386.7	390.4	3.7	4.58	123.8
13R	390.4	396.4	6.0	5.00	83.3
14R	396.4	406.0	9.6	3.85	40.1
15R	406.0	415.7	9.7	0.19	2.0
16R	415.7	418.8	3.1	0.18	5.8
17R	418.8	425.3	6.5	2.67	41.1
18R	425.3	434.9	9.6	4.69	48.9
19R	434.9	444.6	9.7	3.36	34.6
20R	444.6	454.2	9.6	5.20	54.2
21R	454.2	463.8	9.6	4.79	49.9
22R	463.8	475.0	11.2	6.42	57.3
Cored			194.0	50.36	26.0
Drilled			281.0		
Total			475.0		

Table 2.2 - Summary of holes, cores, total depth below sea floor and recovery (modified from Kanazawa, Sager, et al., submitted)

Lithological Unit IV (? – early Cretaceous) is 93.2 m thick and comprises cherty layers with soft porcelanite and chalk intervals. Unit IV is found in 191-1179C-26X-CC through to 191-1179D-11R-1, 15 cm. An overview of the Lithological Units can be found in Table 2.3 and a lithology depth plot in Figure 2.6 (Kanazawa, Sager *et al.*, submitted).

2.6 Paleomagnetism

Natural remnant magnetism (NRM) intensities were measured every 5 cm from the archive halves of all soft sediment cores (191-1179A-1H, 0 cm through 191-1179C-26X-CC). The soft sediment cores contain excellent magnetic polarity reversal sequences from the early Miocene (Chron C5Dr) to the present (Chron 1Cn, Brunhes). The single core 191-1179A-1H records the present Chron C1n. The six cores from 1179B record five magnetic polarity reversals and Cobb Mountain cryptochron (C1r.2r-1n). Cores 191-1179C-2H through 25H span from Chrons C1r.2r, Matuyama, to C4Dr. Figure 2.6 shows the magnetostratigraphy on the lithology depth plot and Figure 2.7 shows the magnetic polarity reversals for Site 1179 (Kanazawa, Sager *et al.*, submitted).

2.7 Biostratigraphy

Siliceous microfossils, such as diatoms, radiolarians and silicoflagellates, are common and well preserved in Lithological Units I and II. Unit III is barren of all types of microfossils. Numerous radiolarian data were established and late Miocene to late Pleistocene zones for the mid-latitudes were determined, which are the focus of this thesis.

Lithological Unit	Description	Intervals	Depth	Thickness
I	Clay- and radiolarian bearing diatom ooze	191-1179A-1H to 191-1179C-20H	0.0 – 223.5 mbsf	223.5 m
II	Clay- and diatom-bearing radiolarian ooze	191-1179C-20H to 191-1179C-22H	223.5 – 246.0 mbsf	22.5 m
III	Pelagic clay	191-1179C-22H to 191-1179C-26X	246.0 – 283.53 mbsf	37.53 m
IV	Chert	191-1179C-26X to 191-1179D-11R	283.53 – 377.15 mbsf	92.62 m

Table 2.3 – An overview of the Lithologic Units of ODP site 1179, including lithological description, intervals, depth and thickness (based on information from Kanzawa, Sager, et al., submitted)

Few other microfossil data were produced with non-siliceous microfossils. Sample 191-1179B-4H-CC contained both planktic and benthic foraminifera and calcareous nannofossils. The foraminifera were not useful biostratigraphically, but the nannofossils helped to constrain and early Quaternary age for this sample (Figure 2.6). There is no explanation for the occurrence of calcareous microfossils within the core because the drilling site is well below the CCD for the Northwest Pacific Ocean. Geochemical analysis yielded anomalously high carbonate readings elsewhere in Units I and II. There were no calcareous microfossils in Unit III and IV, and no anomalous readings were observed. Agglutinated foraminifera of middle to late Miocene age were observed in sample 191-1179C-20H-CCC (Figure 2.6) (Kanazawa, Sager et al., submitted).

Palynomorphs (terrestrial spores and pollen, dinocysts and acritarches) were observed in samples 191-1179A-CC to 191-1179C-10H-CC and are moderately to well preserved, ranging from Pliocene to early Pleistocene (Figure 2.6). All samples below 191-1179C-11H-CC, in Units I, II and III, are barren of palynomorphs (Figure 2.6). There is an increase in the abundance of terrestrial pollen in the samples that have anomalously high carbonate contents (Kanazawa, Sager et al., submitted).

Chapter Three – Methods

3.1 Introduction

This chapter outlines the guidelines used in the sample annotation, core description, radiolarian processing method, slide mounting techniques and slide examination.

3.2 Radiolarian Processing

Radiolarians were obtained from the core samples 191-1179B-1H to 191-1179C-3H and core catcher samples 191-1179B-1H-CC to 191-1179C-27X-CC. About 10 cm³ of sediment were disaggregated by using 10% H₂O₂ and about 1% Calgon solutions. Brief treatment of samples in an ultrasonic bath was followed by washing on a 63- μ m mesh sieve. Treating the sample with a 10% HCl solution was not necessary because the sediments were well below the carbonate compensation depth. Radiolaria were obtained from sample 191-1179D-9R-1, 58-62 cm (~358 mbsf) by dissolving small chert fragments in a 5% HF bath for 5hrs. The HF was decanted off the sample and it was then thoroughly washed in distilled water.

The core catcher samples 191-1179B-1H-CC to 191-1179C-27X-CC and 191-1179D-9R-1, 58-62 cm were mounted immediately. The Samples 191-1179B-1H to 191-1179C-3H were filtered using 15 cm diameter filter paper and dried under heat lamps. The samples were stored in 20 ml glass vials for transport.

Core samples 191-1179B-1H to 191-1179C-3H were dried in an oven at 50 °C and the weight was recorded prior to processing.

3.3 Slide Mounting Procedure

Strewn slides were made for the core catcher samples using the greater than 63- μ m fraction with a pipette. The samples were mounted on 50 x 22mm coverslips using Norland Optical Adhesive applied to glass slides and cured under ultraviolet light. Sample 191-1179D-9R-1, 58-62 cm was mounted in Canada Balsam using the strewn pipette method. The use of a pipette to make strewn slides biases the diversity of radiolarians, therefore relative group and species abundance may not be an accurate reflection of the diversity. For this reason the samples are only examined for age estimates.

The method of Roelofs and Pisias (1986) is employed to ensure a random distribution of radiolaria. This allows for accurate species and group diversities to be calculated. This was used to mount core samples 191-1179B-1H to 191-1179C-3H. The washed and dried sample is placed in a beaker containing distilled water and the height of water and diameter of the beaker is measured. The sample is agitated with a sediment stirrer until completely dispersed throughout the water. A stand with two gelatin-covered 50 x 22mm coverslips affixed to it is immersed in the beaker immediately following agitation. The height of the water was measured with the stand immersed. 15-20 minutes was allowed for all the sample particles to settle and the water was siphoned off to just above stand level. The additional water was allowed to evaporate overnight, until it was below stand level. This method may have been employed several times, adjusting the stand height to obtain optimum particle coverage. The coverslips were removed from the stand and allowed to air dry before mounting with Norland Optical Adhesive and curing in ultra-violet light. The particles were washed off the stand and back into their

beaker (Roelofs and Pias, 1986). The sample in the beaker was then sieved using a 63- μm mesh to concentrate the particles and return them to vials. A complete list of apparatus and set up can be found in Figure 3.1.

3.4 Radiolarian Examination

Overall radiolarian abundance was determined based on strewn slide evaluation at 100X, using the following convention:

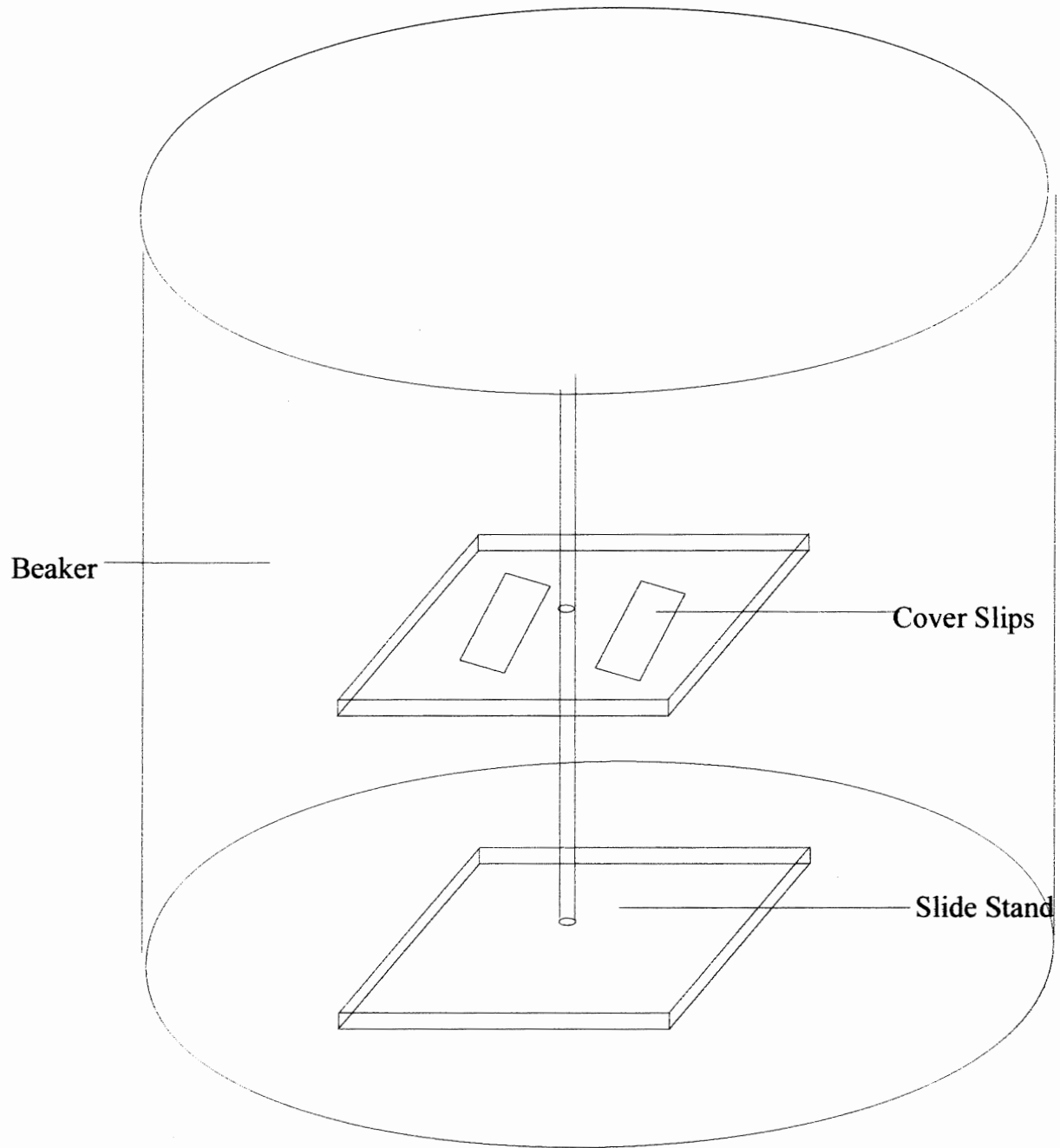
- A (abundant) = >100 specimens per slide traverse;
- C (common) = 50-100 specimens per slide traverse;
- F (few) = 10-50 specimens per slide traverse;
- R (rare) = < 10 specimens per slide traverse;
- T (trace) = <1 specimens per slide traverse; and
- B (barren) = no radiolarians in the sample.

The abundance of total individual species was recorded relative to the fraction of the total assemblage as follows:

- A (abundant) = >10% of the total assemblage;
- C (common) = 5-10% of the total assemblage;
- F (few) = <5% of the total assemblage;
- R (rare) = a few or more specimens per slide;
- T (trace) = present in slide; and
- B (barren) = absent.

Preservation was recorded as follows:

- E (excellent) = nearly pristine, complete skeleton, lacking any indications of dissolution, recrystallization, or breakage;
- G (good) = majority of specimens complete, with minor dissolution, recrystallization, and/or breakage;



List of apparatus

Slide Stand: 2 plexiglass squares (4.5 cm x 4.5cm), all thread, bolts, glue
 500 mL Beaker water siphoning hose
 ruler sediment stirrer processed sample

Figure 3.1 - Setup of apparatus used in the slide mounting procedure.

M (moderate) = minor but common dissolution, with a small amount of recrystallization or breakage of specimen; and

P (poor) = strong dissolution, recrystallization, or breakage, many specimens unidentifiable.

3.5 Biostratigraphic Framework

The conventions for the Cenozoic biostratigraphic zonation used in this thesis can be found in Nigrini and Sanfilippo (1992, 2001). These results were derived from tropical and equatorial site in the Pacific Ocean. In suggesting 'absolute' ages for radiolarian datum levels and zonal boundaries, Nigrini and Sanfilippo (1992, 2001) was used. These schemes were based on results of DSDP Leg 85 sites in the equatorial Pacific.

Chapter Four – Results

4.1 General Statement

The core-catcher samples 191-1179B-2H to 191-1179C-21H were examined and radiolarian datums were produced. During the examination of samples 191-1179B-1H to 191-1179C-3H, severe breakage of radiolaria was observed; there were no identifiable radiolarians in these samples and they were therefore not used.

4.2 ODP Site 1179 Core Catcher Samples

Common-to-abundant radiolarians are present in most sediments, with the exception of Samples 1179B-4H-CC, 1179C-5H-CC, 1179C-9H-CC, and 1179C-12H-CC (Table 2.2). Samples 1179C-22H-CC (~248 mbsf) to 1179C-25H-CC (~273 mbsf) were barren of radiolarians. Radiolarians reappear in samples 1179C-26R-CC (~283 mbsf) and 1179C-27R-CC (~293 mbsf) and continue down through the chert layers. The range of each species can be found in Figure 4.1. The overall group abundance, preservation and species occurrence for each sample can be observed in Table 4.1. The species that were identified by the author are common marker species for the mid-latitude Pacific. The slides were examined until species adequate for an age assignment were observed.

Amphiropalum ypsilon (Plate 1, Figure 1) was observed in Sample 191-1179C-7H-CC (105.85 mbsf) and 8H-CC (115.74 mbsf); this species was few in occurrence.

Botryostrobus aquilonaris (Plate 1, Figure 2) was observed in Samples 191-1179B-1H-CC (7.48 mbsf) through 1179-C-2H-CC (58.77 mbsf); this species was common in occurrence in Samples 191-1179B-1H-CC (7.58 mbsf) through 4H-CC and was few in

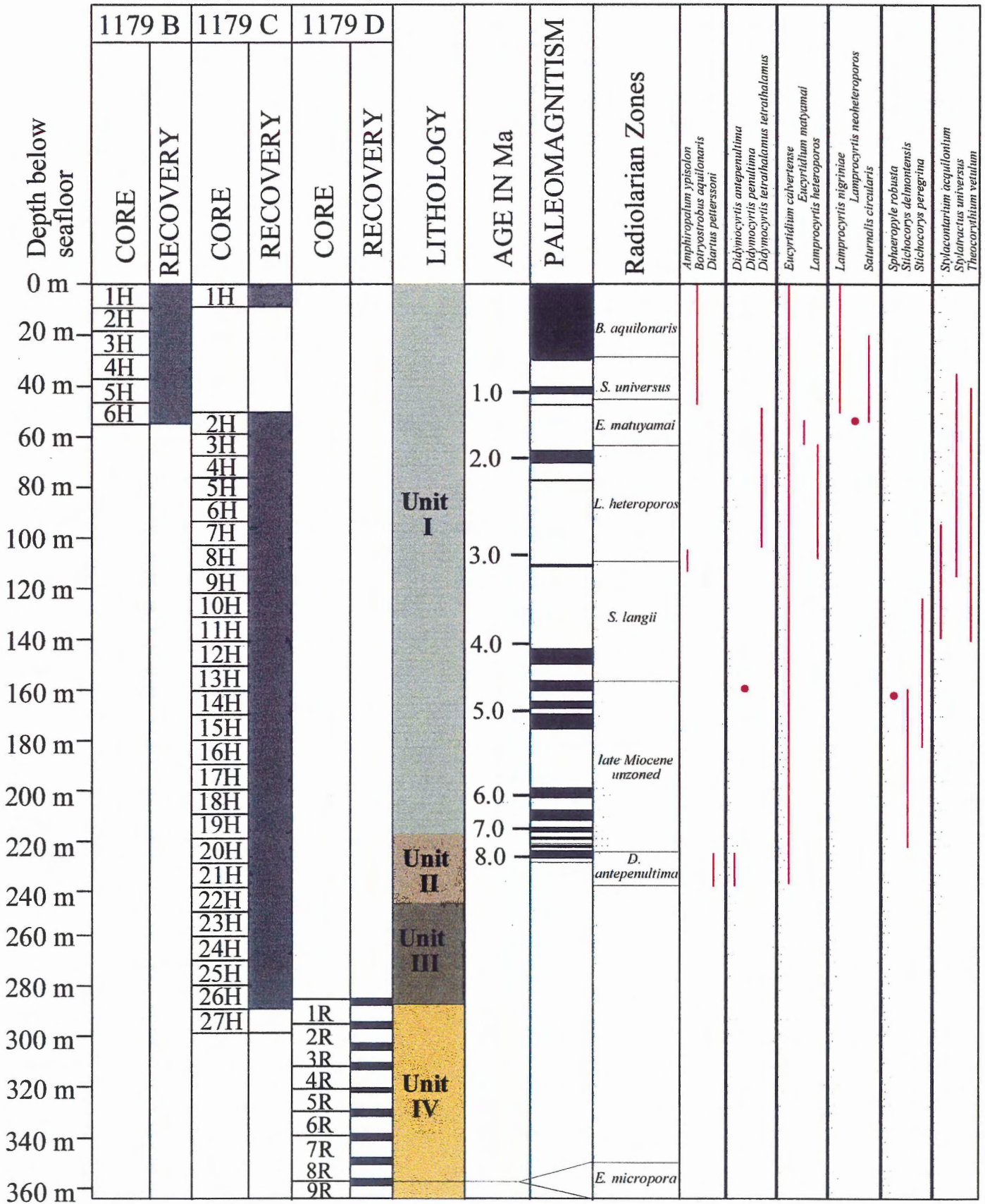


Figure 4.1 - General lithology, magnetostratigraphy, and ranges of radiolarians observed from core-catchers at ODP Site 1179 (after Kanazawa, Sager, et al., submitted)

Lég	Site	H	Core	T	Sct	Depth (mbsf)	Zone To	Zone From	Group Abundance	Group Preservation	<i>Amphithopulum ypsilon</i>	<i>Baryostrobilus aquilonaris</i>	<i>Diartus peterssoni</i>	<i>Didymocorytis antepenultima</i>	<i>Didymocorytis penultima</i>	<i>Didymocorytis terrahalamus terrahalamus</i>	<i>Eucyrtidium cakertensis</i>	<i>Eucyrtidium matuyamai</i>	<i>Emprocorytis heteroporos</i>	<i>Emprocorytis nigritinae</i>	<i>Lamprocorytis neoheteroporos</i>	<i>Saemmadis circularis</i>	<i>Sphaeropyle robusta</i>	<i>Stichocorys delmontensis</i>	<i>Stichocorys peregrina</i>	<i>Sylacanthium acquilonium</i>	<i>Sylactacus universus</i>	<i>Theocorythium vetulum</i>		
191	1179	B	1	H	CC	7.48	<i>B. aquilonaris</i>	<i>B. aquilonaris</i>	C	G	C						C													
191	1179	B	2	H	CC	16.69	<i>B. aquilonaris</i>	<i>B. aquilonaris</i>	C	G	C										C									
191	1179	B	3	H	CC	27.09	<i>S universus</i>	<i>S universus</i>	C	G	C										C					F	F			
191	1179	B	4	H	CC	36.02	<i>S universus</i>	<i>S universus</i>	F	G	C										C					F	F			
191	1179	B	5	H	CC	46.12	<i>E matuyamai</i>	<i>E matuyamai</i>	C	G	F				F		C				C					F	F	C		
191	1179	B	6	H	CC	55.2	<i>E matuyamai</i>	<i>E matuyamai</i>	C	G	F						C	C			C	C				F				
191	1179	C	2	H	CC	58.77	<i>E matuyamai</i>	<i>E matuyamai</i>	F	G	F							C								F				
191	1179	C	3	H	CC	67.81	<i>L. heteroporos</i>	<i>L. heteroporos</i>	C	G													C			F	F	C		
191	1179	C	4	H	CC	77.86	<i>L. heteroporos</i>	<i>L. heteroporos</i>	C	G						F				C						F		C		
191	1179	C	5	H	CC	87.03	<i>L. heteroporos</i>	<i>L. heteroporos</i>	F	G						F				C						F		C		
191	1179	C	6	H	CC	96.83	<i>L. heteroporos</i>	<i>L. heteroporos</i>	A	G										C						F	F	C		
191	1179	C	7	H	CC	105.85	<i>L. heteroporos</i>	<i>L. heteroporos</i>	C	G	F									C						F	F	C		
191	1179	C	8	H	CC	115.74	<i>S langii</i>	<i>S langii</i>	C	G	F															F	F	C		
191	1179	C	10	H	CC	134.57	<i>S langii</i>	<i>S langii</i>	C	G													C							
191	1179	C	11	H	CC	143.84	<i>S langii</i>	<i>S langii</i>	A	G								C					C							C
191	1179	C	12	H	CC	153.87	<i>S langii</i>	<i>S langii</i>	F	M														C						
191	1179	C	13	H	CC	162.89	<i>S peregrina</i>	<i>D penultima</i>	C	G					C									C		C	C			
191	1179	C	14	H	CC	172.87	<i>S peregrina</i>	<i>D penultima</i>	C	M														C	C	C	C			
191	1179	C	15	H	CC	181.94	<i>S peregrina</i>	<i>D penultima</i>	C	M								C							C	C	C			
191	1179	C	16	H	CC	191.79	<i>S peregrina</i>	<i>D penultima</i>	C	M								C							C					
191	1179	C	17	H	CC	201.08	<i>S peregrina</i>	<i>D penultima</i>	C	M								C							C					
191	1179	C	18	H	CC	210.71	<i>S peregrina</i>	<i>D penultima</i>	C	M								C							C					
191	1179	C	20	H	CC	229.72	<i>D antepenultima</i>	<i>D antepenultima</i>	A	G				C	C											C				
191	1179	C	21	H	CC	238.80	<i>D antepenultima</i>	<i>D antepenultima</i>	A	G				C	C											C				

Table 4.1 - Summary of radiolarians examined in core-catcher samples from ODP Site 1179 (after Kanzawa, Sager, et al., submitted)

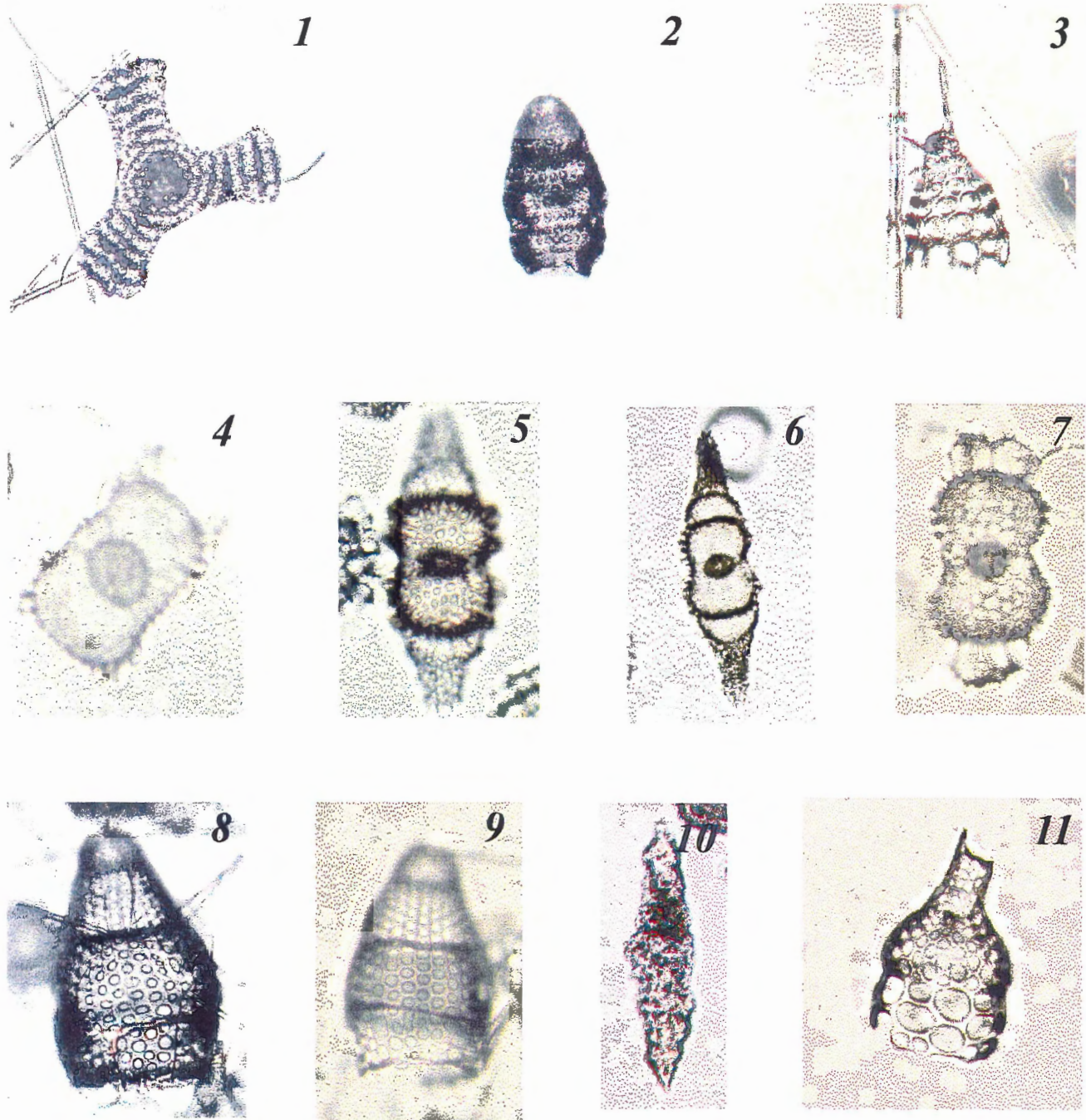


Figure 1 *Amphirhopalum ypsilon* (Hackel, 1887) 191-1179B-6H-CC, slide 2

Figure 2 *Botryostrobos aquilonaris* (Nigrini, 1977) 191-1179-2H-CC, slide 2

Figure 3 *Cycladophora davidsoni davidsoni* (Ehrenburg, 1871) 191-1179B-6H-CC, slide 1

Figure 4 *Diartus petterssoni* (Sanfilippo & Riedel, 1980) 191-1179C-20H-CC, slide 1

Figure 5 *Didymocyrtis antepenultima* (Sanfilippo & Riedel, 1980) 191-1179C-20H-CC, slide 1

Figure 6 *Didymocyrtis penultima* (Sanfilippo & Riedel, 1980) 191-1179C-13H-CC, slide 2

Figure 7 *Didymocyrtis tetrathalamus tetrathalamus* (Sanfilippo & Riedel, 1980) 191-1179C-5H-CC, slide 1

Figure 8 *Eucyrtidium calvertense* (Martin, 1904) under 300X, 191-1179C-2H-CC, slide 2

Figure 9 *Eucyrtidium matyamai* (Hays, 1970) 191-1179C-2H-CC, slide 1

Figure 10 *Eucyrtis micropora* 191-1179C-9R-1W (58-62 cm), slide 2

Figure 11 *Lamprocyrtis heteroporos* (Kling, 1973) 191-1179C-4H-CC, slide 1

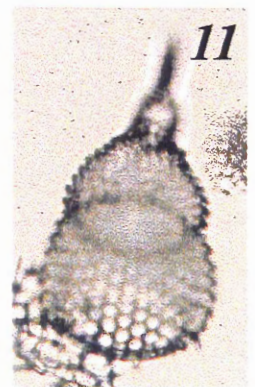
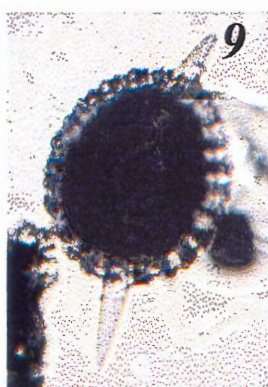
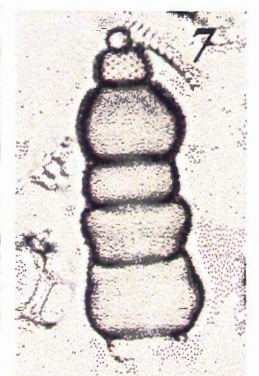
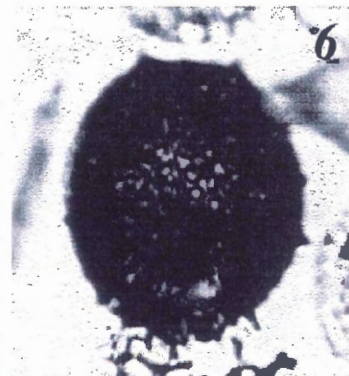
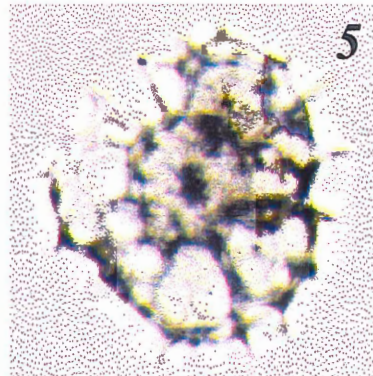
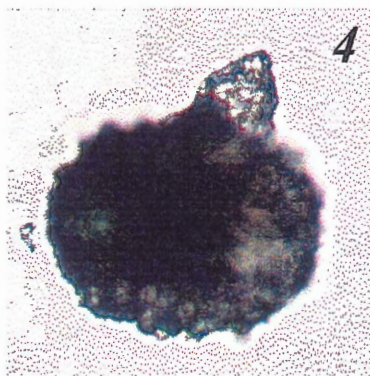
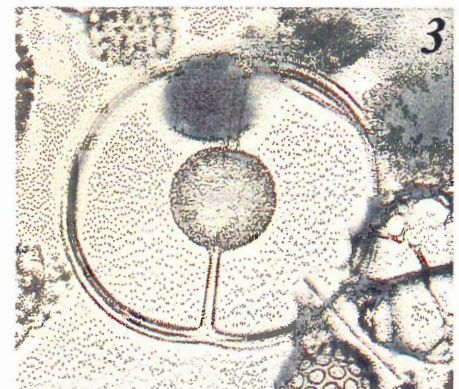


Figure 1 *Lamprocyrtis nigrinia* (Caulet, 1971) 191-1179B-2H-CC, slide 1

Figure 2 *Lamprocyrtis neoheteroporos* (Kling, 1973) 191-1179B-6H-CC, slide 2

Figure 3 *Saturnalis circularis* 191-1179B-3H-CC, slide 2

Figure 4 *Sethocapsa cetia* 191-1179C-9R-1W (58-62 cm), slide 2

Figure 5 *Sphaeropyle langii* (Kling, 1973) 191-1179C-10HCC, slide 2

Figure 6 *Sphaeropyle robusta* (Kling, 1973) 191-1179C-14H-CC, slide 1

Figure 7 *Stichocorys delmontensis* 191-1179C-17H-Cc, slide 1

Figure 8 *Stichocorys peregrina* (Sanfilippo and Riedel, 1970) 191-1179C-12H-CC, slide 1

Figure 9 *Stylocontarium acquilonium* (Kling, 1973) 191-1179B-5H-CC, slide 1

Figure 10 *Stylatractus universus* (Hays, 1970) 191-1179B-4H-CC, slide 2

Figure 11 *Theocorythium vetulum* (Nigrini, 1971) 191-1179B-5H-CC, slide 1

occurrence from Sample 1179B-5H-CC (46.12 mbsf) through 1179C-2H-CC (58.77 mbsf). *Cycladophora davisoni davisoni* (Plate 1, Figure 3) was common in occurrence in sample 191-1179B-4H-CC (32.02 mbsf). *Diatrus petersoni* (Plate 1, Figure 4) and *Didymocyrtis antepenultima* (Plate 1, Figure 5) were common in occurrence and were only observed in Sample 191-1179C-20H-CC (229.72 mbsf) to 191-1179-21H-CC (238.8 mbsf). *Didymocyrtis penultima* (Plate 1, Figure 6) was common in occurrence and was observed in Sample 191-1179C-13H-CC (162.89 mbsf). *Didymocyrtis tetrathalamus tetrathalamus* (Plate 1, Figure 7) was low in occurrence and was found in Samples 191-1179B-5H-CC (46.12 mbsf), 1179C-3H-CC (67.81 mbsf) and 4H-CC (77.86 mbsf).

Eucyrtidium calvertense (Plate 1, Figure 8) was observed in all samples except 191-1179B-6H-CC (58.77 mbsf), 1179C-4H-CC (77.86 mbsf) and 6H-CC (96.83 mbsf) through 8H-CC (115.74 mbsf). *Eucyrtidium matuyamai* (Plate 1, Figure 9) was common in occurrence in Samples 191-1179B-6H-CC (55.2 mbsf) and 1179C-2H-CC (58.77 mbsf). *Lamprocyrtis heteroporos* (Plate 1, Figure 11) is common in Samples 191-1179C-4H-CC (77.86 mbsf) to 7H-CC (105.85 mbsf). *Lamprocyrtis nigriniaie* (Plate 2, Figure 1) is common in occurrence in Samples 191-1179C-2H-CC (16.69 mbsf) to 6H-CC (58.77 mbsf). *Lamprocyrtis neoheteroporos* (Plate 2, Figure 2) was common in occurrence and only observed in Sample 191-1179B-6H-CC.

Saturnalis circularis (Plate 2, Figure 3) was common in Sample 191-1179B-2H-CC (16.69 mbsf) through 6H-CC (55.2 mbsf). *Sphaeropyle robusta* was only observed in Sample 191-1179B-6H-CC (55.2 mbsf). *Stichocorys delmontensis* (Plate 2, Figure 7) is common in Samples 191-1179C-13H-CC (162.89 mbsf) to 20H-CC (229.79 mbsf). *Stichocorys peregrina* (Plate 2, Figure 8) is common in occurrence in Samples 191-

Leg	Site	Hole	Core	Type	Sect	Interval		Volume	Dry weight
191	1179	B	1	HCB	1	25	43	10	20.11
191	1179	B	1	HCB	1	75	93	10	12.5
191	1179	B	1	HCB	2	80	82	10	4.31
191	1179	B	1	HCB	3	80	82	10	5.64
191	1179	B	1	HCB	4	30	32	10	5.69
191	1179	B	1	HCB	5	80	82	10	2.78
191	1179	B	2	HCB	1	76	78	10	3.72
191	1179	B	2	HCB	2	80	82	10	5.87
191	1179	B	2	HCB	3	80	82	10	5.61
191	1179	B	2	HCB	4	80	82	10	8.79
191	1179	B	2	HCB	5	80	82	10	4.48
191	1179	B	2	HCB	6	80	82	10	4.76
191	1179	B	3	HCB	1	80	82	10	8.32
191	1179	B	3	HCB	2	80	82	10	4.98
191	1179	B	3	HCB	3	80	82	10	4.46
191	1179	B	3	HCB	4	80	82	10	7.01
191	1179	B	3	HCB	5	80	82	10	6.78
191	1179	B	3	HCB	6	80	82	10	7.09
191	1179	B	4	HCB	1	80	82	10	3.06
191	1179	B	4	HCB	2	80	82	10	4.36
191	1179	B	4	HCB	3	34	36	10	5.4
191	1179	B	4	HCB	4	34	36	10	4.26
191	1179	B	4	HCB	4	122	124	10	6.23
191	1179	B	4	HCB	5	34	36	10	4.23
191	1179	B	4	HCB	5	122	124	10	3.78
191	1179	B	4	HCB	6	34	36	10	4.09
191	1179	B	4	HCB	6	135	137	10	5.02
191	1179	B	4	HCB	7	6	8	10	6.06
191	1179	B	5	HCB	1	80	82	10	5.61
191	1179	B	5	HCB	1	44	46	10	6.14
191	1179	B	5	HCB	2	30	32	10	4.66
191	1179	B	5	HCB	2	144	146	10	5.05
191	1179	B	5	HCB	3	80	82	10	5.55
191	1179	B	5	HCB	4	30	32	10	4.7
191	1179	B	5	HCB	5	80	82	10	7.5
191	1179	B	5	HCB	6	80	82	10	6.38

Leg	Site	Hole	Core	Type	Sect	Interval		Volume	Dry weight
191	1179	B	5	HCB	7	32	34	10	5.67
191	1179	B	6	HCB	1	32	34	10	5.61
191	1179	B	6	HCB	1	72	74	10	5.79
191	1179	B	6	HCB	2	70	72	10	5.76
191	1179	B	6	HCB	3	72	74	10	5.88
191	1179	B	6	HCB	5	72	74	10	6.9
191	1179	B	6	HCB	6	72	74	10	5.5
191	1179	B	6	HCB	7	42	44	10	4.61
191	1179	C	2	HCB	1	72	74	10	3.5
191	1179	C	2	HCB	2	72	74	10	4.94
191	1179	C	2	HCB	3	72	74	10	5.29
191	1179	C	2	HCB	4	72	74	10	4.41
191	1179	C	2	HCB	5	72	74	10	5.51
191	1179	C	2	HCB	6	72	74	10	5.71
191	1179	C	2	HCB	7	30	32	10	6.23
191	1179	C	3	HCB	1	74	76	10	5.19
191	1179	C	3	HCB	2	2	4	10	3.41
191	1179	C	3	HCB	2	74	76	10	4.76
191	1179	C	3	HCB	2	102	104	10	3.45
191	1179	C	3	HCB	2	146	148	10	5.37
191	1179	C	3	HCB	3	58	60	10	4.56
191	1179	C	3	HCB	4	74	76	10	5.51
191	1179	C	3	HCB	5	74	76	10	5.36
191	1179	C	3	HCB	5	114	116	10	5.95
191	1179	C	3	HCB	6	50	52	10	8.12
191	1179	C	3	HCB	7	6	8	10	5.74
191	1179	C	4	HCB	1	106	108	10	5.42
191	1179	C	4	HCB	1	146	148	10	6.68
191	1179	C	4	HCB	2	74	76	10	4.78
191	1179	C	4	HCB	4	6	8	10	4.09
191	1179	C	5	HCB	2	72	74	10	3.41
191	1179	C	6	HCB	4	8	10	10	4.6
191	1179	C	6	HCB	4	16	18	10	4.55
191	1179	C	6	HCB	4	72	74	10	5.29
191	1179	C	6	HCB	4	74	76	10	4.41
191	1179	C	6	HCB	4	84	86	10	4.42

Table 4.2 - Summary of core samples processed.

Leg	Site	Hole	Core	Type	Sect	Interval		Volume	Dry weight
191	1179	C	6	HCB	5	3	5	10	5.6
191	1179	C	6	HCB	5	76	78	10	7.24
191	1179	C	6	HCB	5	80	82	10	5.46
191	1179	C	6	HCB	5	144	146	10	5.13
191	1179	C	7	HCB	1	74	76	10	3.57
191	1179	C	9	HCB	1	74	76	10	4.09
191	1179	C	9	HCB	2	2	4	10	5.61
191	1179	C	9	HCB	2	104	106	10	3.41
191	1179	C	9	HCB	2	144	146	10	4.17
191	1179	C	9	HCB	3	10	12	10	5.28
191	1179	C	9	HCB	3	74	76	10	4.31
191	1179	C	10	HCB	2	74	76	10	4.11
191	1179	C	10	HCB	4	74	76	10	4.31
191	1179	C	11	HCB	4	74	76	10	3.98
191	1179	C	12	HCB	2	74	76	10	4.74
191	1179	C	13	HCB	1	74	76	10	5.83
191	1179	C	14	HCB	3	64	66	10	4.61
191	1179	C	16	HCB	1	64	66	10	4.56
191	1179	C	17	HCB	4	64	66	10	5.87
191	1179	C	18	HCB	6	64	66	10	7.9
191	1179	C	19	HCB	1	64	66	10	5.51
191	1179	C	20	HCB	5	74	76	10	5.99
191	1179	C	21	HCB	1	20	22	10	10.68
191	1179	C	21	HCB	1	74	76	10	4.56
191	1179	C	22	HCB	6	74	76	10	8.4
191	1179	C	23	HCB	1	2	4	10	8.7

Table 4.2 - Summary of core samples processed.

1179C-10H-CC (134.57 mbsf) to 15H-CC (181.94 mbsf). *Stylocontarium acqilonium* (Plate 2, Figure 9) is common in occurrence in Samples 191-1179B-3H-CC (27.09 mbsf) to 6H-CC (58.77 mbsf) and few appear in Samples 191-1179C-6H (96.83 mbsf) to 8H-CC (115.74 mbsf). Few *Stylatractus universus* (Plate 2, Figure 10) were observed in Samples 191-1179B-4H-CC (36.02 mbsf) to 5H-CC (46.12 mbsf), 1179C-3H-CC (67.81 mbsf) and 1179C-5H-CC (87.03 mbsf) through 7H-CC (105.85 mbsf). *Theocorythidum vetulum* (Plate 2, Figure 11) is common in Samples 191-1179B-4H-CC (36.02 mbsf) and 1179C-3H-CC (67.81 mbsf) through 11H-CC (115.74 mbsf).

4.3 ODP Site 1179 In Core Samples

Samples 191-1179B-1H to C-3H contained radiolaria with severely broken tests. No recognizable species were observed and the abundance of radiolaria was greatly reduced. A detailed outline of the samples taken and their dry weights can be found in Table 4.2. No calculations were performed to estimate the number of radiolaria present in the samples because of the severe breakage of the specimens.

Sample 191-1179D-9R-1, 58-62 cm (~358 mbsf) was taken from Lithological Unit IV, this sample contained common moderately recrystallized radiolaria. Two species were identified from this sample *Eucyrtis micropora* (Plate 1, Figure 10) and *Sethocapsa cetia* (Plate 2, Figure 4).

Chapter Five - Pacific Zonal Definitions for the Middle Latitudes

This chapter contains the Pacific zonal definitions for the middle latitudes as cited in Nigrini and Sanfilippo (1992, 2001). It provides the framework for the radiolarian zonation of ODP Site 1179 found in chapter six.

PLEISTOCENE

Botryostrobus Aquilonaris Zone Baily 1856, emmend. Nigrini 1967

Eucyrtidium tumidulum Zone Hays 1970

Artostrobium miralestensis Zone Kling 1973

Artostrobium tumidulum Foreman 1975

The late Quaternary *B. aquilonaris* (Bailey, 1856) zone is defined by the occurrence of the species it is named for subsequent to the extinction of *Stylatractus universus*. It is the uppermost Quaternary Zone in middle latitudes and is equivalent to the *Omega* Zone in Antarctic sediments (Hays, 1965). Events included in this zone are:

- Tm *Stylocyrtidium acqilonium*

The base of the *B. aquilonaris* Zone is defined by the disappearance of *Stylatractus universus* and is coincident with the upper limit of the *Stylatractus universus* Zone.

Stylatractus Universus Zone Hays 1970

Axoprunum angelinum Kling 1973 and Foreman 1975

The middle Quaternary *S. universus* is defined by the last occurrence of *S. universus* at the top of the zone and is coincident with the lower limit of the *B.*

aquilonaris Zone. The *S. universus* Zone roughly corresponds to the *Psi* Zone in Antarctic sediments (Hays, 1965). Events included in the zone are:

- Tm *Lamprocyrtis neoheteroporos*
- Tm *Theocorythium vetulum* may be coincident with the base of this zone.

The base of the *S. universus* Zone is defined by the disappearance of *Eucyrtidium matuyamai* and is coincident with the upper limit of the *Eucyrtidium matuyamai* Zone.

***Eucyrtidium Matuyamai* Zone Hays 1970, emend. Foreman 1975**

The top of the zone is defined by the disappearance of *E. matuyamai* and is coincident with the lower limit of the *Stylatractus universus* Zone. The zone corresponds approximately to the *Chi* Zone in Antarctic sediments (Hays, 1965). Events included in the zone are:

- Tm *Lamprocyrtis heteroporos*
- Bm *Lamprocyrtis nigrinae*
- Bm *L. neoheteroporos*
- Tm *Sphaeropyle robusta*

The base of the *E. matuyamai* Zone is defined by the evolutionary transition from *Eucyrtidium calvertense* to *E. matuyamai*. The base of the zone approximates the base of the Pleistocene in the North Pacific.

PLIOCENE

***Lamprocyrtis Heteroporos* Zone Hays, 1970, emend. Foreman, 1975**

The top of the late Pliocene *L. heteroporos* Zone is defined by the evolutionary transition of *E. calvertense* to *E. matuyamai* and is coincident with the lower limit of the

E. matuyamai Zone. The upper limit of this zone is similar to the upper boundary of the *Phi* Zone in Antarctic sediments (Hays, 1965). Kling (1973), in North Pacific sediments, used the occurrence of *E. matuyamai* as the upper limit of this zone. The base of the zone is defined by the disappearance of *Stichocorys peregrina* and is coincident with the upper limit of the *Sphaeropyle langii* Zone.

***Sphaeropyle Langii* Zone Foreman 1975**

The top of the middle Pliocene *S. Langii* Zone is defined by the disappearance of *S. peregrina* and is coincident with the lower limit of the *L. heteroporos* Zone. Events included in the zone are:

- Bm *S. acqilonium*
- Tm *Stichocorys delmontensis*
- Bm *L. heteroporos*
- Tm *Theocorys redondoensis*

The base of the zone is defined by the occurrence of *S. langii* and is coincident with the upper limit of the *S. peregrina* Zone. The range of this zone approximates that of the *Spongaster pentas* Zone in the equatorial Pacific. Subsequent unpublished studies (Nigrini, C. and Sanfilippo, A., 2001) suggest that *S. langii* and *S. robusta* are not stratigraphically useful species and that the radiolarian zonation in this part of the time scale will need to be revised.

LATE MIOCENE

Stichocorys Peregrina Zone Riedel and Sanfilippo, 1970, emend. Foreman, 1975

The top of the late Miocene *S. peregrina* Zone is defined by the occurrence of *S. langii* and is coincident with the lower limit of the *S. langii* Zone. Foreman (1975) emended the top of this zone for the North Pacific where the tropical *Spongaster pentas* Zone cannot be recognized. The base of this zone is defined by the occurrence of *S. peregrina* and is coincident with the upper limit of the *Didymocyrtis penultima* Zone. Subsequent unpublished studies (Nigrini, C. and Sanfilippo, A., 2001) suggest that *S. langii* and *S. robusta* are not stratigraphically useful species and that the radiolarian zonation in this part of the time scale will need to be revised. This zone is equivalent to the low-latitude zone of the same name, but the faunal assemblage in the middle latitudes is often different and important marker species are frequently missing.

Didymocyrtis Penultima Zone Riedel and Sanfilippo, 1970

The top of the middle late Miocene *D. penultima* Zone is defined by the occurrence of *S. peregrina* and is coincident with the lower limit of the *S. peregrina* Zone. The base of the zone is defined by the occurrence of *D. penultima* and is coincident with the upper limit of the *Didymocyrtis antepenultima* Zone. This zone is equivalent to the low-latitude zone of the same name, but the faunal assemblage in the middle latitudes is often different and important marker species are frequently missing.

***Didymocyrtis antepenultima* Zone** Riedel and Sanfilippo, 1970

The top of the early late Miocene *Didymocyrtis antepenultima* zone is defined by the occurrence of *D. penultima* and is coincident with the lower limit of the *D. penultima* Zone. The base of the zone is defined by the occurrence of *D. antepenultima* and is coincident with the upper limit of the *Diartus petterssoni* Zone. This zone is equivalent to the low-latitude zone of the same name, but the faunal assemblage in the middle latitudes is often different and important marker species are frequently missing.

Chapter Six – Discussion

6.1 General Statement

This chapter discusses the abundance and preservation of radiolaria assemblages observed from sediments at ODP Site 1179 in Lithological Units I, II and IV and assigns them to mid-latitude radiolaria zones. It discusses the relative rate of sedimentation and compares it to the rate of sedimentation based on the magnetostratigraphy of the site. It also includes a detailed comparison of ODP Site 1179 with other sites drilled on the abyssal sea floor in the Northwest Pacific Basin and suggests the relative position of the Kuroshio/Oyashio convergence boundary since the onset of biosiliceous sedimentation in the middle to late Miocene.

6.2 Radiolarian Biostratigraphy of ODP Site 1179

The radiolarians present in sediments from core-catcher samples of Lithological Units I and II from holes drilled at Site 1179 range in age from late Miocene to Quaternary (Figure 4.1); this corresponds to Unit A in Northwest Pacific stratigraphy (Figure 2.3). Common-to-abundant radiolarians are present in most sediments, with the exception of Samples 1179B-4H-CC, 1179C-5H-CC, 1179C-9H-CC, and 1179C-12H-CC (Table 1179-E-1). The small concentration of radiolarians in Samples 1179C-5H-CC, 1179C-9H-CC, and 1179C-12H-CC (Table 1179-E-1) possibly resulted from an increase in diatom and silicoflagellate production. The concentration of radiolaria in Sample 1179B-4H-CC was decreased by the presence of volcanic ash. Samples 1179C-22H-CC (~248 mbsf) to 1179C-25H-CC (~273 mbsf) were barren of radiolaria, but fish teeth were present in these samples. Radiolaria reappear in Samples 1179C-26R-CC (~283 mbsf)

and 1179C-27R-CC (~293 mbsf) and continue down through the chert layers. Sample 1179D-9R-1, 58-62 cm (~358 mbsf) contained radiolarians from the early Cretaceous.

The radiolarian preservation is good in lithological Unit I (0 to ~220 mbsf) and is moderate in lithological Unit II (~220 to ~246 mbsf). Many of the radiolarians in these samples have broken tests but show little evidence of silica dissolution or recrystallization. Below Units I and II the radiolarian preservation is poor. In Samples 1179C-26R-CC (~283 mbsf) to 1179C-27R-CC (~293 mbsf), identification of species was hindered due to a high degree of silica recrystallization. Sample 1179D-9R-1, 58-62 cm, had a moderately high degree of silica recrystallization. Certain species were less affected by the recrystallization, allowing identification.

6.2.1 Biostratigraphy of Leg 191, Site 1179, Hole D

Sample 191-1179D-9R-1, 58-62 cm (~358 mbsf) contained radiolarians from the early Cretaceous. This is evident from the occurrence of *Eucyrtis micropora* and *Sethoscapsa cetia*, indicating that this sample ranges in age from Valanginian to Barremian.

6.2.2 Biostratigraphy of Leg 191, Site 1179, Hole C

The early late Miocene *D. antepenultima* Zone (Riedel and Sanfilippo, 1970) begins in sample 191-1179C-21H-CC (238.8mbsf) (Figure 4.1); this zone is marked by the presence of *D. antepenultima* and *Diartus hughesi*. These species are also found in Sample 191-1179C-20H-CC (229.72 mbsf) (Figure 4.1). Radiolarians present in Samples 191-1179C-19H-CC (210.71 mbsf) to 191-1179C-13H-CC (162.95 mbsf) (Figure 4.1).

indicate that the section is of middle to late Miocene age, based on the presence of *S. delmontensis*, *S. peregrina* and *S. robusta*. This unzoned section of the core must have the *D. penultima* Zone (Riedel and Sanfilippo, 1970) at its lower boundary with the *D. antepenultima* Zone between cores 191-1179C-20H-CC and 1179C-19H-CC. The unzoned section of the core also must have the *S. peregrina* Zone (Riedel and Sanfilippo, 1970, 1978) at its upper boundary with the *S. langii* Zone (Foreman, 1975). This boundary is marked by the first occurrence of *S. delmontensis* and abundant *S. peregrina*, this occurs between Samples 191-1179C-12H-CC (153.97 mbsf) and 191-1179C-13H-CC (Figure 4.1).

The faunal assemblage suggests that the sediments remain in the *S. langii* Zone through to Sample 191-1179C-H-CC (115.81 mbsf) (Figure 4.1). The boundary between the middle Pliocene *S. langii* Zone and the *L. heteroporos* Zone (Hays, 1970; Foreman 1975) is marked by the first occurrence of *S. acquilonium* in Sample 191-1179C-7H-CC (115.81 mbsf) (Figure 4.1). The *L. heteroporos* Zone continues through to Sample 191-1179C-3H-CC (105.92 mbsf) (Figure 4.1). The faunal assemblage in Sample 191-1179C-2H-CC (28.77 mbsf) (Figure 4.1) suggests that the boundary between the early Pliocene *L. heteroporos* Zone and the *E. matuyamai* Zone (Hays, 1970; Foreman 1975) occurs between cores 191-1179C-3H and 1179C-2H (Figure 4.1). Sediments in Sample 191-1179C-2H-CC (58.28 mbsf) (Figure 4.1) have been assigned to the early Quaternary *E. matuyamai* Zone on the basis of the presence of *Eucyrtidium matuyamai*.

6.2.3 Biostratigraphy of Site 1179, Hole B

Sediments in Samples 191-1179B-6H-CC (55.25 mbsf) and 191-1179B-5H-CC (46.16 mbsf) (Figure 4.1) have been assigned to the early Quaternary *E. matuyamai* Zone on the basis of the presence of *E. matuyamai*. The first occurrence of *S. universus* in sample 1179B-4H-CC (36.06 mbsf) confirms that we are in the *S. universus* Zone (Hays, 1970) (Figure 4.1). The end of the middle Quaternary *S. universus* Zone is marked by the last occurrence of *S. acqulonium* in Sample 1179B-3H-CC (27.14 mbsf). The late Quaternary *B. aquilonaris* Zone (Hays, 1970) is found in Samples 1179B-2H-CC (16.74 mbsf) and 1179B-1H-CC (7.53 mbsf) based on the absence of *S. acqulonium* (Figure 4.1).

6.3 Sedimentation Rate based of Radiolaria Zones and Magnetostratigraphy at ODP Site 1179

The *B. aquilonaris*, *S. universus*, and *E. matuyamai* Zones encompass all of the Quaternary in the mid-latitude Pacific Ocean. Cores 191-1179B-1H-CC through 191-1179C-2H-CC contain these zones. This suggests that 67 m of sediment was deposited at this site during the Quaternary, a sedimentation rate of roughly 37 m/Ma. The *L. heteroporos* and *S. langii* Zone encompasses most of the Pliocene (from 1.8 – 4.5 Ma), cores 191-1179C-3H-CC through 191-1179C-12H-CC contain these zones. This suggests that over 90 m of sediment was deposited during the Pliocene (from 1.8 – 4.5 Ma), a sedimentation rate of roughly 34 m/Ma. The *S. peregrina* Zone encompasses the earliest part of the Pliocene (from 4.5 – 5.2 Ma), this zone was not identified at ODP Site 1179 as it belonged to an unzoned section of the core. The unzoned section of the core

and the *D. antepenultima* Zone contain the earliest part of the Pliocene (from 4.5 – 5.2 Ma) and all of the late Miocene. Cores 191-1179C-13H-CC through 191-1179C-21H-CC contain these zones. This suggests that over 80 m of sediment was deposited during the late Miocene and the earliest part of the Pliocene, a sedimentation rate of roughly 13 m/Ma. Cores 191-1179B-1H through 191-1179C-21H-CC correspond to the topmost layer in Northwest Pacific Basin Stratigraphy, this unit has an average sedimentation rate of roughly 22 m/Ma.

The magnetostratigraphy at ODP Site 1179 indicates that 65.42 m of sediment were deposited during the Quaternary, a rate of 36.3 m/Ma. There were 92.4 m of sediments deposited from 4.5 Ma to the Pliocene/Quaternary boundary, this give a sedimentation rate of 34.2 m/Ma. There were 88.35 m of sediments deposited from the late Miocene to 4.5 Ma, this give a sedimentation rate of 13.6 m/Ma. There were 245 m of sediments were deposited since the late Miocene, suggesting an average sedimentation rate of 22.2 m/ Ma. These rates are nearly the same as the average sedimentation obtained through radiolarian biostratigraphy; this can be verified in Figure 6.1.

6.4 Comparison of Site 1179 with DSDP and ODP Sites in the Northwest Pacific

The radiolarian biostratigraphy done in the Northwest Pacific Basin of the abyssal seafloor by the DSPD (Leg 6 (Heezen, Pimm *et al.*, 1971), Leg 20 (Heezen, MacGregor *et al.*, 1973), Leg 32 (Larson, Moberly *et al.*, 1975), Leg 86 (Heath, Burckle *et al.*, 1979)) and ODP (Leg 145, and Leg 185 (Plank, Ludden, Escutia, 2000)) shows a similar zonation to ODP Site 1179. Figure 6.2 contains a map showing the location of the DSDP/ODP sites in the Northwest Pacific Ocean, the precise location of these sites can

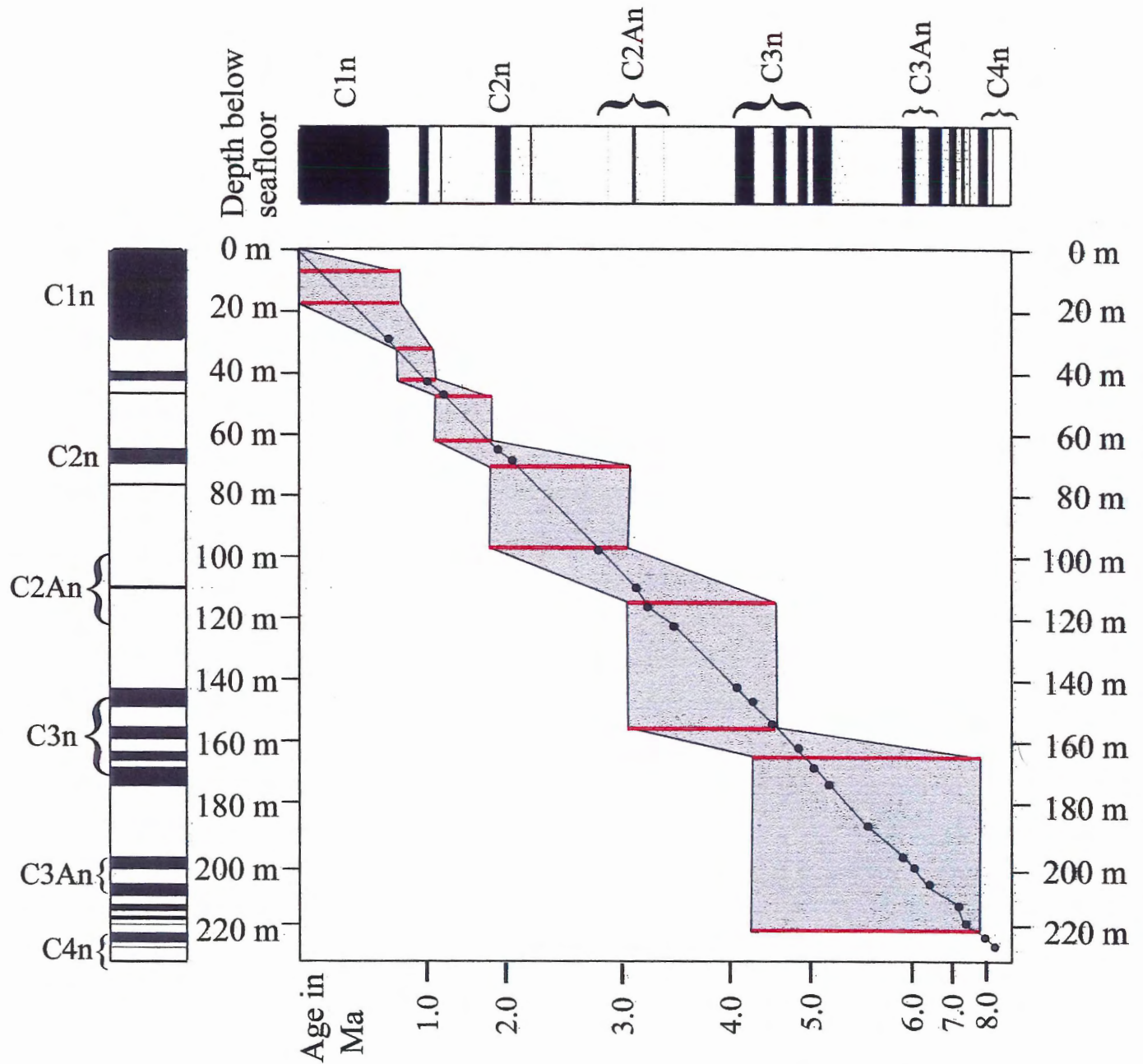


Figure 6.1 - Sedimentation rate diagram based on radiolaria and paleomagnetic data. Range of radiolarian zones shown in gray (modified from Kawanza, Sager et al., submitted).

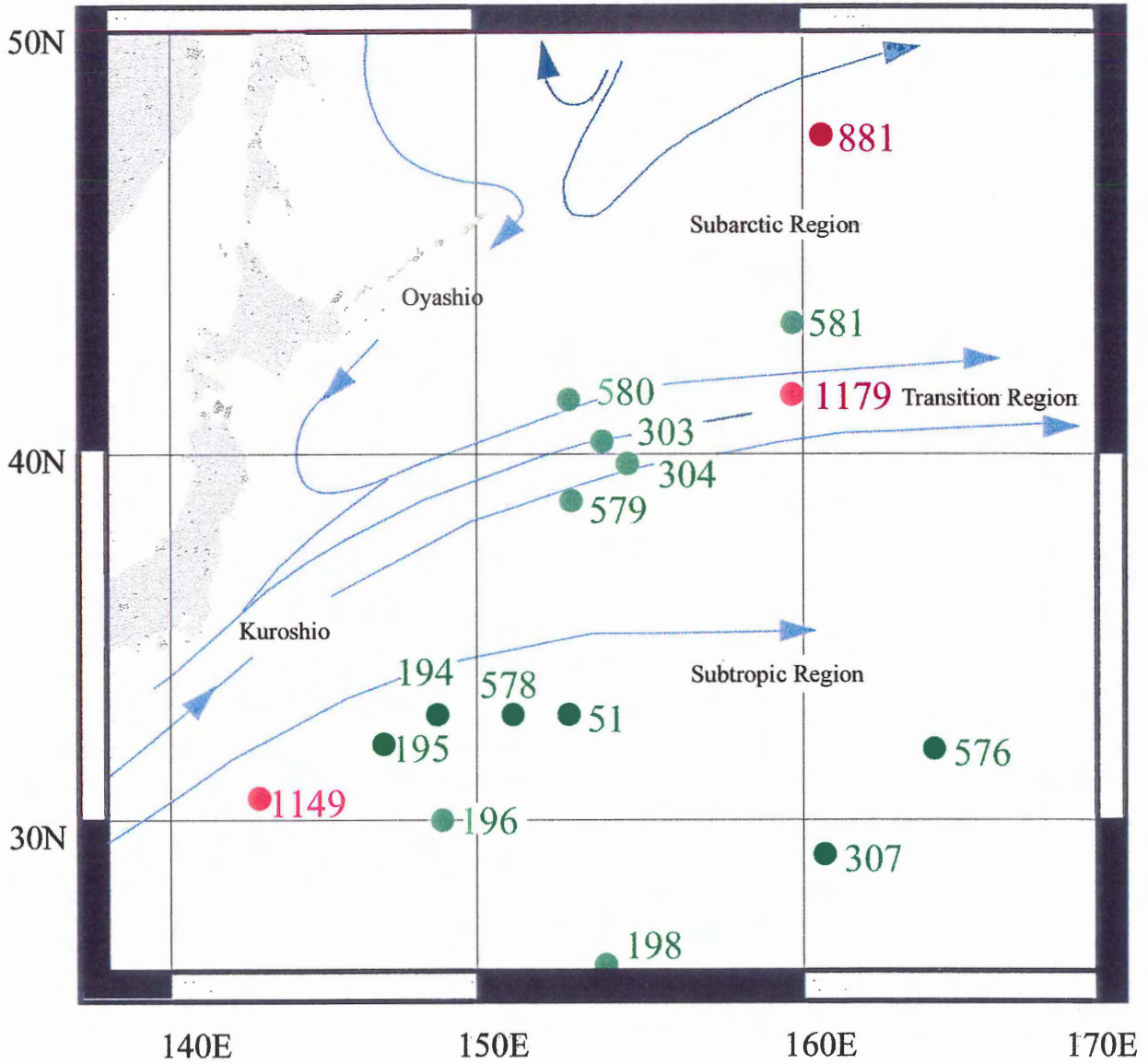


Figure 6.2 - Map showing location of DSDP/ODP sites drilled on the abyssal seafloor in the Northwest Pacific Basin and the location of the modern Kuroshio and Oyashio Currents according to Koizumi (1985). DSDP sites are shown in green and ODP sites are shown in red.

be found in Table 6.1. Other DSDP and ODP Sites from the Northwest Pacific were not used because they are located above the CCD.

Unit A, a Miocene to Pleistocene olive green to gray siliceous clay and ooze with numerous ash layers (Figure 6.3 and 6.4), has been observed to be greater than 200m in thickness resulting from a high productivity in the convergent waters of the Kuroshio and Oyashio currents (Kanazawa, Sager *et al.*, submitted). This unit is the main focus of the comparison between ODP Site 1179 and other sites in the Northwest Pacific Basin.

6.4.1 DSDP and ODP sites of interest

Sites to the south of ODP Site 1179 include DSDP Sites 51 (Leg 6 (Heezen, Pimm *et al.*, 1971)), 194, 195, 196, 198 (Leg 20 (Heezen, MacGregor *et al.*, 1973)), 307 (Leg 32 (Larson, Moberly *et al.*, 1975)), 576, and 578 (Leg 86 (Heath, Burckle *et al.*, 1979)). A summary of the number of cores, intervals, recovery, lithology and radiolarian zonation can be found in Table 6.2. At DSDP Site 51 (Heezen, Pimm *et al.*, 1971) the cores of specific interest to this thesis are 6-51.0-1H (114.0 – 123.1 mbsf) and 6-51.1-1H (22.9 – 32.0 mbsf). Core 6-51.0-1H belongs to the *S. peregrina* Zone and core 6-51.1-1H belongs to the *E. matuyamai* Zone (Fischer *et al.*, 1971). DSDP Site 51 (Heezen, Pimm *et al.*, 1971) is not suitable for a detailed comparison with ODP Site 1179 because cores were not continuously recovered. This site was abandoned before the barren zone was reached making it impossible to estimate a sedimentation rate.

At DSDP Sites 194, 195, 196 and 198 (Heezen, MacGregor *et al.*, 1973) the cores of specific interest to this thesis are 20-194-1H (37.5 – 47.0 mbsf) and 20-194-2H (142.0 – 151.5 mbsf), 20-195A-1H (63.0 – 72.5 mbsf) and 20-195A-2H (120.0-129.5 mbsf), 32-

Leg	Hole #	Latitude	Longitude	Water Depth
6	51	33 ⁰ 28.5N	153 ⁰ 24.3E	5981.0
20	194	33 ⁰ 28.5N	148 ⁰ 48.6E	5744.0
20	195	32 ⁰ 46.48N	146 ⁰ 58.7E	5958.0
20	196	30 ⁰ 07.0N	148 ⁰ 57.70E	6184.0
20	198	25 ⁰ 29.5N	154 ⁰ 35.0E	5848.0
32	303	40 ⁰ 48.50N	154 ⁰ 27.07E	5609.0
32	304	39 ⁰ 20.27N	155 ⁰ 4.19E	5640.0
32	307	28 ⁰ 35.26N	161 ⁰ 00.28E	5696.0
86	576	32 ⁰ 21.37N	164 ⁰ 16.52E	6219.3
86	578	33 ⁰ 55.56N	151 ⁰ 37.74E	6010.0
86	579	38 ⁰ 37.68N	153 ⁰ 50.14E	5736.6
86	580	41 ⁰ 37.47N	153 ⁰ 58.58E	5375.0
86	581	43 ⁰ 55.62N	159 ⁰ 47.76E	5467.0
145	881	47 ⁰ 6.14N	161 ⁰ 29.52E	5531.1
185	1149	31 ⁰ 20.55N	143 ⁰ 21.0E	5818.0

Table 6.1 - Summary of location and water depth at DSDP and ODP Sites in the Northwest Pacific Basin.

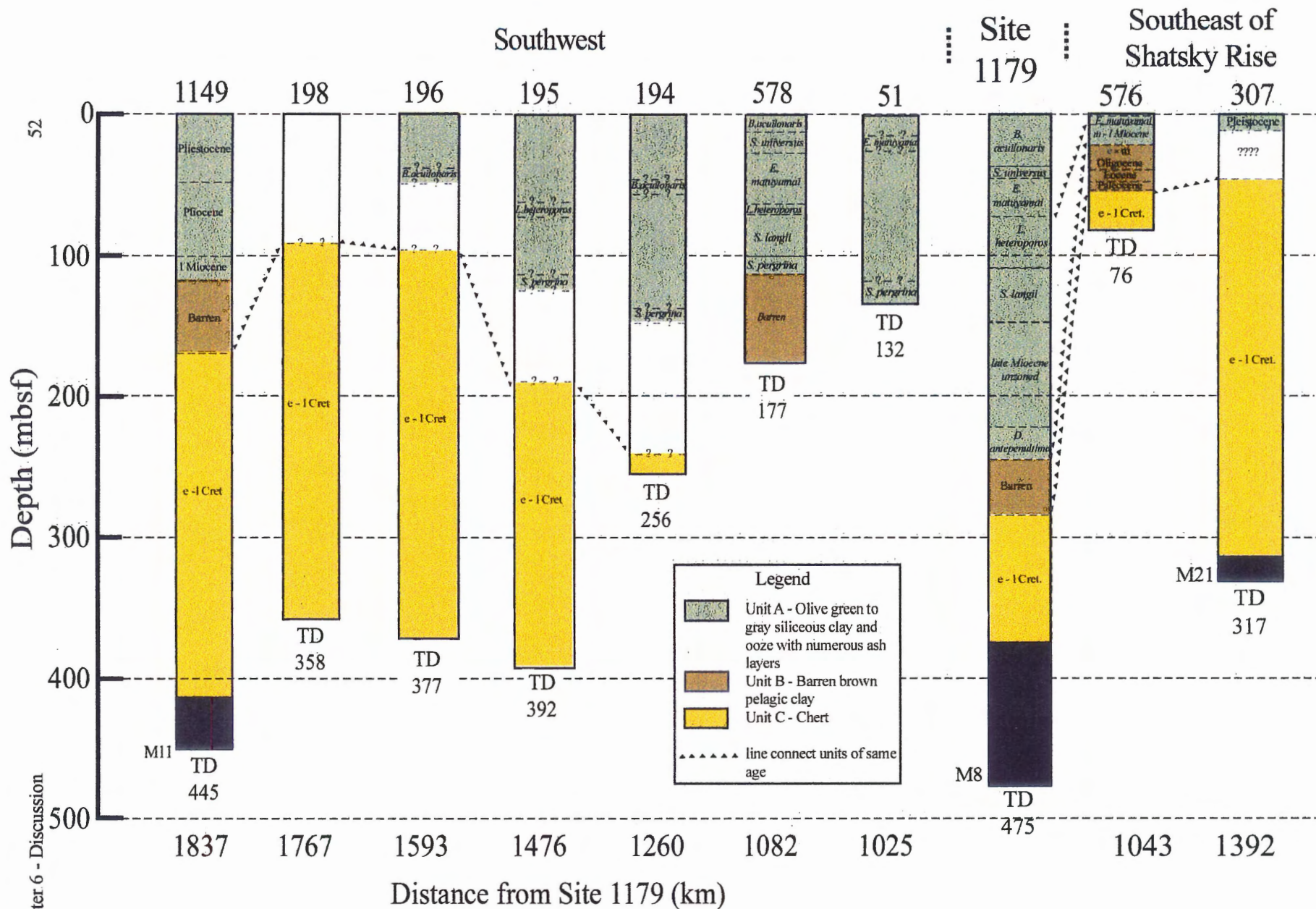


Figure 6.3 - Biostratigraphic zonation of DSDP/ODP sites South of Site 1179, DSDP Leg 6 (Heezen, Pimm et al., 1971), Leg 20 (Heezen, MacGregor et al., 1973), Leg 32 (Larson, Moberly et al., 1975), Leg 86 (Heath, Burckle et al., 1979) and ODP Leg 145, and Leg 185 (Plank, Ludden, Escutia, 2000).

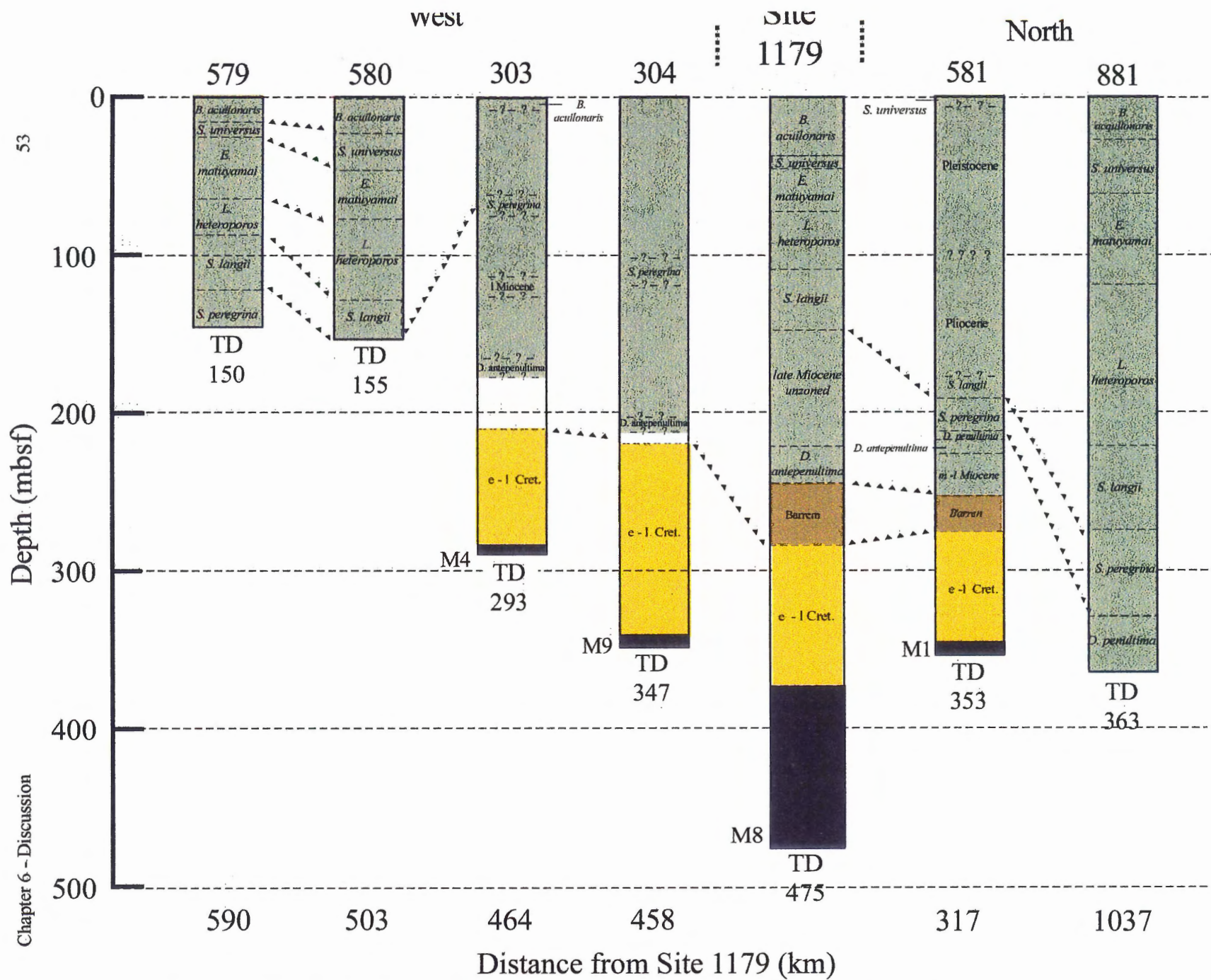


Figure 6.4 - Biostratigraphic zonation of DSDP/ODP sites to the West and North of Site 1179; Leg 6 (Heezen, Pimm et al., 1971), Leg 20 (Heezen, MacGregor et al., 1973), Leg 32 (Larson, Moberly et al., 1975), Leg 86 (Heath, Burckle et al., 1979) and ODP Leg 145, and Leg 185 (Plank, Ludden, Escutia, 2000).

Leg	Site	Core #	Interval (mbsf)	Recovery (m)	Recovery (%)	Lithological Description	Zones
6	51.0	1	114.0 - 123.1	9.1	100	Dark brown zeolitic clay w/ yellowish-brown diatom ooze mottles and ash layers	<i>Stichocorys peregrina</i> to <i>Didmocyrtilis penultima</i>
		2	123.7 - 132.0	0.3	3	Barren	-----
	51.1	1	22.9 - 32.0	9.1	100	Radiolarian - Diatom rich clay w/ ash layers	<i>Eucyrtis matuyamai</i> to <i>Lamprocyrtis heteroporos</i>
		2	120.7 - 126.8	1.8	30	Barren	-----
20	194	1	37.5 - 47.0	8.5	89	Pale green radiolarian clay	<i>Botryostrobilus aquilonaris</i>
		2	142.0 - 151.5	6.5	68	Pale green radiolarian clay	<i>Stichocorys peregrina</i>
		3	227.5 - 237.0	cc	1	Chert	early Cretaceous
		4	237.0 - 246.5	cc	1	Chert	
		5	246.5 - 248.0	cc	1	Chert	
	195A	1	63.0 - 72.5	8.5		Mottled silty radiolarian clay w/ ash layers	<i>Lamprocyrtis heteroporos</i>
		2	12.0 - 129.5	5.0		Brown clay	<i>Stichocorys peregrina</i>
		3	190.0 - 196.0	0.5		Chert/Limestone	Valanginian to Hauterivian
	195B	1	357.5 - 367.0	cc		Chert/Chalk	
		2	367.0 - 371.0	cc		Chert	
		3	389.0 - 392.0	1.0		Chert/Chalk/Limestone	

Table 6.2 – Summary of DSPD and ODP Sites in the Northwest Pacific Basin (Leg 6 (Heezen, Pimm et al., 1971), Leg 20 (Heezen, MacGregor et al., 1973), Leg 32 (Larson, Moberly et al., 1975), Leg 86 (Heath, Burckle et al., 1979)) and ODP (Leg 145, and Leg 185 (Plank, Ludden, Escutia, 2000)).

Leg	Site	Core #	Interval (mbsf)	Recovery (m)	Recovery (%)	Lithological Description	Zones
20	196	1	37.5 – 47.0	1.0		Palagonitic silty red clay	<i>Botryostrobus aquilonaris</i>
		2	104.0 – 110.0	6.0		Zeolitic red clay	late Cretaceous
		3	197.0 – 203.0	1.0		Limestone/Chert/Siltstone	Valanginian to Hauterivian
		4	300.5 – 310.0	0.5		Limestone/Chert	
	198	1	90.5 – 100.0	8.0		Brown zeolitic clay	Cretaceous
		2	100.5 – 109.5	2.5			
		3	109.5 – 119.0	6.0			
		4	119.0 – 125.0	6.0			
		5	125.0 – 134.5	cc		Brown zeolitic clay/Chert	
	32	303	1	0.0 – 12.0	0.5	5	Diatom – Radiolarian ooze w/ radiolarian-bearing pelagic clay
2			62.0 – 72.0	9.0	100	<i>Stichocorys peregrina</i>	
3			117.0 – 126.0	8.0	89	late Miocene	
4			174.0 – 183.0	8.3	92	<i>Didymocyrtis antepenultima</i>	
5			212.0 – 220.0	tr	<1	Zeolitic pelagic clay/Chert	
303A		2	220.0 – 229.25	tr	<1	Chert	Albian
		3	229.25 – 238.5	0.2	2		Aptian to Barremian
		4	238.5 – 247.5	0.4	4		Barremian to Hauterivian
		5	247.75 – 257.0	1.5	16		
		6	257.0 – 266.75	0.4	4		
		7	266.25 – 275.5	0.5	5		
		8	275.5 – 284.75	0.4	4		Clayey nanno ooze/Chert

Table 6.2 – Summary of DSDP and ODP Sites in the Northwest Pacific Basin (Leg 6 (Heezen, Pimm et al., 1971), Leg 20 (Heezen, MacGregor et al., 1973), Leg 32 (Larson, Moberly et al., 1975), Leg 86 (Heath, Burckle et al., 1979)) and ODP (Leg 145, and Leg 185 (Plank, Ludden, Escutia, 2000)).

Leg	Site	Core #	Interval (mbsf)	Recovery (m)	Recovery (%)	Lithological Description	Zones
32	304	1	105.5 – 115.0	5.5	58	Radiolarian diatom ooze	<i>Stichocorys peregrina</i>
		2	216.0 – 225.5	2.8	29	Pelagic clay/Chert	<i>Didymocyrtilis antepenultima</i>
		3	235.0 – 244.0	9	100		late Albian
		4	244.0 – 253.0	tr	<1		Albian to Aptian
		5	253.0 – 262.5	0.4	4		Aptian to Barremian
		6	262.0 – 271.5	tr	<1		
		7	271.5 – 281.0	0.4	4		
		8	281.0 – 290.0	0.4	4		
		9	290.0 – 299.5	0.5	5		Barremian to Hauterivian
		10	299.5 – 308.5	0.4	4		
		11	308.5 – 318.0	0.3	3		
		12	318.0 – 327.0	0.3	3		
		13	327.0 – 331.0	tr	<1	Nanno ooze/ Chert	
		14	331.0 – 334.5	1.4	43		
	307	1	0.0 – 9.0	7.5	83	Zeolitic pelagic clay	Pliocene
		2	37.5 – 47.0	0.4	4	Chert/Porcellenite/Zeolitic pelagic clay	late Albian
		3	56.5 – 65.5	0.4	4		Albian
		4	84.5 – 85.5	0.2	2		Aptian to Barremian
		5	103.0 – 112.5	0.1	1		Barremian to Valanginian
		6	121.5 – 130.5	0.3	3		
		7	158.0 – 167.0	1.7	19		
		8	195.0 – 204.0	1.2	13	Chert/Nanno Chalk/Calcareous Porcellenite	

Table 6.2 – Summary of DSPD and ODP Sites in the Northwest Pacific Basin (Leg 6 (Heezen, Pimm *et al.*, 1971), Leg 20 (Heezen, MacGregor *et al.*, 1973), Leg 32 (Larson, Moberly *et al.*, 1975), Leg 86 (Heath, Burckle *et al.*, 1979)) and ODP (Leg 145, and Leg 185 (Plank, Ludden, Escutia, 2000)).

Leg	Site	Core #	Interval (mbsf)	Recovery (m)	Recovery (%)	Lithological Description	Zones	
32	307	9	232.5 – 241.5	1.3	14	Chert/Nanno Chalk/Calcareous Porcellanite	Valanginian	
		10	270.0 – 277.5	0.8	9		Valanginian to Berriasian	
		11	288.5 – 297.5	0.7	8			
		12	297.5 – 307.0	0.6	6			
86	576	1	0.0 – 2.7	2.71	100	Pelagic brown clay	<i>Botryostrobus aquilonaris</i> to <i>Stylatractus universus</i> <i>Eucyrtidium matuyamai</i>	
		2	2.7 – 12.2	9.78	103		middle to late Miocene	
		3	12.2 – 21.7	6.64	70			
		4	21.7 – 31.2	10.05	106		Barren of radiolaria (ages based on Ichthyoliths)	early to middle Oligocene
		5	31.2 – 40.7	9.81	103			
		6	40.7 – 50.2	9.78	103			
		7	50.2 – 59.7	9.68	102		Calcareous ooze/Pelagic brown clay	Eocene
		8	59.7 – 69.2	9.68	102			Paleocene Cretaceous
	578		1	0.0 – 4.8	4.77	99	Olive grey siliceous clay	<i>Botryostrobus aquilonaris</i>
			2	4.8 – 14.3	8.25	87		<i>Stylatractus universus</i>
			3	14.3 – 23.8	9.70	102		
			4	23.8 – 33.3	9.01	95		<i>Eucyrtidium matuyamai</i>
			5	33.3 – 42.8	9.63	101		
			6	42.8 – 52.3	10.00	105		
			7	52.3 – 61.8	9.68	102		Yellow brown to brown clay
8			61.8 – 71.3	9.76	103			
9			71.3 – 80.8	9.75	103			

Table 6.2 – Summary of DSPD and ODP Sites in the Northwest Pacific Basin (Leg 6 (Heezen, Pimm et al., 1971), Leg 20 (Heezen, MacGregor et al., 1973), Leg 32 (Larson, Moberly et al., 1975), Leg 86 (Heath, Burckle et al., 1979)) and ODP (Leg 145, and Leg 185 (Plank, Ludden, Escutia, 2000)).

Leg	Site	Core #	Interval (mbsf)	Recovery (m)	Recovery (%)	Lithological Description	Zones	
86	578	10	80.8 – 90.3	8.93	94	Yellow brown to brown clay	<i>Sphaeropyle langii</i>	
		11	90.3 – 99.8	9.44	99		<i>Stichocorys peregrina</i>	
		12	99.8 – 109.3	9.06	95			
		13	109.3 – 118.8	9.48	100			
		14	118.8 – 128.3	10.18	107			
		15	128.3 – 137.8	9.76	103	Brown pelagic clay		Barren
		16	137.8 – 147.3	8.36	88			
		17	147.3 – 155.3	7.86	96			
		18	156.8 – 163.3	6.20	95			
		19	166.3 – 171.3	4.57	91			
			20	175.8 – 176.8	0.81	81	Brown pelagic clay / Chert	
		579	1	0.0 – 8.4	8.44	100	Siliceous clay	<i>Botryostrobus aquilonaris</i>
			2	8.4 – 17.9	8.46	89		<i>Stylatræus universus</i>
		579A	1	14.0 – 23.5	9.3	98		<i>Eucyrtidium matuyamai</i>
			2	23.5 – 33.0	9.7	102		
			3	33.0 – 42.5	8.88	93		
			4	42.5 – 52.0	5.36	56		
			5	52.0 – 61.5	9.03	95		
			6	61.5 – 71.0	7.94	84		
			7	71.0 – 80.5	8.27	87		
	8		80.5 – 90.0	9.66	102			
	9		90.0 – 99.5	7.68	81			
	10		99.5 – 109.0	7.59	80	<i>Sphaeropyle langii</i>		
	11		109.0 – 118.5	7.30	77			
	12		118.5 – 128.0	8.34	88	<i>Stichocorys peregrina</i>		
	13	128.0 – 137.5	6.95	73				
	14	137.5 – 147.0	7.50	79				

Table 6.2 – Summary of DSPD and ODP Sites in the Northwest Pacific Basin (Leg 6 (Heezen, Pimin et al., 1971), Leg 20 (Heezen, MacGregor et al., 1973), Leg 32 (Larson, Moberly et al., 1975), Leg 86 (Heath, Burckle et al., 1979)) and ODP (Leg 145, and Leg 185 (Plank, Ludden, Escutia, 2000)).

Leg	Site	Core #	Interval (mbsf)	Recovery (m)	Recovery (%)	Lithological Description	Zones	
86	579A	15	147.0 – 149.5	2.37	95	Siliceous clay	<i>Stichocorys peregrina</i>	
	580	1	0.0 – 3.3	3.32	101	Siliceous clay	<i>Botryostrobos aquilonaris</i>	
		2	3.3 – 12.8	8.39	88			
		3	12.8 – 22.3	8.62	91			
		4	22.3 – 31.8	8.88	93			
		5	31.8 – 41.3	9.14	96			
		6	41.3 – 50.8	8.80	93			
		7	50.8 – 60.3	7.74	81	Calcareous siliceous clay	<i>Eucyrtidium matuyamai</i>	
		8	60.3 – 69.8	9.27	98			
		9	69.8 – 79.3	7.51	79			
		10	79.3 – 88.8	8.65	91	Siliceous clay	<i>Lamprocyrtis heteroporos</i>	
		11	88.8 – 98.3	7.30	77			
		12	98.3 – 107.8	9.29	98			
		13	107.8 – 117.3	9.08	96	Clayey diatom ooze		
		14	117.3 – 126.8	9.14	96			
		15	126.8 – 136.3	8.45	89	Siliceous clay	<i>Sphaeropyle langii</i>	
		16	136.3 – 145.8	8.97	94			
		17	145.8 – 155.3	7.72	81			
	581	1	0.0 – 1.0	0.93	93	Biogenic siliceous clay	<i>Stylatractus universus</i>	
		2	181.5 – 191.0	6.83	67		<i>Sphaeropyle langii</i>	
		3	191.0 – 200.5	8.52	90		<i>Stichocorys peregrina</i>	
		4	200.5 – 210.0	9.45	99			
		5	210.0 – 219.5	5.32	56		<i>Didymocyrtis penultima</i>	
		6	219.5 – 229.0	9.44	99		<i>Didymocyrtis antepenultima</i>	
		7	229.0 – 238.5	8.98	95		<i>Diartus pettersoni</i>	
		8	238.5 – 248.0	7.59	80		<i>Dorcadosphyris alata</i>	
		9	248.0 – 257.5	5.48	58		Pelagic brown clay	

Table 6.2 – Summary of DSPD and ODP Sites in the Northwest Pacific Basin (Leg 6 (Heezen, Pimm et al., 1971), Leg 20 (Heezen, MacGregor et al., 1973), Leg 32 (Larson, Moberly et al., 1975), Leg 86 (Heath, Burckle et al., 1979)) and ODP (Leg 145, and Leg 185 (Plank, Ludden, Escutia, 2000)).

Leg	Site	Core #	Interval	Recovery (m)	Recovery (%)	Lithological Description	Zones
86	581	10	257.5 – 267.0	8.52	90	Pelagic brown clay	Barren
		11	267.0 – 276.5	0.40	4		
		12	276.5 – 286.0	0.35	4		
		13	286.0 – 295.5	0.16	2	Chert	Cretaceous
		14	295.5 – 305.0	0.27	3		
		15	305.0 – 314.5	0.55	6		
		16	314.5 – 324.0	0.18	2		
		17	324.0 – 333.5	1.07	11		
		18	333.5 – 343.0	0.35	4		
		19	343.0 – 352.5	3.65	38		
145	881C	1	0.0 – 3.8	3.92	103	Clayey diatom ooze	<i>Bostrychobolus aquilonaris</i>
		2	3.8 – 13.3	9.63	11		<i>Stylatractus universus</i>
		3	13.3 – 22.8	8.81	92		
		4	22.8 – 32.3	9.84	103		
		5	32.3 – 41.8	8.80	92		
		6	41.8 – 51.3	9.84	103		
		7	51.3 – 60.8	9.29	98		<i>Eucyrtidium matuyamai</i>
		8	60.8 – 70.3	10.05	106		
		9	70.3 – 79.8	8.57	90		
		10	79.8 – 89.3	9.59	11		<i>Lamprocyrtis heteroporos</i>
		11	89.3 – 98.8	9.26	98		
		12	98.8 – 108.3	9.91	104		
		13	108.3 – 117.8	9.32	98		
		14	117.8 – 127.3	10.00	05		
		15	127.3 – 136.8	9.75	102		
		16	136.8 – 146.3	9.96	105		
		17	146.3 – 155.8	9.48	99		

Table 6.2 – Summary of DSPD and ODP Sites in the Northwest Pacific Basin (Leg 6 (Heezen, Pimm *et al.*, 1971), Leg 20 (Heezen, MacGregor *et al.*, 1973), Leg 32 (Larson, Moberly *et al.*, 1975), Leg 86 (Heath, Burckle *et al.*, 1979)) and ODP (Leg 145, and Leg 185 (Plank, Ludden, Escutia, 2000)).

Leg	Site	Core #	Interval	Recovery (m)	Recovery (%)	Lithological Description	Zones
145	881	18	155.8 – 162.3	3.9	60	Diatom ooze	<i>Lamprocyrtis heteroporos</i>
		19	162.5 – 171.9	cc	<1		
		20	171.9 – 181.7	cc	<1		
		21	181.7 – 191.2	9.5	100		
		22	191.2 – 200.6	cc	<1		
		23	200.6 – 209.7	9.32	102		
		24	209.7 – 219.0	cc	<1		
		25	219.0 – 228.7	5.28	54		<i>Sphaeropyle langii</i>
		26	228.7 – 238.3	cc	<1		
		27	238.3 – 248.0	8.65	89		
		28	248.0 – 257.6	cc	<1		
		29	257.6 – 267.2	4.08	42		<i>Stichocorys peregrina</i>
		30	267.2 – 276.9	9.44	97		
		31	276.9 – 286.5	cc	<1		
		32	286.5 – 296.2	3.85	39		
		33	296.2 – 305.8	cc	<1		
		34	305.8 – 315.4	cc	<1		
		35	315.4 – 325.1	7.46	77		
		36	325.1 – 334.8	9.65	99		
37	334.8 – 344.5	cc	<1				
38	344.5 – 354.1	cc	<1				
		39	354.1 – 363.8	cc	<1		

Table 6.2 – Summary of DSPD and ODP Sites in the Northwest Pacific Basin (Leg 6 (Heezen, Pimm et al., 1971), Leg 20 (Heezen, MacGregor et al., 1973), Leg 32 (Larson, Moberly et al., 1975), Leg 86 (Heath, Burckle et al., 1979)) and ODP (Leg 145, and Leg 185 (Plank, Ludden, Escutia, 2000)).

196-1H (37.5 – 47.0 mbsf), and no cores from Site 198. Cores 20-194-1H and 20-196-1H belong to the *B. aquilonaris* Zone, core 20-195A-1H belongs to the *L. heteroporos* Zone and 20-194-2H belongs to the *S. peregrina* Zone (Heezen et al, 1971). DSDP Sites 194, 195, 196, and 198 (Heezen, MacGregor et al., 1973) were not suitable for comparison with ODP Site 1179 because only discrete intervals of sediment from Unit A were recovered, the lower boundary of Unit A was not recovered at these site making it impossible to estimate a sedimentation rate.

At DSDP Site 307 (Larson, Moberly et al., 1975), core 32-307-1H (0.0 – 9.0 mbsf) is the only core of interest. The zonation of core 32-307-1H was not determined but the faunal assemblage suggests that it is of Pleistocene age. DSDP Site 307 is not suitable for comparison because only a single core was recovered from Unit A.

At DSDP Sites 576 and 578 (Heath, Burckle et al., 1979) the cores of interest are 86-576-1H (0.0 – 2.7 mbsf) to 86-576-3H (12.2 – 21.7 mbsf) and 86-578-1H (0.0 – 4.8 mbsf) through 13H (109.3 – 118.8 mbsf). The top of core 86-576-1H and all of cores 86-578-1H to 86-578-2H belong to the *B. aquilonaris* Zone. The bottom of core 86-576-1H and cores 578-3H to 578-4H belong to the *S. universus* Zone. Cores 86-576-2H, 86-578-5H through 86-578-7H belong to the *E. matuyamai* Zone. Cores 86-578-8H, 86-578-9H through 86-578-11H and 86-578-12H to 86-578-13H belong to the *L. heteroporos*, *S. langii*, and *S. peregrina* Zone, respectively. Core 86-576-3H is of middle to late Miocene in age, this datum is based on the Ichthyolith assemblage and corresponds to the *D. antepenultima* to *D. penultima* Zones. DSDP Site 576 is not comparable to ODP Site 1179 because the Unit A sediment package is very thin (~ 10 m). This site was drilled on the western flank of Shatsky Rise at a depth of roughly

6200m, the increased depth may have an effect on the sedimentation rate as does its proximity to Shatsky Rise. DSDP Site 578 is comparable to ODP Site 1179 because of its continuous record and it reaches the barren zone, radiolarian zones were determined throughout Unit A allowing us to compare the rate of sedimentation in various zones in the core.

ODP Site 1149 (Leg 185 (Plank, Ludden, Escutia, 2000)) is located to the south of ODP Site 1179. This site is comparable even though analysis of the radiolarian assemblages and zonation was not performed because the magnetostratigraphy shows the important boundaries in Unit A and where the boundary with the barren zone occurs allowing for a sedimentation rate estimate.

Sites to the west of ODP Site 1179 include DSDP Sites 303 and 304 (Leg 32 (Larson, Moberly et al., 1975)) and Sites 579 and 580 (Leg 86 (Heath, Burckle et al., 1979)). A summary of the number of cores, intervals, recovery, lithology and radiolarian zonation can be found in Table 6.2. At DSDP Sites 303 and 304 (Larson, Moberly et al., 1975) the cores of interest are 32-303-1H (0.0 – 12.0 mbsf), 32-303-2H (62.0 – 72.0 mbsf), 32-303-3H (117.0 – 126.0 mbsf), 32-303-4H (174.0 – 183.0 mbsf), 32-304-1H (105.5 – 115.0 mbsf) and 32-304-2H (216.0 – 225.5 mbsf). Core 32-303-1H belongs to the *B. aquilonaris* Zone. Cores 32-303-2H and 32-304-1H belong to the *S. peregrina* Zone. Core 32-303-3H belongs to the late Miocene and had no discernible radiolarian zonation. Core 32-303-4H belongs to the *D. antepenultima* Zone. DSDP Sites 303 and 304 are not comparable to ODP Site 1179 because cores were not continuously recovered. These sites did not recover the boundary with the barren zone making it impossible to estimate a sedimentation rate.

At DSDP Sites 579 and 580 (Heath, Burckle et al., 1979) the cores of interest include 86-579-1H (0.0 – 8.4 mbsf) to 86-579-2H (8.4 – 17.9 mbsf), 86-579A-1H (14.0 – 23.5 mbsf) through 86-579A-15H (147.0 – 149.5 mbsf) and 86-580-1H (0.0- 3.3 mbsf) through 86-580-17H (145.8 – 155.33 mbsf). Cores 86-579-1H to 86-579-2H and 86-580-1H to 86-580-3H belong to the *B. aquilonaris* Zone. Cores 86-579A-1H to 86-579A-2H and 86-580-4H to 86-580-6H belong to the *S. universus* Zone. Cores 86-579A-3H to 86-579A-5H and 86-580-7H to 86-580-10H belong to the *E. matuyamai* Zone. Cores 86-579A-6H to 86-579A-8H and 86-580-11H to 86-580-15H contain the *L. heteroporos* Zone. Cores 86-579A-9H to 86-579A-12H and 86-580-16H to 86-580-17H contain the *S. langii* Zone. Cores 86-579A-13H to 86-579A-14H belong to the *S. peregrina* Zone. DSDP Sites 579 and 580 (Heath, Burckle et al., 1979) are comparable to ODP Site 1179 because cores were continuously recovered and radiolarian zones were determined throughout Unit A. These sites did not recover the boundary with the barren zone but it is possible to estimate a sedimentation rate because of continuous recovery.

Sites to the north of ODP Site 1179 include Sites 581 (Leg 86 (Heath, Burckle et al., 1979)) and 881 (Leg 145). A summary of the number of cores, intervals, recovery, lithology and radiolarian zonation can be found in Table 6.2. At DSDP Site 581 (Heath, Burckle et al., 1979) the cores of interest are 86-581-1H (0.0 – 1.0 mbsf) and 86-581-2H (181.5 – 191.0 mbsf) through 86-581-6H (219.5 – 229.0 mbsf). Core 86-581-1H belongs to the *B. aquilonaris* Zone. Core 86-581-2H contains the *S. langii* Zone. Cores 86-581-3H to 86-581-4H belong to the *S. peregrina* Zone. Core 86-581-5H belongs to the *D. penultima* Zone. Core 86-581-6H belongs to the *D. antepenultima* Zone. ODP Site 581 is comparable to ODP Site 1179 even though the upper part of Unit A not continuously

recovered. Radiolarian zonation was established for the lower part of Unit A and this site did recover the boundary with the barren zone making possible to estimate a sedimentation rate.

At DSDP Site 881 the cores of interest are 145-881C-1H (0.0 – 3.8) through 145-881C-39H (345.1 – 363.8 mbsf). Cores 145-881C-1H to 145-881-C-3H belong to the *B. aquilonaris* Zone. Cores 145-881-4H through 145-881-7H belong to the *S. universus* Zone. Cores 145-881C-8H through 145-881C-13H belong to the *E. matuyamai* Zone. Cores 145-881C-14H to 145-881C-25H contain the *L. heteroporos* Zone. Cores 145-881C-26H through 145-881C-30H contain the *S. langii* Zone. Cores 145-881C-31H to 145-881C-35H belong to the *S. peregrina* Zone. Core 145-881C-36H through 145-881C-39H belong to the *D. penultima* Zone. ODP Site 881 is comparable to ODP Site 1179 because cores were continuously recovered and radiolarian zones were determine throughout Unit A. This site did recover the boundary with the barren zone but it is possible to estimate a sedimentation rate.

6.4.2 Sedimentation rates of comparable DSDP and ODP Sites in the Northwest Pacific

The sedimentation rates were estimated for suitable sites (578, 579, 580, 581, 881, and 1149) in the Northwest Pacific Basin. Figure 6.5 shows the radiolarian biostratigraphy of the comparable sites and the sedimentation rates for the Quaternary, Pliocene and late Miocene sediments are given in Table 6.3.

In estimating the sedimentation rates the following ages were used for each epoch, these ages are based on the time-scale from Berggren et al. (1980) and correspond

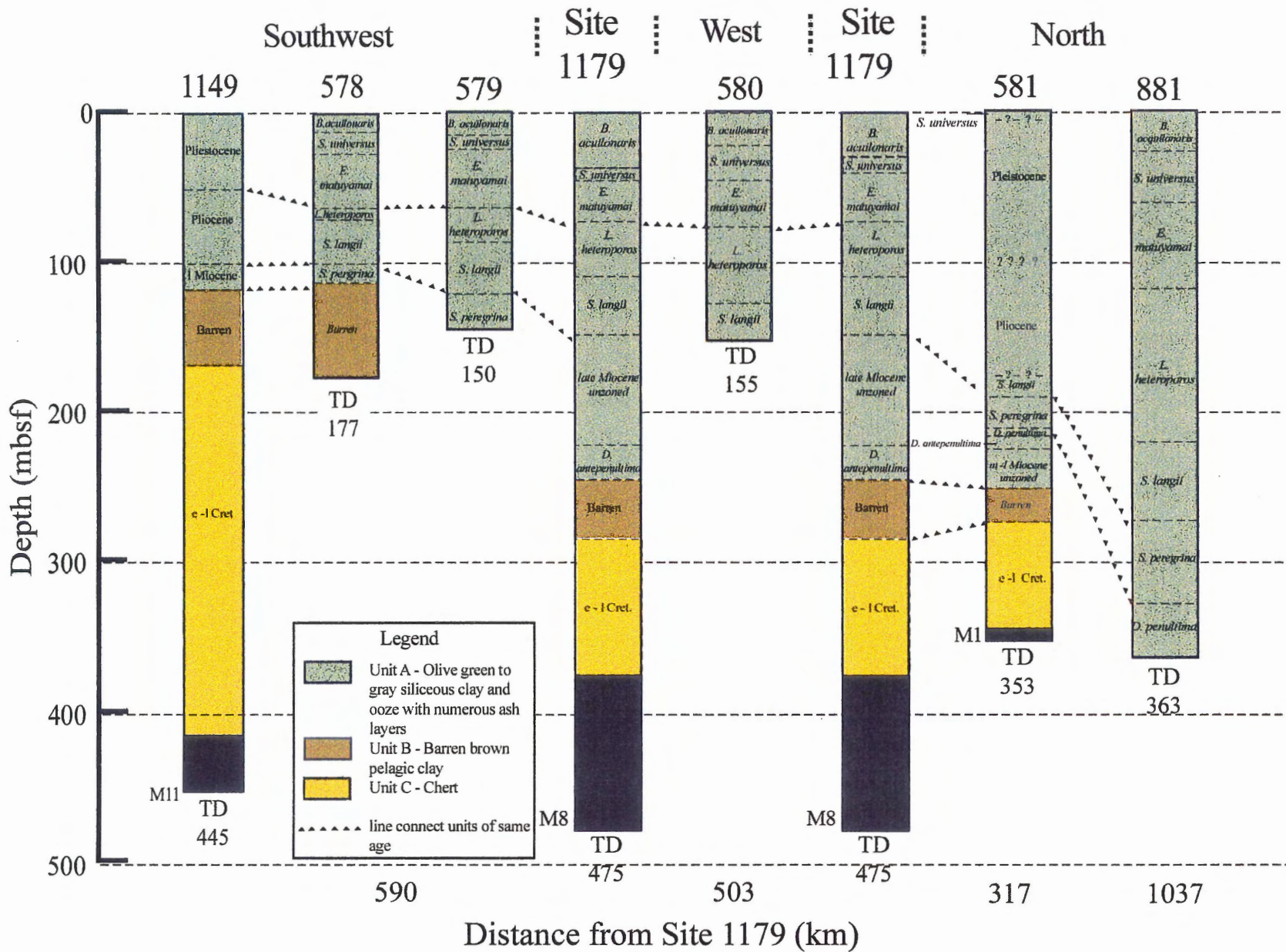


Figure 5.5 - Biostratigraphic zonation of comparable DSDP/ODP sites, Leg 6 (Heezen, Pimm et al., 1971), Leg 20 (Heezen, MacGregor et al., 1973), Leg 32 (Larson, Moberly et al., 1975), Leg 86 (Heath, Burckle et al., 1979) and ODP Leg 145, and Leg 185 (Plank, Ludden, Escutia, 2000).

to those of Nigrini and Sanfilippo (1992, 2001). The Quaternary ranges from present to 1.8 Ma. The Pliocene contains the *L. heteroporos*, *S. langii* and part of the *S. pergrina* Zones. The late Miocene/Pliocene boundary is not clearly distinguishable from the radiolarian zonation, therefore, the sedimentation rates for the Pliocene are determined strictly from the *L. heteroporos* and *S. langii* Zones ranging from 1.8 – 4.5 Ma. The late Miocene contains the part of the *S. pergrina* Zone and all of the *D. penultima* and *D. antepenultima* Zones. The late Miocene/Pliocene boundary is not clearly distinguishable from the radiolarian zonation, therefore, the sedimentation rates for the late Miocene are determined from the *S. pergrina*, *D. penultima* and *D. antepenultima* Zones ranging from 4.5 – 11.0 Ma. The same convention was used in calculating the sedimentation rates at ODP Site 1179 (see section 6.3).

The sedimentation rates during the late Miocene range from 23.1 m/Ma at the most northern site to 3.4 m/Ma at the most southern site. The sedimentation rates during the Pliocene range from 58.4 m/Ma at the most northern site to 14.0 m/Ma at the most southern site. The sedimentation rates during the Quaternary range from 65.4 m/Ma at the most northern site to 27.7 m/Ma at the most southern site. See Table 6.3 for the sedimentation rate at DSDP Sites 578, 579, 580, and 581, and ODP Sites 881, and 1149.

6.4.3 Late Miocene to Recent Paleooceanographic Changes of the Northwest Pacific Ocean

The Northwest Pacific Ocean contains three distinct water masses (Figure 6.2): (i) the subarctic, (ii) the subtropic and (iii) a transition region containing the mixed waters of the subarctic and subtropic water masses (Koizumi, 1985). The modern transition

zone lies between 40 and 42⁰N latitude (Koizumi, 1985). The water in this region is derived off the coast of Japan, where the warm Kuroshio current, which originates in the central water mass, converges with the Oyashio current, which originates in the Bering Sea and Sea of Okhotsk (Figure 6.2) (Koizumi, 1985). The mixed surface water in the transition zone moves east with the West Wind Drift (Koizumi, 1985). New data from ODP Sites in the Northwest Pacific indicate that this transition zone has had north/south fluctuations through out the Quaternary. The position of the Kuroshio/Oyashio transition zone during the late Quaternary as indicated by radiolarian data is not consistent with Koizumi (1985); it ranges from 39 to 41⁰N. This a slight drift in the apparent latitude of the Kuroshio/Oyashio convergence boundary from paleoceanographic indicators to sea surface currents to sedimentation

The subarctic region has a higher concentration of nutrient salts than the subtropic region. This is due to upwelling of the nutrient-rich deep water occurring in the center of the gyres in the subarctic region, therefore, the primary productivity in the subarctic region is higher than that of the subtropic region (Koizumi, 1985). The key controlling factor on sediment accumulation on the abyssal sea floor is plankton primary productivity not the transport of detrial sediment, this is evident from the composition of the sediments in Unit A of the Northwest Pacific Stratigraphy (Corresponding to Lithologic Units I and II of ODP Site 1179). Unit A is classified as biogenic siliceous ooze, indicating that the siliceous component (diatoms, radiolarians, and silicoflagellates) is greater than 50 %.

The initiation of Miocene biosiliceous sedimentation in the Northwest Pacific Ocean is recorded at DSDP Sites 578 and 581 and ODP Site 1179. This event marks the

time when each specific site exited the low productivity central gyre region and moved into the high productivity transition zone between the Kuroshio and Oyashio currents (Morely, 1985).

At DSDP Site 581 the onset of biosiliceous sedimentation is marked by the transition from barren pelagic clay to radiolarian bearing clay and occurs at 248.0 mbsf (Table 6.2). The radiolarian assemblage indicates we are in the middle – late Miocene *Dorcadospyris alata* Zone. At ODP Site 1179 this event is marked by the transition from barren pelagic clay to radiolarian bearing clay and occurs at 238.8 mbsf. The radiolarian assemblage indicates we are in the late Miocene *D. antepenultima* Zone. At DSDP Site 578 this event is marked by the transition from barren pelagic clay to radiolarian bearing clay and occurs at 118.8 mbsf (Table 6.2). The radiolarian assemblage indicates we are in the late Miocene – early Pliocene *S. peregrina* Zone. This shows that the initiation of Miocene biosiliceous sedimentation is transitional in the Northwest Pacific Ocean, indicating that the region of convergence between the Kuroshio and Oyashio currents began to move south during the middle Miocene.

Sedimentation rates in the Northwest Pacific Ocean give a good estimate of primary productivity rates and to the relative movement of the Kuroshio/Oyashio convergence zone after the middle Miocene. At ODP Site 881 the sedimentation rate for the late Miocene is 23.4 m/Ma (Table 6.3), this rate is significantly higher than the rates of the other DSDP and ODP sites in the North West Pacific suggesting that the Kuroshio/Oyashio convergence zone was located to the north of this site during the late Miocene (Figure 6.6). The sedimentation rate at DSDP Site 581 and ODP Sites 1179 and 1149 were 11.1m/Ma, 13 m/Ma and 3.4m/Ma, respectively. This suggests that the

Epoch	1149	578	579	580	581	881
Quaternary	27.7 m/Ma	34.3 m/Ma	34.1 m/Ma	49.3 m/Ma	42.4 m /Ma	65.4 m/Ma
Pliocene	14.0 m/Ma	11.7 m/Ma	19.5 m/Ma	19.5 m/Ma		58.4 m/Ma
late Miocene	3.4 m/Ma	-----	-----	-----	11.1 m/Ma	24.3 m/Ma

Table 6.3 – Sedimentation rates in the Northwest Pacific Basin during the late Miocene, Pliocene and Quaternary.

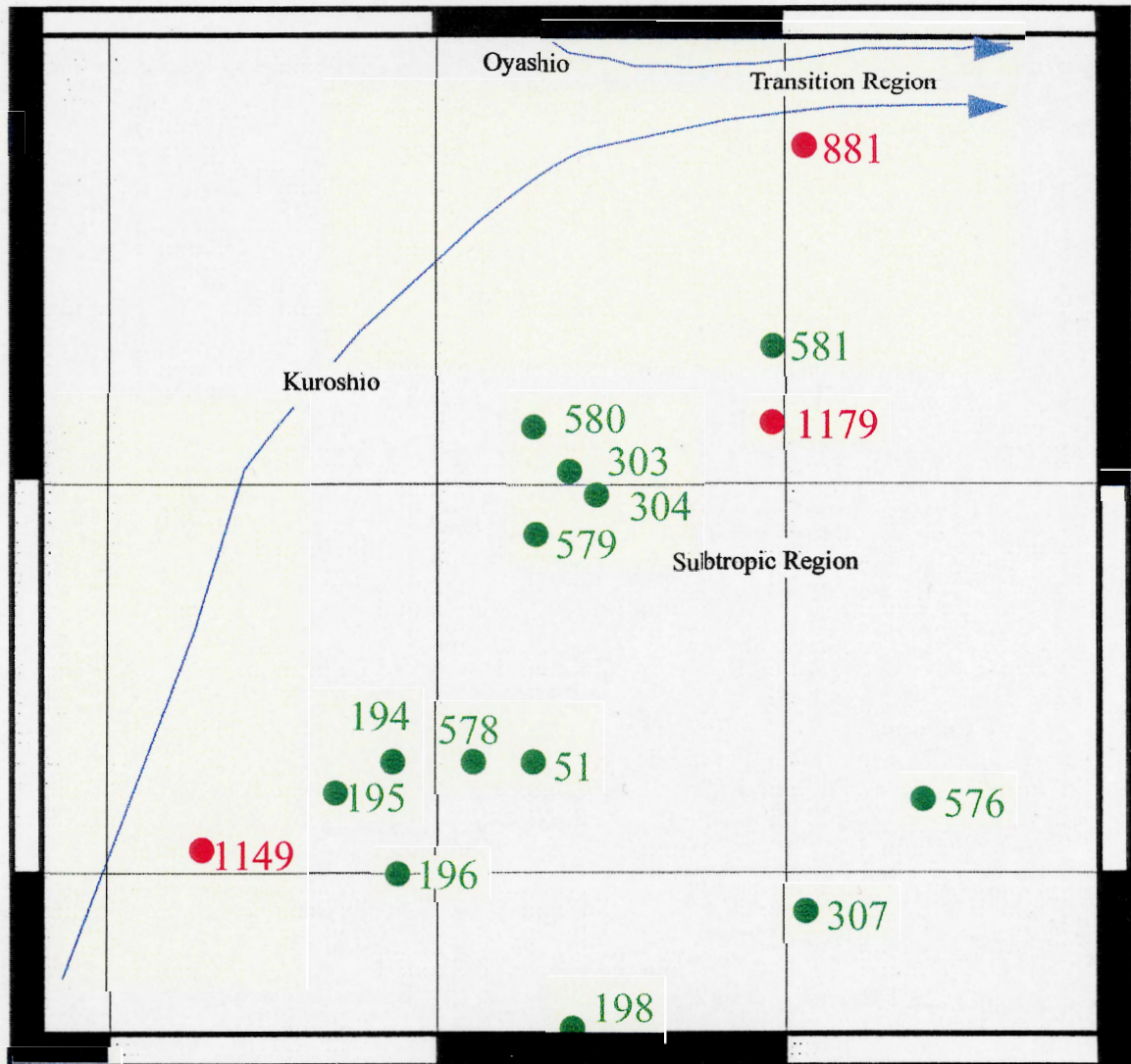


Figure 6.6 - Map showing relative location of DSDP/ODP sites drilled on the abyssal seafloor in the Northwest Pacific Basin and the relative location of the Kuroshio and Oyashio Current convergence during the late Miocene.

convergence boundary was north of Site 1179 (Figure 6.6). The extremely low sedimentation rate of ODP Site 1149 is caused by its proximity to the subtropic gyre region during the late Miocene.

During the Pliocene the Kuroshio/Oyashio convergence boundary continued to move southward. Evidence for the southward movement of the transition zone can be found at DSDP Site 581. The sedimentation rate at this site increases dramatically from 11.1 m/Ma for the late Miocene to 42.4 m/Ma for the Pliocene through Quaternary. This sedimentation rate suggests that the transition zone has moved past DSDP Site 581 but is not very far away from it (Figure 6.7). This is evident because the sedimentation rate for the Pliocene through Quaternary at ODP Site 881 is 62.2 m/Ma, if the transition zone had moved well past DSDP Site 581 you would expect the sedimentation rate to be similar to ODP Site 881. The convergence boundary during the Pliocene was centered around ODP Site 1179 (Figure 6.7) suggested by a sedimentation rate higher than the sites to the west and south. ODP Site 1179 has a sedimentation rate of 34 m/Ma through the Pliocene where as DSDP Sites 579 and 580 have a sedimentation rate of 19.5 m/Ma and DSDP Site 578 has a sedimentation rate of 11.7 m/Ma.

The Kuroshio/Oyashio convergence boundary has undergone fluctuations since the Pliocene, even though the changes in the average rate of sedimentation through the Quaternary is similar at DSDP Sites 578 and 579 and ODP Site 1179. The rate of sedimentation at DSDP Sites 578 and 579 is roughly 34 m/Ma and at ODP Site 1179 is roughly 36 m/Ma. The rate of sedimentation at DSDP Site 580 is 49.3 m/Ma, an indication that the convergence zone boundary is just south of this site during the Quaternary.

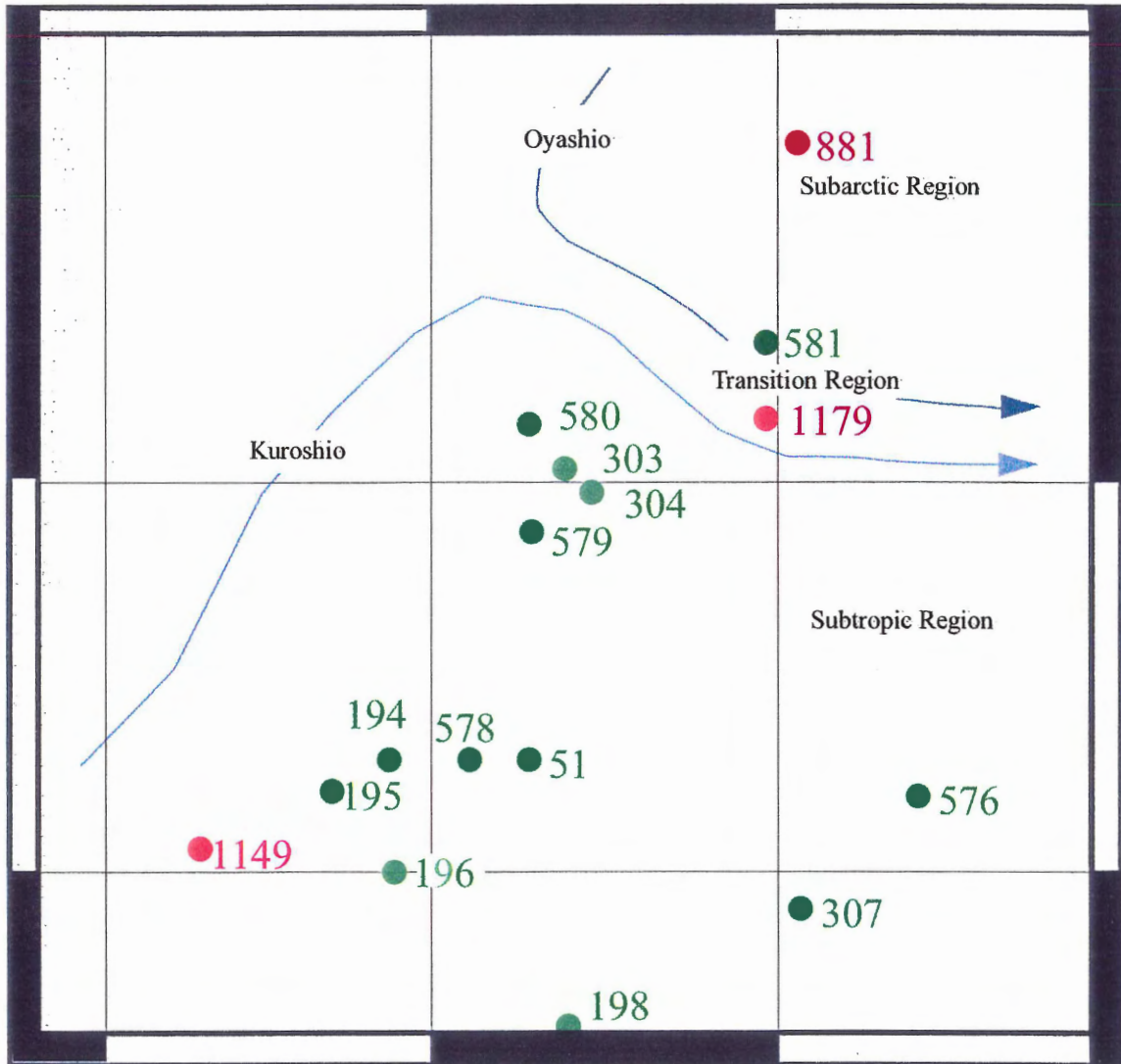


Figure 6.7 - Map showing the relative location of DSDP/ODP sites drilled on the abyssal seafloor in the Northwest Pacific Basin and the relative location of the Kuroshio and Oyashio Current convergence during the Pliocene.

Fluctuations in the position of the transition zone are evident upon close examination of the radiolarian zones at DSDP Sites 578, 579, and 580 and ODP Site 1179. During the early Quaternary *E. matuyamai* Zone (1.0 – 1.8 Ma) the rate of sedimentation is similar at DSDP Sites 578, 579, and 580 (Figure 6.5); there are roughly 29 m of sediment in this zone, suggesting a sedimentation rate of about 36 m/Ma. At ODP Site 1179 the rate of sedimentation is lower, there are roughly 13 m of sediment deposited in the *E. matuyamai* Zone suggesting a sedimentation rate of about 16.25 m/Ma. This indicates that the transition zone moved to the north of ODP Site 1179 but was centered around DSDP Site 578, 579 and 580 (Figure 6.8). The middle Quaternary *S. universus* Zone (0.46 – 1.0 Ma) at DSDP Sites 578, 579 and ODP site 1179 had roughly 18 m of sediment was deposited in this zone suggesting a sedimentation rate of roughly 33 m/Ma. This intermediate rate of sedimentation indicated that this area remained in the transition zone the middle Quaternary (Figure 6.9). DSDP Site 580 has roughly 30 m of the *S. universus* Zone, this is double the amount of sediment present at sites to the south and west indicating a sedimentation rate of about 57 m/Ma. The convergence zone boundary during the middle Quaternary is located to the south of DSDP Site 580 (Figure 6.9). The early Quaternary *B. aquilonaris* Zone (present – 0.46Ma) remains of constant thickness, roughly 10 m, at DSDP Sites 578 and 579 suggesting a rate of 21 m/Ma. This is an indication that they remain closer to the central gyre (Figure 6.10). DSDP Site 580 and ODP Site 1179 has roughly 25 m of sediment deposited in the *B. aquilonaris* Zone, suggesting a sedimentation rate of about 54 m/Ma. This indicates that these sites are located in the subarctic region and the transition zone is located to the south (Figure 6.10).

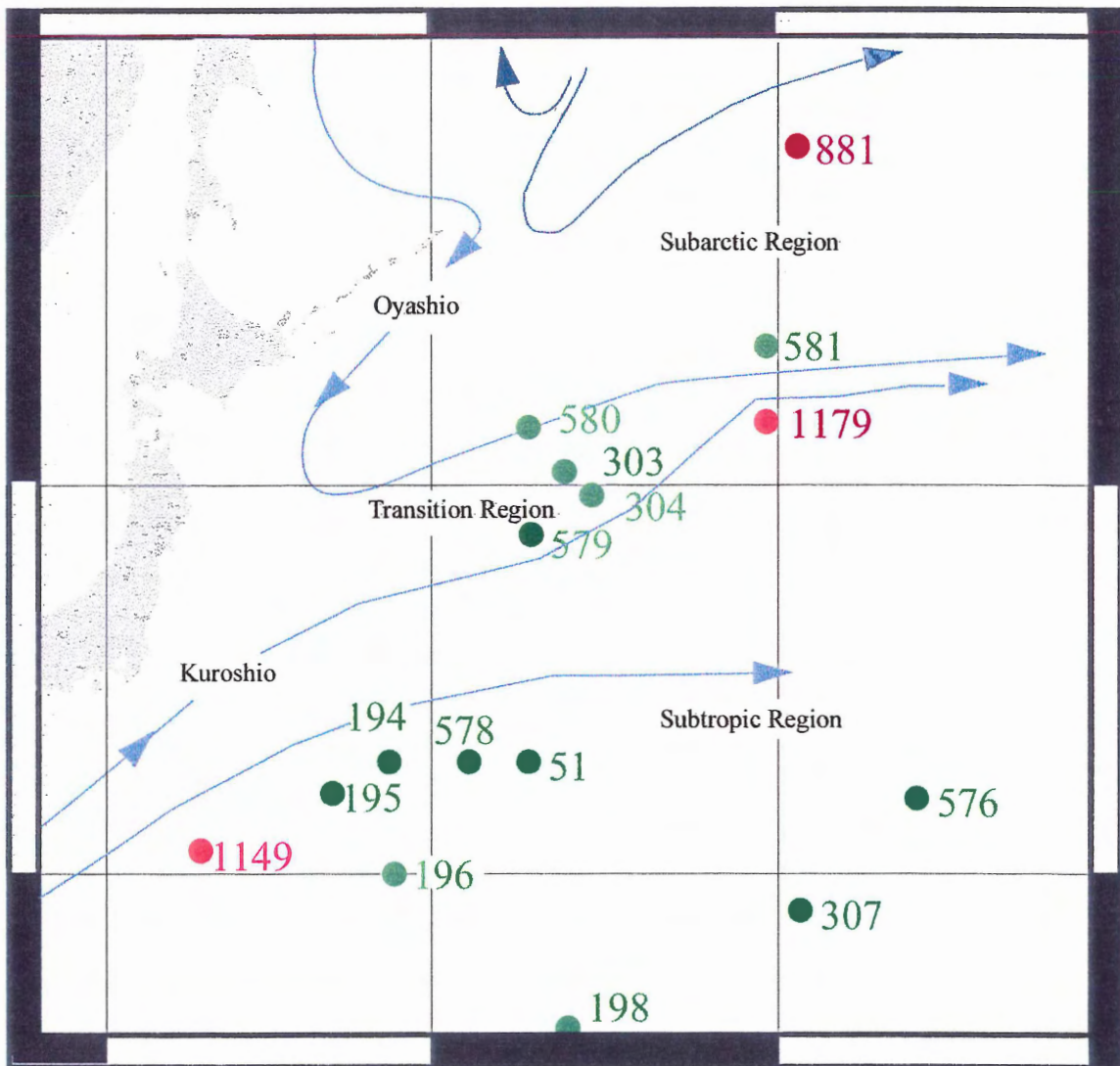


Figure 6.8 - Map showing the relative location of DSDP/ODP sites drilled on the abyssal seafloor in the Northwest Pacific Basin and the relative location of the modern Kuroshio and Oyashio Currents during the early Quaternary.

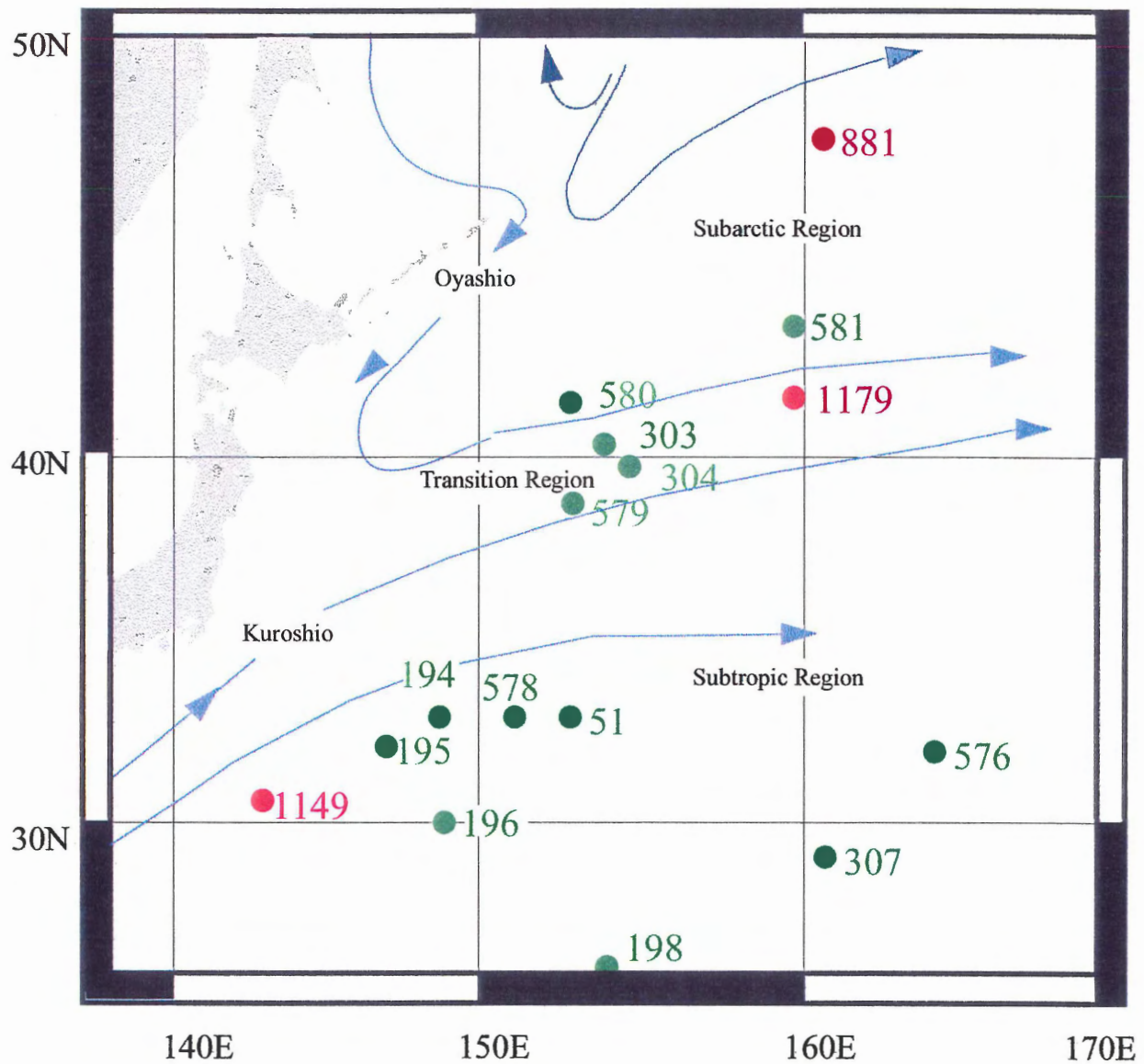


Figure 6.9 - Map showing location of DSDP/ODP sites drilled on the abyssal seafloor in the Northwest Pacific Basin and the location of the modern Kuroshio and Oyashio Currents during the middle Quaternary.

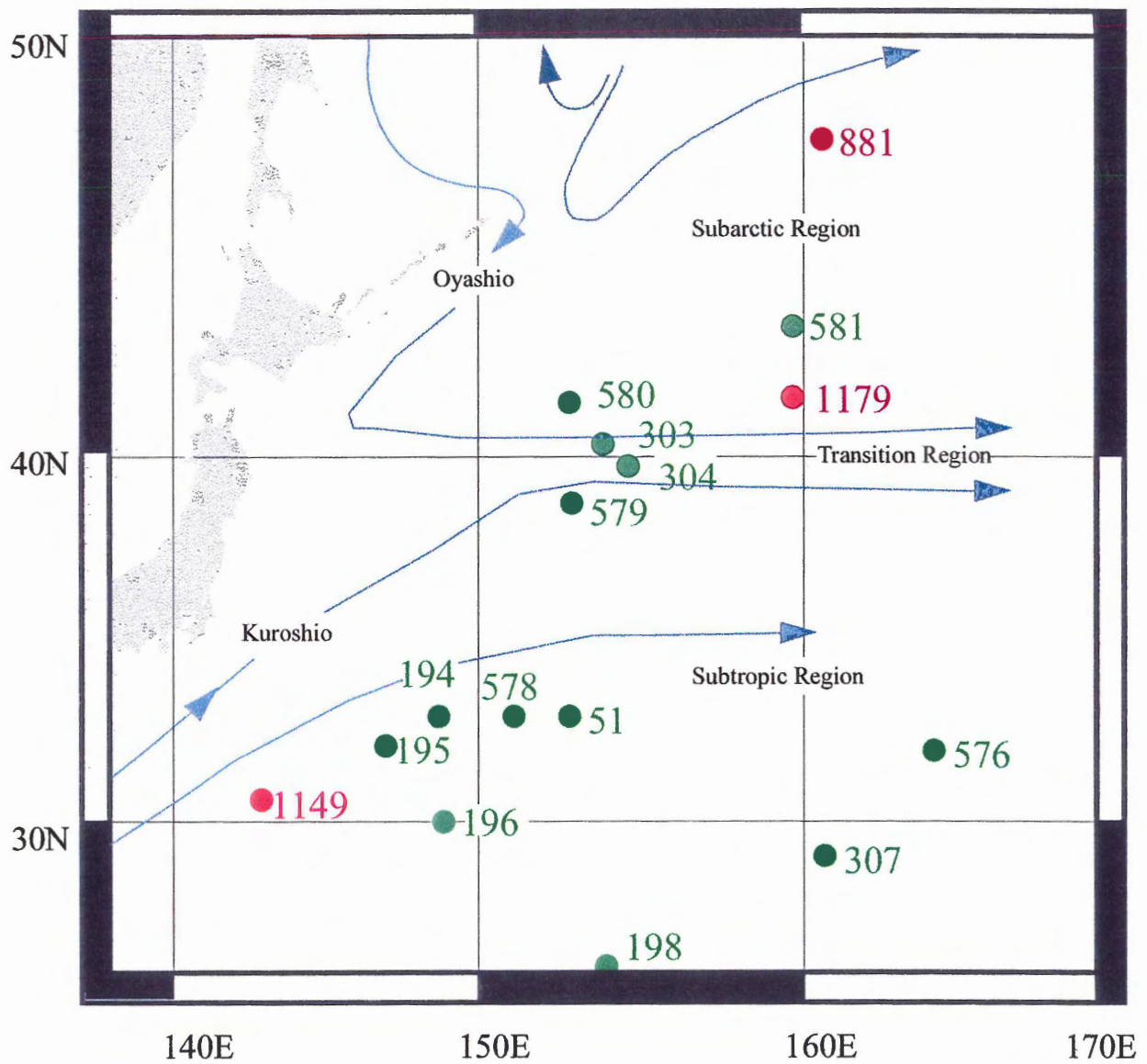


Figure .10 - Map showing location of DSDP/ODP sites drilled on the abyssal seafloor in the Northwest Pacific Basin and the location of the modern Kuroshio and Oyashio Currents during the late Quaternary.

Chapter Seven – Conclusions

Five radiolarian zones and one unzoned section were observed from core-catcher samples at ODP Site 1179. The data indicate that the soft sediments recovered from Unit A range from late Miocene to Recent. The radiolaria biostratigraphy of ODP Site 1179 yielded reliable results even though only core-catcher samples were studied for analysis, as seen by the comparison of the radiolarian based sedimentation rates and those based on the magnetostratigraphy of the site.

Many of the sites (194, 195, 196, 198, 303, 304, 307, 581) drilled in the Northwest Pacific Basin did not yield continuous sections, only small portions of the core were recovered and the rest of the core was washed. Correlation between the radiolarian zones is not because the thickness of the zones is uncertain. The more recently drilled sites (578, 579, 580, 581, 881, and 1149) are continuous and have comparable radiolarian zonations allowing for estimates of sedimentation rates from the late Miocene to Quaternary. The sedimentation rates during the late Miocene range from 23.1 m/Ma at the most northern site to 3.4 m/Ma at the most southern site. The sedimentation rates during the Pliocene range from 58.4 m/Ma at the most northern site to 14.0 m/Ma at the most southern site. The sedimentation rates during the Quaternary range from 65.4 m/Ma at the most northern site to 27.7 m/Ma at the most southern site.

The initiation of Miocene biosiliceous sedimentation in the Northwest Pacific Ocean as recorded at DSDP Sites 578 and 581 and ODP Site 1179 indicates that this event was diachronous. The onset of biosiliceous sedimentation began in the middle Miocene at DSDP Site 581 and moved southward during the late Miocene. Since this time the

Kuroshio/Oyashio transition zone has been migrating north and south and the current path does not move straight to the east, instead its path is curved..

The position of the Kuroshio/Oyashio transition zone during the late Quaternary as indicated by radiolarian data occurs between 39 to 41⁰N, this is not consistent with Koizumi (1985). This a slight drift in the apparent latitude of the Kuroshio/Oyashio convergence boundary from paleoceanographic indicators to sea surface currents to sedimentation

Systematic Taxonomy

The information for this section is a combination of citations from several sources. The bulk of the systematic classification of radiolarians comes from Nigrini & Sanfilippo (1992, 2001) and Takahashi (1991).

Kingdom PROTISTA Haeckel, 1866
 Phylum SARCONDINA Hertwig and Lesser, 1874
 Class ACTINOPODIA Calkins, 1909
 Subclass RADIOLARIA Müller, 1858
 Order POLYCYSTINA Ehrenburg, 1875
 Suborder SPUMELLARIA Ehrenburg, 1875
 Family COLLOSPHAERIDAE Müller, 1858

Definition: Lattice-shelled colonial spumellarians (Riedel, 1971). Lower Miocene to Recent. (Casey, 1993)

Genus *Acrosphaera* Haeckel, 1881

Acrosphaera spinosa Haeckel *longispina* Takahashi

Acrosphaera spinosa Haeckel, 1881; Popofsky, 1917, p. 253, fig. 16;
 Strelkov and Reshetnyak, 1971, p. 340, pl. 6, figs. 39, 41.

Polysolenia flammabunda Haeckel, 1881; Nigrini, 1967, p. 15, pl. 1, fig. 2;
 Nigrini and Moore, 1979, p. S13, pl. 2, fig. 2.

Acrosphaera flammabunda Haeckel, 1881; Johnson and Nigrini, 1980, p. 116, pl. 1, fig. 1

Acrosphaera spinosa longispina Takahashi, 1991, p. 53, pl. 1, figs. 1, 4.

Genus *Collosphaera* Müller, 1855

Collosphaera huxleyi (Huxleyi)

Thalassicola punctata Huxleyi, 1851, p. 434, pl. 14, fig. 6.

Collosphaera huxleyi Müller, 1855, p. 238; Müller, 1858, p. 55, pl. 8, figs. 6-9; Popofsky, 1917, p. 241, pl. 13, figs. 1-9; Strelkov and Reshetnyak, 1971, p. 332, pl. 4, figs. 21, 23; Boltovskoy and Riedel, 1980, p. 103, pl. 1, fig. 5.

Family ACTINOMMIDEA Haeckel, 1862; emend. Sanfilippo and Riedel, 1980

Definition: Solitary spumellarians, spherical to ellipsoidal tests or modifications there of, but not discoidal or equatorially constricted ellipsoids. Paleozoic?, Triassic to Recent. (Casey, 1993)

Genus *Stylacontarium* Popofsky, 1912

Stylacontarium aquilonium Kling

Drupptractus aquilonius Hays, 1970, p. 214, pl. 1, figs. 4-5; Ling, 1975, p. 717, pl.1, figs. 17-18.

Stylacontarium aquilonium Kling, 1973, p.634, pl. 1, figs. 1-4; Ling, 1973, p. 777, pl.1. figs. 6-7.

Genus *Stylatractus* Haeckel 1887

Stylatractus universus Hays

Stylatractus sp. Hays, 1965, p. 167, pl. 1. fig. 6.

Stylatractus universus Hays, 1970, p. 215, pl. 1, figs. 1-2.

Subfamily ARTISCINAE Haeckel 1881, emend. Riedel 1967b

Definition: Elliptical cortical lattice shelled with equatorial constriction and caps. Oligocene to Recent (Casey, 1993)

Genus *Diartus* Sanfilippo and Riedel 1980

Diartus hughesi (Campbell and Clark)

Ommatocampe hughesi Campbell and Clark, 1944, p.23, pl.3, fig.12; Riedel and Sanfilippo, 1970, p.521

Diartus hughesi Sanfilippo and Riedel, 1980, p.1010

Diartus petterssoni (Riedel and Funnell)

Camartus(?) petterssoni conditional manuscript name proposed in Riedel and Funnell, 1964, p.310; Riedel and Sanfilippo, 1970, p.520, pl.14, fig.3

Diartus petterssoni Sanfilippo and Riedel, 1980, p.1010

Genus *Didymocyrtis* Haeckel 1860*Didymocyrtis antepenultima* (Riedel and Funnell)

Panarium antepenultimum conditional manuscript name proposed by
Riedel and Funnell, 1964, p.311

Ommatartus antepenultimus Riedel and Sanfilippo, 1970, p.521, pl.14,
fig.4

Didymocyrtis antepenultima Sanfilippo and Riedel, 1980, p.1010

Didymocyrtis penultima (Riedel and Funnell)

Panarium penultimum Riedel, 1957, p.76, pl.1, fig.1; Riedel and Funnell,
1964, p.311

Ommatartus penultimus sensu stricto, Riedel and Sanfilippo, 1970, p.521

Didymocyrtis penultima Sanfilippo and Riedel, 1980, p.1010

Didymocyrtis tetrathalamus Haeckel *tetrathalamus* Nigrini

Panartus tetrathalamus Haeckel, 1887, p.378, pl.40, fig.3; Nigrini, 1967,
p.30, pl.2, figs.4a-4d (with synonymy)

Panartus tetrathalamus tetrathalamus Nigrini, 1970, p.168, pl.1, fig.12

Didymocyrtis tetrathalamus tetrathalamus Sanfilippo and Riedel, 1980,
p.1010

Family SPONGODISCISAE Haeckel 1862, emend. Riedel 1967b

Definition: Group of spongy and discoidal nature. Devonian to Recent (Casey, 1993).

Genus *Amphiropalum* Haeckel 1887, emend. Nigrini 1967*Amphiropalum ypsilon* Haeckel

Amphiropalum ypsilon Haeckel, 1887, p.522; Nigrini, 1967, p.35, pl. 3,
3a-d.

Family PYLONIIDDAE Haeckel 1881

Definition: Ellipsoid test of girdles with holes. Eocene to Recent (Casey, 1993).

Genus *Sphaeropyle* Dreyer 1889*Sphaeropyle langii* Dreyer

Sphaeropyle langii Dreyer, 1889, p.13, pl.4, fig.54; Kling, 1973, p.634, pl.1, figs.5-10, pl.13, figs.6-8 (with synonymy); Foreman, 1975, p.618, pl.9, figs.30-31 (with synonymy)

Sphaeropyle robusta Kling

Sphaeropyle robusta Kling, 1973, p.634, pl.1, figs.11-12, pl.6, figs.9-13, pl.13, figs.1-5

Order NASSELARIA Ehrenberg 1875

Suborder CYRTIDA Haeckel 1862, emend. Petrushevskaya 1971

Family THEOPERIDAE Haeckel 1881, emend. Riedel 1967b

Genus *Cycladophoria* Ehrenberg 1838*Cycladophora davisoni* Ehrenberg *davisoni* Petrushevskaya

Cycladophora(?) davisoni Ehrenberg, 1871, p. 297.

Theocalyptra davisoni Riedel, 1958, p. 239, pl. 4, figs. 2,3; Nigrini and Moore, 1979, p. N59, pl. 24, figs. 2a, 2b

Cycladophora davisoni davisoni Petrushevskaya, 1967, p. 122, pl. 69, figs. I-VIII; Ling, 1973, p. 780, pl.2, fig. 2.

Genus *Eucyrtidium* Ehrenberg 1847b, emend. Nigrini 1967*Eucyrtidium calvertense* Martin

Eucyrtidium calvertense Martin, 1904, p.450, pl.130, fig.5; Hays, 1965, p.181, pl.III, fig.6

Eucyrtidium matuyamai Hays

Eucyrtidium matuyamai Hays, 1970, p.213, pl.1, figs.7-9

Genus *Stichocorys* Haeckel 1881*Stichocorys delemontensis* (Cambell and Clark)

Eucyrtidium delmontense Campbell and Clark, 1944, p.56, pl.7, figs.19-20

Stichocorys delmontensis Sanfilippo and Riedel, 1970, p.451, pl.1, fig.9
(with synonymy)

Stichocorys pergrina Sanfilippo and Riedel

Eucyrtidium elongatum peregrinum Riedel, 1953, p.812, pl.85, fig.2;
Riedel, 1957, p.94

Stichocorys peregrina Sanfilippo and Riedel, 1970, p.451, pl.1, fig.10;
Westberg and Riedel, 1978, p.22, pl.3, figs.6-9

Family Pterocorythidae Haeckel 1881, emend. Riedel 1967b, emend. Moore 1972

Genus *Lamprocyrtis* Kling 1973

Lamprocyrtis heteroporos (Hays)

Lamprocyclas heteroporos Hays, 1970, p.214, pl.1, fig.3

Lamprocyrtis heteroporos Kling, 1973, p.639, pl.5, figs.19-21, pl.15, fig.6

Lamprocyrtis neoheteroporos Kling

Lamprocyrtis neoheteroporos Kling, 1973, p.639, pl.5, figs.17-18, pl.15,
figs.4-5

Lamprocyrtis nigrinae Caulet

Conarachnium ? sp. Nigrini, 1968, p.56, pl.1, fig.5a (partim.)

?*Conarachnium*? sp. Nigrini, 1968, p.56, pl.1, fig.5b (partim.)

Lamprocyrtis nigrinae Caulet, 1971, p.3, pl.3, figs.1-4, pl.4, figs.1-4

Family ARTOSTROBIIDAE Riedel 1967a, emend. Foreman 1973

Definition: Tube like cephalis with many postcephalic chambers. Cretaceous to Recent.

Genus *Botryostobus* Haeckel 1887, emend. Nigrini 1977

Botryostobus aquilonaris (Bailey)

Eucyrtidium aquilonaris Bailey, 1856, p.4, pl.1, fig.9

Artostrobium miralestensis Riedel & Sanfilippo, 1971, p.1599, pl.1H,
figs.9-13 (partim.); Kling, 1973, p.639, pl.5, figs.31-34 (partim.)

Botryostobus aquilonaris Nigrini, 1977, p.246, pl.1, fig.1 (with
synonymy)

References

- Anderson, O.R., 1983. *Radiolaria*. New York: Springer-Verlag, 355 pp.
- Bailey, J.W., 1856. Notice of microscopic forms found in the soundings of the Sea of Kamtschatka-with a plate. *Am. J. Sci. Arts, Ser. 2*, 22:1-6.
- Berggren, W.A., Burckle, L.H., Cita, M.B., Cooke, H.B.S., Funnell, B.M., Gartner, S., Hays, J.D., Kennett, J.P., Opdyke, N.D., Pastouret, L., Shackleton, N.J., and Takayanagi, Y., 1980. Towards a Quaternary time scale. *Quat. Res.*, 13:277-302.
- Boltovskoy, D. and Riedel, W. R., 1980. Polycystine radiolaria from the southwestern Atlantic Ocean plankton. *Revista Española de Micropaleontología*, 23 (1): 114-126.
- Calkins, G.N., 1909. *Protozoology*, Lea and Feboger Co., New York, 339 pp.
- Campbell, A.S., and Clark, B.L., 1944. Miocene radiolarian faunas from Southern California. *Spec. Pap. Geol. Soc. Am.*, 51:1-76.
- Casey, R.E., 1971. Radiolarian as past and present water-masses in Funnell, B.M. and Riedel, W.R. (eds.) *The Micropaleontology of Oceans*. Cambridge University Press, Cambridge.
- Casey, R.E., 1993. Radiolaria in Lipps, J.H. ed (1993) *Fossil Prokaryotes and Protists*. Cambridge, Blackwell Scientific Publication.
- Caulet, J.-P., 1971. Contribution a l'étude de quelques Radiolaires Nassellaires des boues de la Méditerranée et du Pacifique (Study of some nassellarian Radiolaria from Mediterranean and Pacific sediments). Archives originale, Centre de Documentation, C.N.R.S., No. 498. *Cah. Micropaleontol., Ser. 2*, 10:1-10.
- Caulet, J.P., 1986. Radiolarians from the southwest Pacific in Kennett, J.P., von der Borch, C.C., et al., *Init. Repts. DSDP*, 90: Washington (U.S. Govt. Printing Office), 835-861.
- Dreyer, F., 1889. Morphologische Radiolarienstudien. 1. Die Pylombildungen in vergleichend-anatomischer und entwicklungsgeschichtlicher Beziehung bei Radiolarien und bei Protisten überhaupt, nebst System und Beschreibung neuer und der bis jetzt bekannten pylomatischen Spumellarien. *Jena. Z. Naturwiss.*, 23:1-138.
- Ehrenberg, C.G., 1872b. Mikrogeologische Studien über das kleinste Leben der Meeres-Tiefgrunde aller Zonen und dessen geologischen Einfluss. *Abh. K. Akad. Wiss. Berlin*, 131-399.

- Ehrenberg, C.G., 1847. Beobachtungen über die mikroskopischen kieselschaligen Polycystinen als mächtige Gebirgsmasse von Barbados und über das Verhältniss der aus mehr als 300 Neuen Arten bestehenden ganz eigenthümlichen Formengruppe jener Felsmasse zu den jetzt lebenden Thieren und zur Kreidebildung. Eine neue Anregung zur Erforschung des Erdlebens. K. Preuss. Akad. Wiss. Berlin, Monatsberichte, Jahre
- Ehrenberg, C.G., 1860. Über den Tiefgründ des stillen Oceans zwischen Californien und den Sandwich-Inseln aus bis 15600' Tiefe nach Lieutenant Brooke. K. Preuss. Akad. Wiss. Berlin, Monatsberichte, Jahre 1860: 819-833.
- Ehrenberg, C.G., 1875. Fortsetzung der mikrogeologischen Studien als Gesamt-Uebersicht der mikroskopischen Paläontologie gleichartig analysirter Gebirgsarten der Erde, mit specieller Rücksicht auf den Polycystinen-Mergel von Barbados. Abh. K. Akad. Wiss. Berlin, 1875: 1-225.
- Ewing, J., Ewing, M., Aitken, T., and Ludwig, W.J., 1968. North Pacific sediment layers measured by seismic profiling in Knopoff, L., Drake, C.L. and Hart, P.J. (eds) *The Crust and Upper Mantle of the Pacific Area*. Geophys. Monogr. Ser., Am. Geophys. Union, 12: 147-173.
- Foreman, H.P., 1975. Radiolarians from the North Pacific, Deep Sea Drilling Project, Leg 32. in Larson, R.L., Moberly, R., and the Leg 32 Scientific Party, *Init. Repts. DSDP*, 32: Washngton (U.S. Govt. Printing Office), 572-676.
- Gradstein, F.M., Agterberg, F.P., Ogg, J.G., Hardenbol, J., van Veen, P., Thierry, J. and Huang, Z., 1994. A Mesozoic Time Scale. *J. Geophys. Res.*, 99: 24051-24074.
- Hays, J.D., 1965. Radiolaria and late Tertiary and Quaternary history of Antarctic Seas. in Llano, G.A. (Ed.), *Biology of Antarctic Seas II*. American Geophysical Union, Antarctic Research 5: 125-184.
- Hays, J.D., 1970. Stratigraphy and evolutionary trends of radiolarians in North Pacific deep sediments. In Hays, J.D. (Ed.), *Geological Investigations of the North Pacific*. Mem. - Geol. Soc. Am., 126: 185-218.
- Haeckel, E., 1860. Fernere Abbildungen und Diagnosen neuer Gattungen und Arten von lebenden Radiolarien des Mittelmeeres (Supplementary illustrations and diagnosis of new genera and species of living radiolarians of the Mediterranean Sea). K. Preuss. Akad. Wiss. Berlin, Monatsberichte, 835-845.
- Haeckel, E., 1862. *Die Radiolarien (Rhizopoda Radiolaria)* Berlin (Reimer).
- Haeckel, E., 1866. *Generelle Morphologie der Organismen*, 2, Berlin (Reimer).

- Haeckel, E., 1881. Entwurf eines Radiolarien-Systems auf Grund von Studien der Challenger-Radiolarien (Basis for a radiolarian classification from the study of Radiolaria of the Challenger collection). *Jena. Z. Med. Naturwiss.*, 15 (Vol. 8, Pt. 3):418-472.
- Haeckel, E., 1887. Report on the Radiolaria collected by H.M.S. Challenger during the years 1873-1876. *Rep. Sci. Results Voy. H.M.S. Challenger, 1873-1876, Zool.*, 18:1-1803.
- Heath, G.R., Burckle, L.H. and the Leg 86 Scientific Party, 1979. *Init. Repts. DSDP*, 86: Washington (U.S. Govt. Printing Office).
- Hetwigg, R. and Lesser, E., 1874. Der Organismus der Radiolarien, *Jena*, Fisher, G., pp. 1-149. Organesmen, *Arch. Mikr. Anat.*, 10(Suppl.): 35-243.
- Heezen, B.C., MacGregor, I. D. and the Leg 20 Scientific Party, 1973. *Init. Repts. DSDP*, 20: Washington (U.S. Govt. Printing Office).
- Heezen, B.C., Pimm, A.C. and the Leg 6 Scientific Party, 1971. *Init. Repts. DSDP*, 6: Washington (U.S. Govt. Printing Office).
- Huesser, L.E. and Morley, J.J., 1996. Pliocene climate of Japan and environs between 4.8 and 2.8 Ma: a joint pollen and marine faunal study. *Marine Micropaleontology*, 27:85-106.
- Huxley, Th., 1851. Zoological notes and observations made onboard the H.M.S. "Rattlesnake." III. Upon *Thalassicolla* a new Zoophyte. *Ann. Mag. Nat. Hist., London, Ser. 2*, 8: 433-442.
- Johnson, D.A., and Nigrini, C., 1980. Radiolarian biogeography in surface sediments of the western Indian Ocean. *Mar. Micropaleontol.*, 5:111-152.
- Kanazawa, T., Sager, W. and the Shipboard Scientific Party of Leg 191, 2000. *Preliminary Summary of Drilling Results: Ocean Drilling Program Leg 191*. Submitted.
- Kling, S.A., 1973. Radiolaria from the eastern North Pacific, Deep Sea Drilling Project, Leg 18. in Kulm, L.D., von Huene, R., et al., *Init. Repts. DSDP*, 18: Washington (U.S. Govt. Printing Office), 617-671.
- Kiozumi, I., 1985. Late Neogene Paleooceanography in the Western North Pacific in Heath, G.R., Burckle, L.H., et al., *Init. Repts. DSDP*, 86: Washington (U.S. Govt. Printing Office), 429-438.
- Larson, R.L., Moberly, R. and the Leg 32 Scientific Party, 1975. *Init. Repts. DSDP*, 32: Washington (U.S. Govt. Printing Office).

- Larson, R.L., Steiner, M.B., Erba, E., and Lancelot, Y., 1992. Paleolatitude and tectonic reconstructions of the oldest portion of the Pacific plate: A comparative study. *Proc. ODP Sci. Res.*, 129:615-631.
- Martin, G.C., 1904. Radiolaria in Clark, W.B., Eastman, C.R., Glenn, L.C., Bagg, R.M., Bassler, R.S., Boyer, C.S., Case, E.C., and Hollick, C.A. eds., *Systematic Paleontology of the Miocene Deposits of Maryland: Baltimore*. Maryland Geol. Surv., Johns Hopkins Press, 447-459.
- Moore, T.C., 1972. Mid-Tertiary evolution of the radiolarian genus *Calocycletta*. *Micropaleontology*, 18:144-152.
- Morely, J.J., 1985. Radiolarians from the Northwest Pacific, Deep Sea Drilling Project Leg 86 in Heath, G.R., Burckle, L.H., et al., *Init. Repts. DSDP*, 86: Washington (U.S. Govt. Printing Office), 399-428.
- Morely, J.J. and Hays, J.D., 1979. Comparison of Glacial and Interglacial Oceanographic Conditions in the South Atlantic from Variations in Calicum Carbonate and Radiolarian Distributions. *Quaternary Research*, 12:396-408.
- Müller, J., 1855. Über Sphaerozoum und Thalassicolla. Königl. Preuss. Akad. Wiss. Berlin, Bericht, 229-253.
- Müller, J., 1858. Über die Thalassicollen, Polycystinen und Acanthometren des Mittelmeeres. K. Preuss. Akad. Wiss. Berlin, Abh., 1-62.
- Nakanishi, M., Sager, W.W. and Klaus, A., 1999. Magnetic lineations within Shatsky Rise, northwest Pacific Ocean: Implications for hot-spot triple junction interaction and ocean plateau formation. *J. Geophys. Res.*, 104: 7539-7556.
- Nigrini, C., 1967. Radiolaria in pelagic sediments from the Indian and Atlantic Oceans. *Bull. Scripps Inst. Oceanogr.*, 11:1-125.
- Nigrini, C., 1970. Radiolarian assemblages in the North Pacific and their application to a study of Quaternary sediments in core V20-130 in Hays, J.D. ed., *Geological Investigations of the North Pacific*. Mem. Geol. Soc. Am., 126:139-183.
- Nigrini, C., and Moore, T.C., 1979. *A Guide to Modern Radiolaria*. Spec. Publ. Cushman Found. Foraminiferal Res., 16.
- Nigrini, C. and Sanfilippo, A., 1992. *Cenozoic radiolarian stratigraphy for low and middle latitudes with descriptions of biomarkers and stratigraphically useful species*, ODP Tech. Note.

- Nigrini, C. and Sanfilippo, A., 2001. *Cenozoic radiolarian stratigraphy for low and middle latitudes with descriptions of biomarkers and stratigraphically useful species*, ODP Tech. Note, 27 [Online]. Available from World Wide Web: <<http://www-odp.tamu.edu/publications/tnotes/tn27/index.html>>. [Cited 2001-02 16]
- Petrushevskaya, M.G., 1971. *Radiolyarii Nassellaria v planktone Mirovogo Okeana (Radiolarians of the Ocean)*. Issled. Fauny Morei, 9:1-294.
- Plank, T., Ludden, J.N., Escutia, C., and Shipboard Scientific Party, 2000. *Proc. ODP, Init. Repts.*, 185: College Station, TX (Ocean Drilling Program).
- Popofsky, A., 1912. Die Sphaerellarien des warmwassergebietes. *Deutsche Sudpolar-Expedition 1901-1903*, 1901-1903, Zoologie, 13 (Vol. 5):73-159.
- Popofsky, A., 1917. Die Collosphaeriden, mit Nachtrag zu den Spumellarien und Nassellarien. *Deutsche Sudpolar-Expedition 1901-1903*, Zoologie, 16 (Vol. 8): 253-278.
- Riedel, W.R., 1953. Mesozoic and late Tertiary Radiolaria of Rotti. *J. Paleontol.*, 27:805-813.
- Riedel, W.R., 1957. Radiolaria: a preliminary stratigraphy in Petterson, H. ed, *Rep. Swed. Deep-Sea Exped.*, 1947-1948 (Vol. 6): Goteborg (Elanders Boktryckeri Aktiebolag), 59-96.
- Riedel, W.R., 1959. Oligocene and Lower Miocene Radiolaria in tropical Pacific sediments. *Micropaleontology*, 5:285-302.
- Riedel, W.R., 1967. Subclass Radiolaria in Harland, W.B., Holland, C.H., House, M.R., Hughes, N.F., Reynolds, A.B., Rudwick, M.J.S., Satterthwaite, G.E., Tarlo, L.B.H., and Willey, E.C. (Eds.), *The Fossil Record*. Geol. Soc. London, 291-298.
- Riedel, W.R., 1971. The occurrence of pre-Quaternary Radiolaria in deep-sea sediments. In Funnell, B.M. and Riedel, W.R., *The Micropalaeontology of Oceans*: Cambridge (Cambridge University Press) 567-594.
- Riedel, W.R., and Sanfilippo, A., 1970. Radiolarians, Leg 4, Deep Sea Drilling Project. in Bader, R.G., Gerard, R.D., et al., *Init. Repts. DSDP*, 4: Washington (U.S. Govt. Printing Office), 503-575.
- Riedel, W.R., and Sanfilippo, A., 1978. Stratigraphy and evolution of tropical Cenozoic radiolarians. *Micropaleontology*, 24:61-96.

- Robertson, J.H., 1975. Glacial to Interglacial Oceanographic Changes in the Northwest Pacific, Including a Continuous Record of the Last 400,000 Years. Doctoral Dissertation, Columbia University, New York.
- Roelofs, A.K. and Pisias, N.G., 1986. Revised technique for preparing quantitative radiolarian slides from deep-sea sediments. *Micropaleontology*, 32(2):182-185.
- Sanfilippo, A., and Riedel, W.R., 1980. A revised generic and suprageneric classification of the Artiscins (Radiolaria). *J. Paleontol.*, 54:1008-1011.
- Sager, W.W. and Pringle, M.S., 1988. Mid-Cretaceous to early Tertiary apparent polar wander path of the Pacific plate. *J. Geophys. Res.*, 93:11753-11771.
- Strelkov, A. A. and Reshetnyak, V. V., 1971. Colonial spumellarian radiolarians of the World Ocean in Strelkov, A. A. ed., *Radiolarians of the Ocean – Reports on the Soviet Union Expeditions, Explorations of the Fauna of the Seas*, Academy of Sciences of the U.S.S.R., 9 (7): 295-369, (in Russian), [Translated to English by W. R. Riedel].
- Takahashi, K., 1991. Radiolaria: Flux, Ecology, and Taxonomy in the Pacific and Atlantic in Honjo, S ed. (1991) *Ocean Bioscience Series No. 3*. Woods Hole Massachusettes, Woods Hole Oceanographic Institution.
- Tappan, H. and Loeblich, A.R., 1972. Fluctuating rates of protozoan evolution, diversification and extinction. *International Geological Congress 24, Montreal, 1972, Sect. 7, Paleontology*.

Appendix One – Visual Core Barrel Sheets of ODP Site 1179 (after Kawanaza, Sager *et al.*, submitted)

Sedimentologic description

The description of sedimentary units recovered during Leg 191 included estimates of sediment composition based on smear slides, thin sections, carbonate measurements, and XRD, documentation of sedimentary and deformational structures, drilling disturbance, presence and type of fossils, bioturbation intensity, induration, diagenetic alteration, and color. These data were recorded manually for each core section on standard visual core description (VCD) paper forms that are archived by ODP.

Barrel-Sheet Data

Information on the VCDs was summarized and entered into Apple-CORE (version 0.7.5g) software, which generated a one-page graphical log of each core (“barrel sheet”). A wide variety of features, such as sediment lithology, bed thickness, primary sedimentary structures, bioturbation parameters, soft-sediment deformation, and structural and diagenetic features are indicated by patterns and symbols in the graphic logs. A key to the full set of patterns and symbols used on the barrel sheets is shown in Figure F3. The symbols are schematic, but they are placed as close as possible to their proper stratigraphic position, or arrows indicate the interval for which the symbol applies. For exact positions of sedimentary features, copies of the detailed section-by-section VCD forms can be obtained from ODP. The columns on the barrel sheets are as follows:

Lithology

Sediment lithologies are represented by patterns in the “Lithology” column. This column may consist of up to three vertical strips, depending on the number of the major end-member constituents (see “Sediment Classification,”), thus reflecting intermixing of different components. Sediments with only one major component group (i.e., all other component groups are <10% each) are represented by one strip. Because of the limitations of the AppleCORE software, thin intervals of interbedded lithologies cannot be adequately displayed at the scale used for the barrel sheets, but they are described in the “Description” columns of the barrel sheets where appropriate.

Bioturbation, Structures, Accessories, Ichnofossils, and Fossils

Symbols in these columns are explained in Figure F3. The bulk of the clayey sediments recovered during Leg 191 was relatively homogeneous. Stratification, bioturbation, or other sedimentary structures were usually discernible only where textural or compositional differences were present (e.g., close to ash layers). In the homogeneous background sediment, however, it was difficult to distinguish the destruction of primary structures due to bioturbation from the actual absence of primary structures. Given the light gray and reddish colors of the clayey sediments, the absence of lamination, and the very low organic matter contents it is reasonable to assume that the remaining sediment has been pervasively bioturbated as well because benthic burrowing activity was not limited by oxygen deficiency. To convey the maximum amount of information

without confusing interpretation with observation, we used the “Bioturbation” column to display only visible bioturbation or sediment mottling. The bioturbation column of the barrel sheets shows four levels of intensity:

Homogeneous = trace fossils are either absent or invisible because they are in a completely biogenic fabric,

Low = rare, discrete burrows,

Moderate = burrows are generally isolated but locally overlap, and

Intense = abundant, overlapping burrows. Several generations of bioturbation structures cut across each other resulting in almost total disruption of sedimentary structures.

Stratification thickness was characterized by a combination of the terms:

very thick bedded (>1 m thick), thick bedded (30–100 cm thick),

medium bedded (10–30 cm thick), thin bedded (3–10 cm thick),

very thin bedded (1–3 cm thick), thickly laminated (3–10 mm

thick), thinly laminated (1–3 mm thick), and very thinly laminated (<1 mm thick).

Drilling Disturbance

Natural structures (physical or biological) can be difficult to distinguish from disturbance created by the coring process. Deformation and disturbance of sediment that resulted from the coring process are illustrated in the “Drilling disturbance” column with the symbols shown in Figure F3. Blank regions indicate the absence of drilling disturbance. The degree of drilling disturbance for soft sediments was described using the following categories:

Slightly disturbed = bedding contacts slightly bent,

Moderately disturbed = bedding contacts bowed,

Highly disturbed = bedding hardly discernible, sometimes showing flow structures, and

Soupy = water-saturated intervals that have lost all original structure.

Fragmentation in indurated sediments and rock was described using the following categories:

Slightly fragmented = core pieces in place with little drilling slurry or brecciation,

Moderately fragmented = core pieces in place or partly displaced but original orientation preserved or recognizable (drilling slurry may surround fragments),

Highly fragmented = core pieces are from the interval cored and are probably in correct stratigraphic sequence (although they may not represent the entire section), but the original orientation is completely lost, and

Drilling breccia = core pieces have lost their original orientation and stratigraphic position and may have been mixed with drilling slurry.

Samples and Close-Up Photographs

The stratigraphic position of samples taken for shipboard analysis and the location of close-up photographs is indicated in the “Samples” column of the barrel sheet according to the following codes:

CAR = carbonate content,
PAL = biostratigraphy,
PHO = close-up photograph,
SS = smear slide,
THS = thin section,
WR = whole-round sample,
XRD = X-ray diffraction analysis, and
XRF = X-ray fluorescence analysis.

Color

Sediment color was determined visually by comparison with standard color and is reported in the “Description” column of the barrel sheets. In addition to determining color visually, all cores were scanned at 2- to 4-cm intervals using a Minolta CM-2002 spectrophotometer mounted on the AMST. The spectrophotometer measures reflectance in thirty-one 10-nm-wide bands of the visible spectrum (400–700 nm) on the archive half of each core section. Spectrophotometer readings were taken after cleaning the surface of each core section and covering it with the clear plastic film (Glad brand Cling Wrap, a brand of polyethylene food wrap). Calibration of the color scanner did not include a correction for the plastic film because we found that the effect is very minor even with very bright colored lithologies. The measurements were taken automatically and recorded by the AMST at evenly spaced intervals along each section. There was no way to program the AMST software to avoid taking measurements in intervals with a depressed core surface or in disturbed areas of core containing drilling slurry or biscuits. The data are part of the Janus database and can be obtained from ODP.

Description

A summary of the sedimentologic data is given in the “Description” column of the barrel sheet. It consists of four parts: (1) a heading in capital letters that lists only the dominant sediment lithologies observed in the core; (2) a general description of the sediments in the core, including color, composition, sedimentary structures, bed thicknesses, drilling disturbance, as well as any other general features in the core; and (3) descriptions and locations of thin, interbedded, or minor lithologies.

Smear Slides and Thin Sections

Sediments were analyzed petrographically using smear slides and thin sections. Tables summarizing these data include information about the sample location, whether the sample represents a dominant (D) or a minor (M) lithology in the core, and the percentages of sand, silt, and clay size fractions, along with all identified components. We emphasize here that smear-slide and thin-section analyses provide only estimates of the relative abundances of the constituents. The comparison charts were used to refine abundance estimates in thin sections. However, these charts cannot be used for smear slides because they are designed to simulate a field of view that is completely and evenly covered with particles. Quantification of data from smear slides is further aggravated by the difficulty in identifying fine-grained particles using only a microscope and by the tendency to underestimate sand-sized grains because they cannot be incorporated evenly into the smear. Biogenic opal and its diagenetic modifications are particularly difficult to determine from smear slides. Previous experience has shown that the largest variations in smear-slide determination correlate with the change from one observer to another, or with shift changes. The accuracy problem is indicated in the "Explanatory Notes" chapters of several recent ODP volumes in which sedimentologic numerical data in general, and those of smear-slide determination in particular, are consistently de-emphasized and replaced by semiquantitative categories. A limitation to semiquantitative categories, such as the ones proposed during previous legs would have seemed all the more appropriate during Leg 185. Current ODP policies, however, require the input of numerical data; therefore, the reader is warned that the tabulated smear-slide results largely reflect the need to comply with these regulations rather than actual accuracy. Smear-slide and thin-section data were reviewed for internal consistency and correct sedimentologic nomenclature, and the qualitative composition was confirmed by XRD. Accuracy of the carbonate content estimated from smear slides and thin sections was confirmed by chemical analyses.

X-Ray Diffraction Analysis

Selected samples were taken for qualitative mineral analysis by XRD using a Philips diffractometer with Cu K α radiation at 40 kV and 35 mA with a focusing graphite monochromator and the following slit settings:

Focus = fine,
Irradiated length = 12 mm,
Divergence slit = automatic,
Receiving slit = 0.2 mm,
Step size = 0.02° 2 Theta,
Count time per step = 1 s,
Scanning rate = 2° 2 Theta/min,
Ratemeter time constant = 0.2 s,
Spinner = off,
Monochromator = on, and
Scan = continuous.

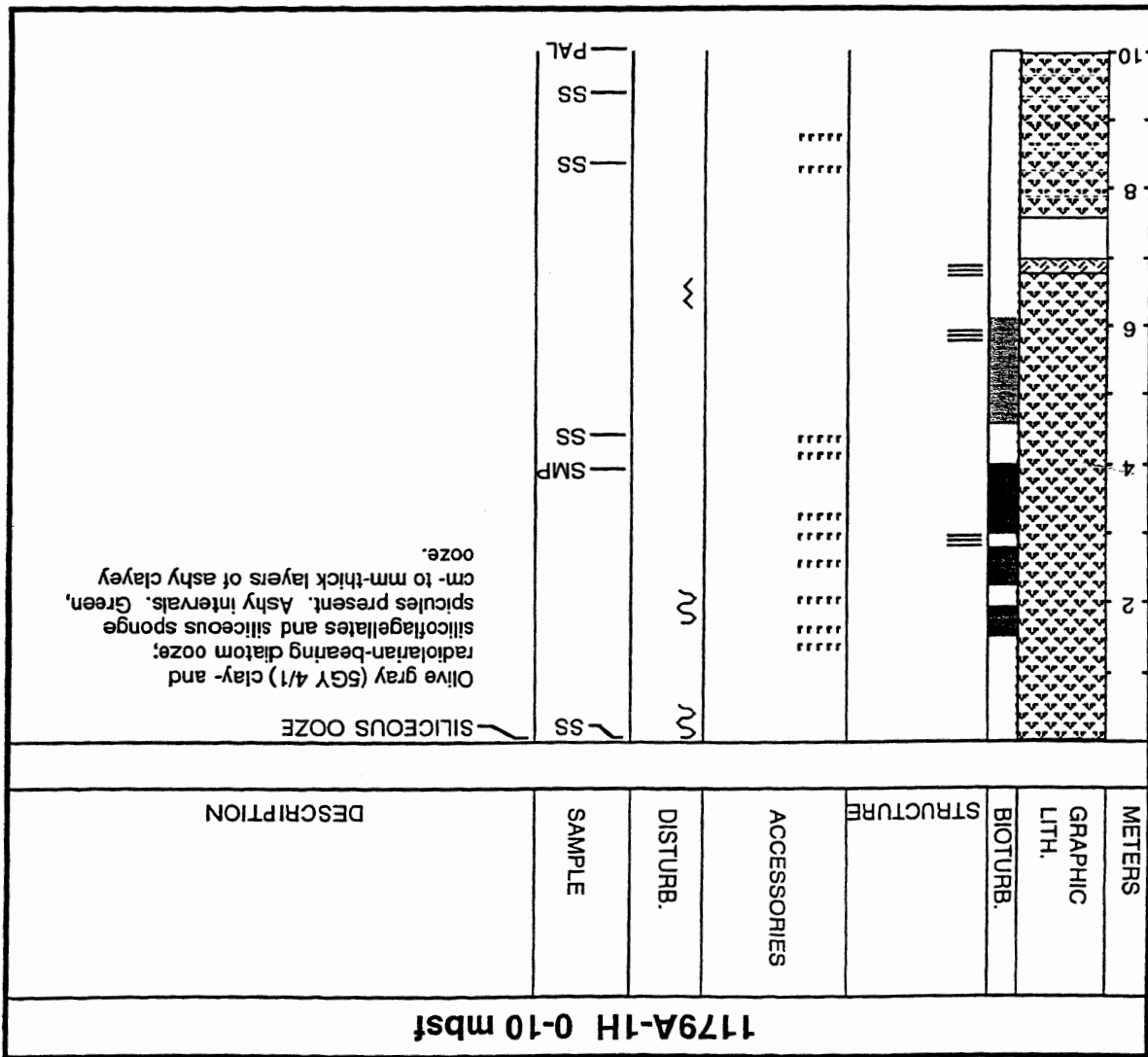
Bulk samples were freeze-dried, ground with an agate mortar and pestle, and packed in sample holders, which, together with the ship's movement, probably imparted some orientation to the mineral powder. These samples were scanned from 2° to 70° 2θ . MacDiff software (v. 4.0.4 PPC, by Rainer Petschick) was used to display diffractograms and to identify the minerals. Most diffractograms were corrected to match the main peaks of quartz, calcite, or clinoptilolite at 3.343, 3.035, and 8.95 Å, respectively. Identifications are based on multiple peak matches with the mineral data base provided with MacDiff. Each site chapter includes selected diffractograms to illustrate which peaks were associated with various minerals. Relative abundances reported in this volume are useful for general characterization of the sediments, but they are not quantitative concentration data.

Sediment Classification

We evaluated the methods and the classification used for sediment description and found that there is a need for a less ambiguous and more flexible classification than the proposed ODP standard classification. Our classification is neither comprehensive nor entirely descriptive, but it is simple to use for the purpose of Leg 191. Notably, it avoids the impression of a level of accuracy that is not achievable under the conditions of most ODP cruises. Also, we tried to use common and relatively simple names, which led us to abandon a number of ambiguous or meaningless terms like "Radiolarite" and "Mixed sediment" (see "Sediment Nomenclature"). We used three end-members (i.e., calcareous, siliceous, and silicate) (Fig. F4).

Sediment Nomenclature

Sediment names consist of a principal name relating to the dominant composition of the sediment (e.g., claystone, marl, or chert) and one or two modifiers that precede the principal name (e.g., ash-bearing siliceous clay). Besides composition, principal names vary according to the grain size and the induration of the sediment.



1179B-1H 0-7.6 mbsf

METERS	GRAPHIC LITH.	BIOTURB.	STRUCTURE	ACCESSORIES	DISTURB.	SAMPLE	DESCRIPTION
<div style="display: flex; flex-direction: column; align-items: center;"> <div style="margin-bottom: 10px;">2</div> <div style="margin-bottom: 10px;">4</div> <div style="margin-bottom: 10px;">6</div> </div>						<div style="display: flex; flex-direction: column; align-items: center;"> <div style="margin-bottom: 10px;">WH</div> <div style="margin-bottom: 10px;">SS</div> <div style="margin-bottom: 10px;">WH</div> <div style="margin-bottom: 10px;">— WH</div> <div style="margin-bottom: 10px;">— WH</div> <div style="margin-bottom: 10px;">— SS</div> <div style="margin-bottom: 10px;">— WH</div> </div>	<p>SILICEOUS OOZE</p> <p>Olive gray (5GY 4/1) clay- and radiolarian-bearing diatom ooze. Moderately mottled by bioturbation. Thin parallel to flaser laminae that consists of dark-green ashy to zeolitic clays</p>

1179B-2H 7.6-17.1 mbsf

METERS	GRAPHIC LITH.	BIOTURB.	STRUCTURE	ACCESSORIES	DISTURB.	SAMPLE	DESCRIPTION
8 10 12 14 16						SS WH SS SS WH	<p>SILICEOUS OOZE</p> <p>Olive gray (5GY 4/1) clay-bearing to clay-rich, radiolarian-bearing to radiolarian-rich diatom ooze. Massive mottled interval alternating with laminated layers of dark greenish gray (5GY 4/1) ashy zeolitic clay.</p> <p>Section 2 (58-60 cm): Light olive gray (5Y 6/1) vitric ash.</p> <p>Mn nodule.</p> <p>Section 5: Dark green (5GY 4/1) zeolitic claystone; altered ash.</p>

1179B-3H 17.1-26.6 mbsf

METERS	GRAPHIC LITH.	BIOTURB.	STRUCTURE	ACCESSORIES	DISTURB.	SAMPLE	DESCRIPTION
18						<ul style="list-style-type: none"> — SS — SS — XRD — SS — WH — SS — SS — SS — SS — SS — SS — PAL 	<p>CLAY-RICH SILICEOUS OOZE</p> <p>Light olive gray (5Y 7/3) clay-rich to clay-bearing, radiolarian-bearing diatom ooze. Sponge spicules, silicoflagellates and zeolites are minor components. A few dark greenish gray (5G 4/1) clayey layers of altered ash. Olive gray to greenish gray massive mottled intervals..</p>

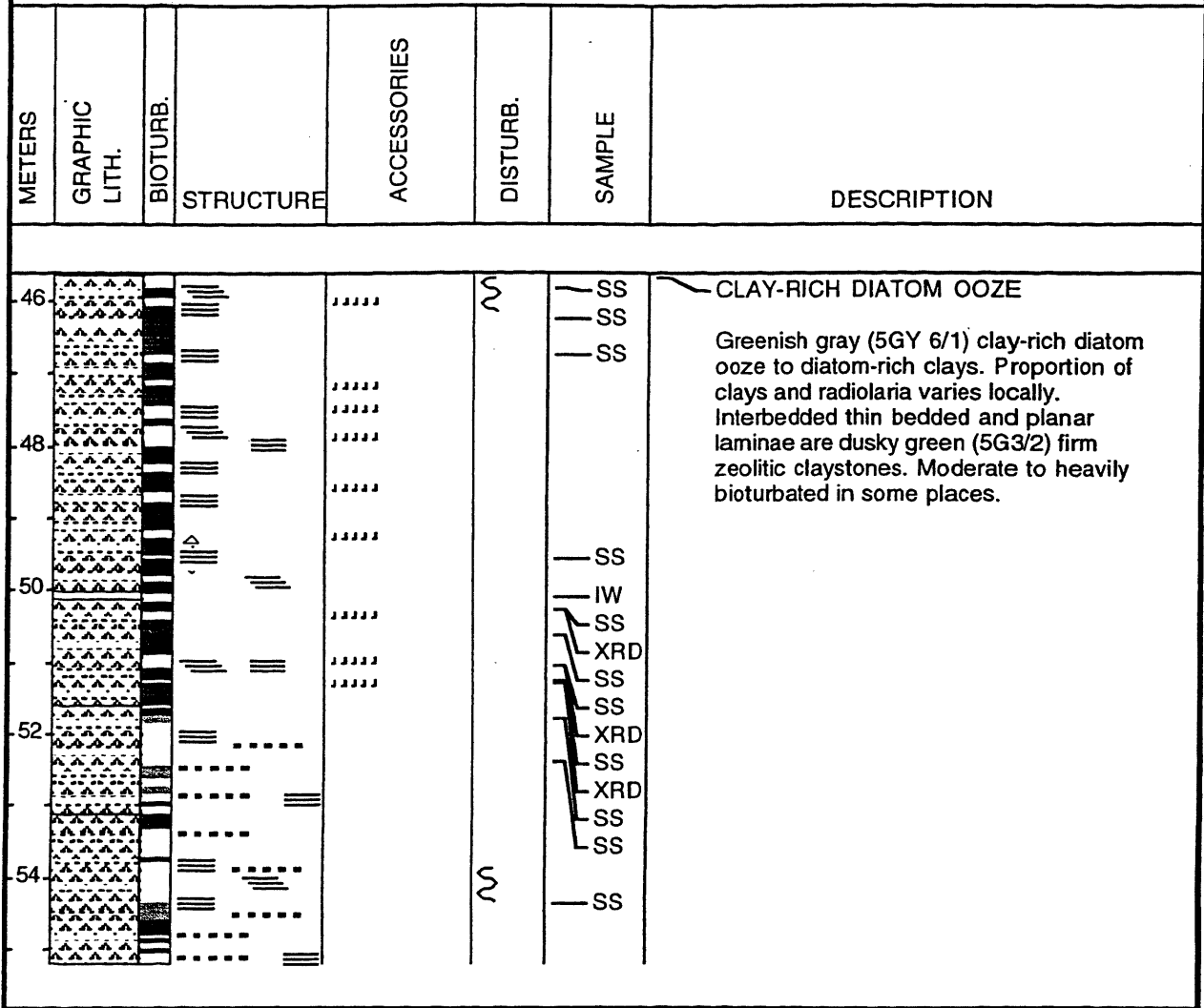
1179B-4H 26.6-36.1 mbsf

METERS	GRAPHIC LITH.	BIOTURB.	STRUCTURE	ACCESSORIES	DISTURB.	SAMPLE	DESCRIPTION
28 30 32 34 36						— SS — SS — WH — SS — SS — SS — SS — PAL	<p>CLAY-RICH SILICEOUS OOZE</p> <p>Greenish gray (5GY 4/1) clay-rich siliceous ooze locally interbedded with pale gray and mottled with various gray shades. Section 1-5 contains clay-rich diatom-radiolarian ooze. Section 6-7 contains volcanic glass bearing siliceous ooze-rich zeolitic clays. This coring interval is possibly largely bioturbated, although it is hard to trace/define due its indistinct appearance.</p> <p>A 10-cm thick ash bed.</p>

1179B-5H 36.1-45.6 mbsf

METERS	GRAPHIC LITH.	BIOTURB.	STRUCTURE	ACCESSORIES	DISTURB.	SAMPLE	DESCRIPTION
38 40 42 44 46						SS SS SS SS WH SS SS SS SS PAL	<p>SILICEOUS CLAY</p> <p>Sections 1-4, 6, and 8, contain diatom-rich zeolitic clays. Sections 5-6, contain clay-rich siliceous ooze. These two lithologies are interbedded with greenish-gray and medium gray beds or laminae. Rarely to moderately bioturbated with laterally oriented subrounded and tubular burrows.</p> <p>A 5-cm bed of vitric ash.</p>

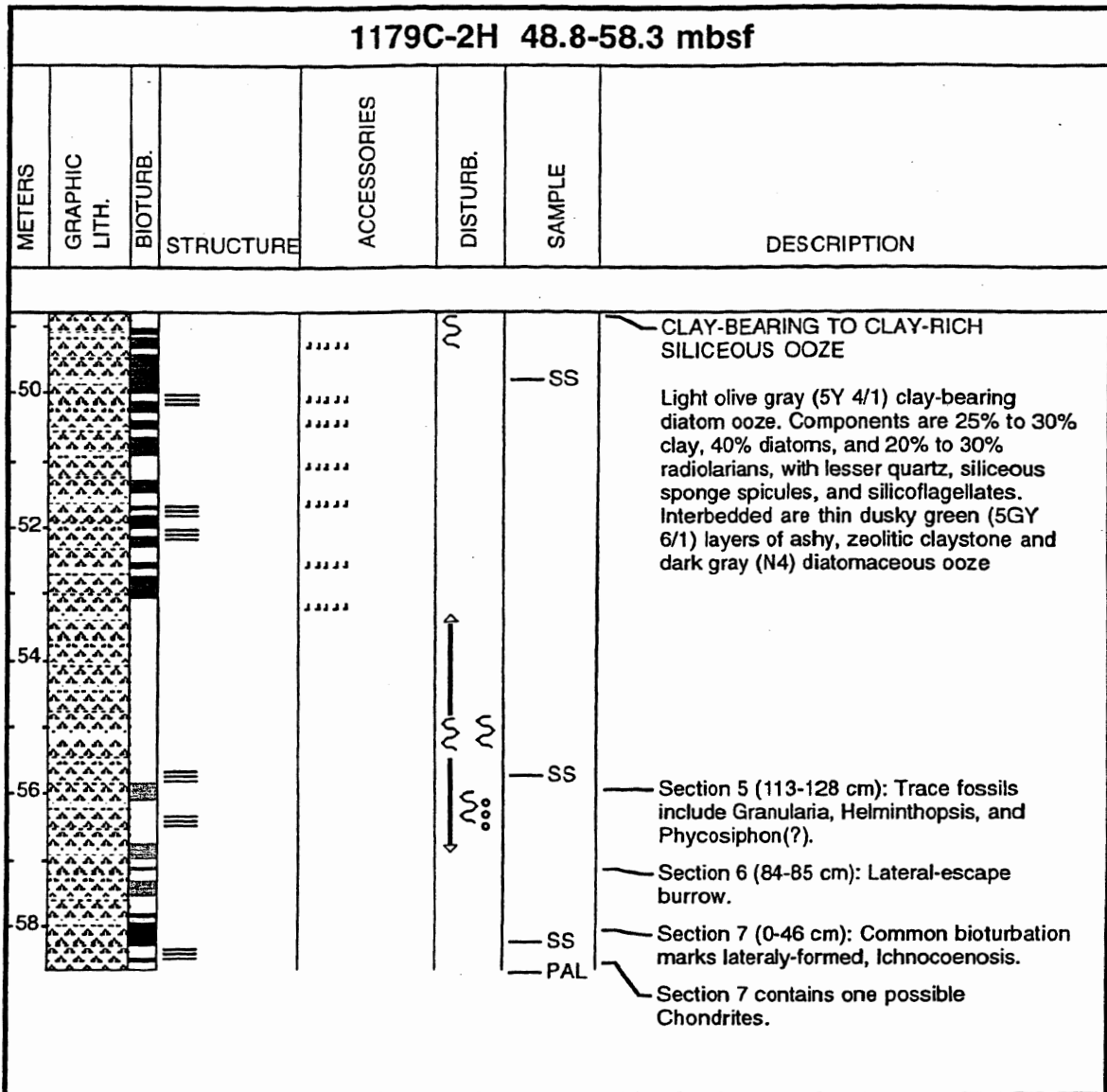
1179B-6H 45.6-55.1 mbsf



1179C-1H 0-5.8 mbsf

METERS	GRAPHIC LITH.	BIOTURB.	STRUCTURE	ACCESSORIES	DISTURB.	SAMPLE	DESCRIPTION
2 4							<p>DIATOM-RICH CLAY</p> <p>Medium brown (5YR 4/4), light brown (5YR 6/4) to olive gray (5Y 4/1) diatom-rich clay. Core components are about 50%-65% clay, 20%-35% diatoms, 5%-10% radiolarians, and traces of quartz, feldspar, light glass, and siliceous-sponge spicules. Laminated interbedded intervals of clayey siliceous ooze and zeolitic claystone.</p> <p>Bioturbation in lower Section 3 (105-145 cm) and upper Section 4 (0-54 cm) include possible Zoophycos, Planolites, and Chondrites.</p> <p>A 4.5-cm diameter piece of firm sediment in core catcher may be a concretion.</p>

1179C-2H 48.8-58.3 mbsf



1179C-3H 58.3-67.8 mbsf

METERS	GRAPHIC LITH.	BIOTURB.	STRUCTURE	ACCESSORIES	DISTURB.	SAMPLE	DESCRIPTION
60						SS	<p>CLAY- AND RADIOLARIAN-BEARING DIATOM OOZE</p> <p>Greenish gray (5GY 6/1) clay- and radiolarian-bearing diatom ooze. About 20% to 25% clay, 15% to 20 % radiolarians, and 45% to 55% diatoms, with lesser volcanic glass, quartz, siliceous sponge spicules, and silicoflagellates. Disturbed section at top of core contains a piece of zeolitic (phillipsite) siltstone. Interbedded are layers of ash-rich siliceous oozes.</p> <p>Section 3 (70-100 cm): Ash-rich interval.</p>
						SS	
						SS	
62						WH	
						SS	
64							
66							
						SS	<p>Section 6 (106-149 cm): Bioturbated interval has Phycosiphon, Granularia, and Helminthopsis.</p>
						SS	
						PAL	

1179C-4H 67.8-77.3 mbsf

METERS	GRAPHIC LITH.	BIOTURB.	STRUCTURE	ACCESSORIES	DISTURB.	SAMPLE	DESCRIPTION
68 70 72 74 76						SS SS PAL	<p>CLAY-BEARING SILICEOUS OOZE</p> <p>Pale olive (10Y 6/2) to greenish gray (5GY 6/1) clay-bearing siliceous ooze. About 20% clay, 30% radiolarians, and 40% diatoms, with lesser volcanic glass.</p> <p>Section 5 (18-27 cm): Bed of vitric ash.</p> <p>Section 7 (0-80 cm): Heavily mottled and bioturbated with possible Planolites, Granularia, and Phycosiphon(?).</p>

1179C-5H 77.3-86.8 mbsf

METERS	GRAPHIC LITH.	BIOTURB.	STRUCTURE	ACCESSORIES	DISTURB.	SAMPLE	DESCRIPTION
78 80 82 84 86						SS WH SS SS PAL	<p>DIATOM-RICH CLAY</p> <p>Light olive gray (5Y 6/1) diatom-rich clay. Abundant diatoms and radiolarians and volcanic glass, with lesser zeolite and sponge spicules. Interbedded are green (firm, zeolitic, ashy) or dark gray (N4) (more diatomaceous and ashy) beds or laminae.</p> <p>Section 4: Contains a 5-cm ash-rich bed.</p>

1179C-6H 86.8-96.3 mbsf

METERS	GRAPHIC LITH.	BIOTURB.	STRUCTURE	ACCESSORIES	DISTURB.	SAMPLE	DESCRIPTION
88 90 92 94 96						<p>SS</p> <p>SS</p> <p>WH</p> <p>SS</p> <p>SS</p> <p>SS</p> <p>PAL</p>	<p>CLAY- AND RADIOLARIAN-BEARING DIATOM-RICH SILICEOUS OOZE</p> <p>Pale olive (10Y 6/2) to greenish gray (5GY 6/1) clay- and radiolarian bearing siliceous ooze. Components are: clay 15% to 25%, radiolarians 15% to 25%, diatoms about 45%, with lesser quartz, glass, and sponge spicules. Mottled massive intervals interbedded with gray ashy clay-poor laminated ooze intervals, and dark green ashy, zeolitic, clay-rich laminae and thin beds.</p> <p>Section 3: Extensive bioturbation, both vertically and laterally oriented, of subrounded, pipe, and tabular shapes; Planolites and Helminthopsis.</p> <p>Section 4: Extensive laterally oriented lensoidal bioturbation, perhaps of Planolites, Helminthopsis, and Granularia.</p> <p>Section 4 (113-118): Ash bed.</p> <p>Section 8 (28-31 cm): Ash bed.</p>

1179C-7H 96.3-105.8 mbsf

METERS	GRAPHIC LITH.	BIOTURB.	STRUCTURE	ACCESSORIES	DISTURB.	SAMPLE	DESCRIPTION
<p>98</p> <p>100</p> <p>102</p> <p>104</p>						<p>SS</p> <p>WH</p> <p>SS</p> <p>SS</p> <p>PAL</p>	<p>CLAY- AND RADIOLARIAN-BEARING DIATOM OOZE</p> <p>Greenish gray (5GY 6/1) to pale olive (10Y 6/2) clay-and radiolarian bearing diatom ooze. Clay about 20% to 25%, radiolarians about 15%, and diatoms about 55% to 60%, with lesser zeolite, feldspar, and quartz. Mottled massive intervals interbedded with gray ashy clay-poor laminated ooze intervals, and dark green ashy, zeolitic, clay-rich laminae and thin beds.</p> <p>Section 5: Planolites, Helmiathopsis, Granularia, and Phycosiphon seen through lower part of core.</p>

1179C-8H 105.8-115.3 mbsf

METERS	GRAPHIC LITH.	BIOTURB.	STRUCTURE	ACCESSORIES	DISTURB.	SAMPLE	DESCRIPTION
106 108 110 112 114						SS WH SS PAL	<p>CLAY-BEARING TO CLAY-RICH RADIOLARIAN-BEARING DIATOM OOZE</p> <p>Greenish gray (5GY 6/1) to pale olive (10Y 6/2) clay-bearing to clay-rich radiolarian-bearing siliceous ooze to diatom ooze. Clay about 10% to 35%, radiolarians about 15%, diatoms about 40% to 70%, with lesser quartz, glass, and sponge spicules. Mottled intervals interbedded with gray ashy clay-poor laminated ooze intervals and dark green ashy, zeolitic, clay-rich laminae and thin beds.</p> <p>Section 5: Increase in diatom content.</p> <p>Section 7: Heavy bioturbation of horizontal and relatively large (1 to 5 cm) burrows.</p>

1179C-9H 115.3-124.8 mbsf

METERS	GRAPHIC LITH.	BIOTURB.	STRUCTURE	ACCESSORIES	DISTURB.	SAMPLE	DESCRIPTION
116 118 120 122 124						SS HS SS PAL	<p>CLAY- AND RADIOLARIAN-BEARING DIATOM OOZE</p> <p>Pale olive (10Y 6/2) clay-bearing, radiolarian-rich diatom ooze. Clay 25% to 30%, radiolarians 15% to 30%, diatoms about 40 to 50%, with lesser zeolite, glass, and sponge spicules. Mottled intervals interbedded with gray ashy clay-poor laminated ooze intervals and dark green ashy, zeolitic, clay-rich laminae and thin beds.</p> <p>Section 5: Planolites, Phycosiphon, and Granularia(?).</p> <p>Section 6: Burrowing largely lateral, subrounded, lensoidal, and tubular, maybe related to Planolites, Helminthopsis, and Zoophycos.</p>

1179C-10H 124.9-134.4 mbsf

METERS	GRAPHIC LITH.	BIOTURB.	STRUCTURE	ACCESSORIES	DISTURB.	SAMPLE	DESCRIPTION
126 128 130 132 134							<p>CLAY- AND RADIOLARIAN-BEARING DIATOM OOZE</p> <p>Grayish green (5GY 6/1) clay- and radiolarian-bearing diatom ooze. Clay about 25%, radiolarians about 10% to 15%, diatoms about 60% to 65%, with lesser feldspar, glass, and zeolite. Mottled intervals interceded with gray ashy clay-poor laminated (planar and flaser) ooze intervals, and dark green ashy, zeolitic, clay-rich laminae and thin beds. Clay is more zeolitic lower in core.</p> <p>Section 3: Contains a 9-cm bed of vitric ash.</p> <p>Section 4: Contains a 1-cm piece of zeolitic ash pebble.</p> <p>Section 5: Bioturbation marks are lateral, subrounded, and tabular; Planolites, Granularia, Zoophycus</p> <p style="text-align: right;">PAL</p>

1179C-11H 134.4-143.9 mbsf

METERS	GRAPHIC LITH.	BIOTURB.	STRUCTURE	ACCESSORIES	DISTURB.	SAMPLE	DESCRIPTION
<p>136</p> <p>138</p> <p>140</p> <p>142</p> <p>144</p>						<p>THS</p> <p>XRD SS</p> <p>XRD SS IW</p> <p>SS XRD</p> <p>SS THS XRD SS SS</p> <p>XRD SS</p> <p>PAL</p>	<p>RADIOLARIAN-BEARING CLAY-RICH DIATOM OOZE</p> <p>Sections 1 to 3 are extensively deformed/soupy. Proportion of clay decreases whereas proportion of radiolarian oozes increases down the core. Core lithology is characterized by olive gray (5Y 4/1) massive radiolarian-bearing clay-rich sediments which are locally banded by purplish gray clay-bearing diatom ooze. The undeformed sections show moderate degree of bioturbation.</p> <p>Section 1: Has two (4 cm) burrow fillings (or clasts?, nodules?)</p>

1179C-12H 143.9-153.4 mbsf

METERS	GRAPHIC LITH.	BIOTURB.	STRUCTURE	ACCESSORIES	DISTURB.	SAMPLE	DESCRIPTION
<p>146</p> <p>148</p> <p>150</p> <p>152</p> <p>154</p>						<p>XRD</p> <p>SS</p> <p>SS</p> <p>SS</p> <p>PAL</p>	<p>CLAY- AND RADIOLARIAN-BEARING DIATOM OOZE</p> <p>Olive gray (5Y 4/1) clay- and radiolarian-bearing diatom ooze. Massive mottled intervals interbedded with purplish gray beds in which proportion of radiolarians increases and that of clay decreases. The cores are moderately to highly bioturbated largely with laterally oriented marks. There are a few flaser laminae, planer lamanae, and indurated yellowish-brown concretions.</p> <p>Section 6: Indurated concretion(?) or burrow-filling(?).</p>

1179C-13H 153.4-162.9 mbsf

METERS	GRAPHIC LITH.	BIOTURB.	STRUCTURE	ACCESSORIES	DISTURB.	SAMPLE	DESCRIPTION
<p>154</p> <p>156</p> <p>158</p> <p>160</p> <p>162</p>						<p>XRD SS</p> <p>XRD SS</p> <p>SS SS</p> <p>SS</p> <p>PAL</p>	<p>RADIOLARIAN-BEARING, CLAY-RICH DIATOM OOZE</p> <p>Pale olive (10Y 6/2) radiolarian-bearing, clay-rich diatomaceous ooze. Interbedded are greenish-gray zeolitic clay and purplish-gray clay-bearing siliceous oozes. Sedimentary features include flaser and planar laminae, and bioturbation. Bioturbation is rare to moderate in Sections 2 and 3, and moderate to common in Sections 5 and 6.</p>

1179C-14H 162.8-172.3 mbsf

METERS	GRAPHIC LITH.	BIOTURB.	STRUCTURE	ACCESSORIES	DISTURB.	SAMPLE	DESCRIPTION
<p>164</p> <p>166</p> <p>168</p> <p>170</p> <p>172</p>						<p>XRD</p> <p>SS</p> <p>SS</p> <p>SS</p> <p>XRD</p> <p>SS</p> <p>SS</p> <p>XRD</p> <p>WH</p> <p>SS</p> <p>PAL</p>	<p>CLAY-RICH SILICEOUS OOZE</p> <p>Sections 1 to 3 consist of pale olive gray (10Y 6/2) massive clay-rich siliceous ooze, which becomes clay- and radiolarian-bearing diatomaceous ooze in Sections 4 to 8. Sedimentary features observed largely in the lower sections include flaser laminae and bioturbation.</p> <p>Section 4: Contains a 3-cm bed of vitric ash.</p>

1179C-15H 172.3-181.8 mbsf

METERS	GRAPHIC LITH.	BIOTURB.	STRUCTURE	ACCESSORIES	DISTURB.	SAMPLE	DESCRIPTION
<p>174</p> <p>176</p> <p>178</p> <p>180</p>						<p>SS</p> <p>SS</p> <p>SS</p> <p>PAL</p>	<p>CLAY-BEARING, RADIOLARIAN-RICH DIATOM OOZE</p> <p>Sections 1 to 5: Pale olive (10Y 6/2) clay-bearing and radiolarian-rich diatom ooze.</p> <p>Sections 5 to 8: Zeolitic clay-rich radiolarian-bearing diatom ooze.</p> <p>A 6-cm thick light-gray vitric ash layer. Section 6 also contains 3 dark-gray chert nodules, and bioturbation.</p>

1179C-16H 181.8-191.3 mbsf

METERS	GRAPHIC LITH.	BIOTURB.	STRUCTURE	ACCESSORIES	DISTURB.	SAMPLE	DESCRIPTION
182 184 186 188 190						SS SS PAL	<p>CLAY-RICH, RADIOLARIAN-BEARING SILICEOUS OOZE</p> <p>Pale olive (10Y 6/2) clay-rich radiolarian-bearing ooze. Massive intervals are interbedded with dusky green (5G3/2) ashy beds and siliceous zeolitic mud. Sedimentary features include planar/flaser laminae and bioturbation.</p> <p>Section 4: Contains a 1-cm vitric ash bed.</p>

1179C-18H 200.8-210.3 mbsf

METERS	GRAPHIC LITH.	BIOTURB.	STRUCTURE	ACCESSORIES	DISTURB.	SAMPLE	DESCRIPTION
<p>202</p> <p>204</p> <p>206</p> <p>208</p> <p>210</p>						<p>SS</p> <p>SS</p> <p>SS</p> <p>XRD</p> <p>PAL</p>	<p>ZEOLITIC CLAY-RICH, RADIOLARIAN-BEARING DIATOM-RICH SILICEOUS OOZE</p> <p>Greenish gray (5GY 5/1) clay-rich, radiolarian-bearing diatom ooze. Zeolite counted with clay; zeolitic clay is about 40 %, radiolarians about 20 %, and diatoms about 40 %. Stiff; approaching claystone or diatomite. Most of the core is massive; a few burrowed, or parallel- or flaser-laminated, intervals. A piece of filled burrow at top of core; perhaps from section above.</p>

1179C-19H 210.3-219.8 mbsf

METERS	GRAPHIC LITH.	BIOTURB.	STRUCTURE	ACCESSORIES	DISTURB.	SAMPLE	DESCRIPTION
<p>212</p> <p>214</p> <p>216</p> <p>218</p>						<p>SS</p> <p>SS</p> <p>XRD</p> <p>XRD</p> <p>SS</p> <p>XRD</p> <p>SS</p> <p>XRD</p> <p>SS</p> <p>XRD</p> <p>THS</p> <p>XRD</p> <p>SS</p> <p>SS</p> <p>XRD</p> <p>SS</p> <p>PAL</p>	<p>ZEOLITIC CLAY-RICH, RADIOLARIAN-BEARING DIATOM-RICH SILICEOUS OOZE</p> <p>Pale olive (10Y 6/2) clay-rich, radiolarian-bearing diatom ooze. Zeolite counted with clay; zeolitic clay is about 30% to 40%, radiolarians about 25%, and diatoms about 30% to 45%. Volcanic glass to 5%. Stiff; approaching a claystone or diatomite. Most of core is massive; a few burrowed, or parallel- or flaser-laminated intervals.</p> <p>Section 5: Contains three pieces of solid burrow fillings. Surfaces are patterned, as if the animal selected particles (2 x 4 mm prism-like forms) to line burrow (c.f. Ophiomorpha).</p>

1179C-20H 219.8-229.3 mbsf

METERS	GRAPHIC LITH.	BIOTURB.	STRUCTURE	ACCESSORIES	DISTURB.	SAMPLE	DESCRIPTION
220 222 224 226 228						XRD SS XRD SS SS XRD XRD SS SS SS SS XRD SS XRD SS WH XRD SS SS SS XRD XRD SS XRD XRD SS SS SS PAL	<p>ZEOLITIC CLAY-RICH, DIATOM-BEARING RADIOLARIAN-RICH SILICEOUS OOZE TO RADIOLARIAN OOZE</p> <p>Zeolite counted with clay; zeolitic clay is about 25% to 35%, radiolarians increase downhole from about 40 %to 60%, and diatoms are about 10% to 20%. Stiff; approaching claystone or diatomite. Most of core is massive; rare burrowed, or parallel- or flaser-laminated, intervals.</p> <p>Section 2: Gradational color change from pale olive (10Y 6/2) to yellowish brown 5GY 6/4) result of a gradual relative increase of radiolarians compared to diatoms.</p> <p>Chert concretion in section 6 (highest chert in section).</p>

1179C-21H 229.3-238.8 mbsf

METERS	GRAPHIC LITH.	BIOTURB.	STRUCTURE	ACCESSORIES	DISTURB.	SAMPLE	DESCRIPTION
<p>230</p> <p>232</p> <p>234</p> <p>236</p> <p>238</p>						<p>SS</p> <p>SS</p> <p>XRD</p> <p>SS</p> <p>PAL</p>	<p>CLAY-RICH RADIOLARIAN OOZE</p> <p>Light brown (5YR 5/6), massive zeolitic clay-rich radiolarian ooze, which becomes clay- and diatom-bearing radiolarian ooze downcore in Sections 5 to 7. A few mottles representing bioturbation are present in places. Sediments are moderately compact.</p>

1179C-22H 238.8-248.3 mbsf

METERS	GRAPHIC LITH.	BIOTURB.	STRUCTURE	ACCESSORIES	DISTURB.	SAMPLE	DESCRIPTION
240						<ul style="list-style-type: none"> SS XRD SS SS SS XRD SS XRD SS XRD SS XRD SS SS SS XRD SS XRD SS XRD SS SS SS XRD SS XRD SS XRD SS SS PAL 	<p>CLAYEY RADIOLARIAN OOZE, AND CLAY</p> <p>Sections 1 to 5: Light brown (5YR 5/6), massive clayey radiolarian ooze. A distinct vitric ash layer is present in Section 3.</p> <p>A 3-cm bed of vitric ash.</p> <p>note about crowded sampling column. Interval 22-3-100 through 22-6-100 are sampled for XRD and ss each 50 cm.</p> <p>Section 5: Records the transition (from 125 cm downwards) to pelagic clay (about 95% clay). The pelagic clay contains red colored mottles which represent very subtle bioturbation marks. These clays also contain zeolites in places.</p>

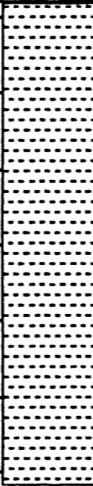
1179C-23H 248.3-257.8 mbsf

METERS	GRAPHIC LITH.	BIOTURB.	STRUCTURE	ACCESSORIES	DISTURB.	SAMPLE	DESCRIPTION
<p>250</p> <p>252</p> <p>254</p> <p>256</p>						<p>SS</p> <p>XRD</p> <p>SS</p> <p>SS</p> <p>XRD</p> <p>SS</p> <p>XRD</p> <p>SS</p> <p>XRD</p> <p>SS</p> <p>SS</p> <p>XRD</p> <p>SS</p> <p>SS</p> <p>XRD</p> <p>XRD</p> <p>SS</p> <p>XRD</p> <p>SS</p> <p>SS</p> <p>SS</p> <p>XRD</p> <p>XRD</p> <p>SS</p> <p>PAL</p>	<p>BROWN PELAGIC CLAY and DARK ZEOLITIC CLAY</p> <p>Yellowish brown (10YR 4/2) pelagic clay. Section 1 is highly deformed/soupy. Core is mottled and burrowed.</p> <p>ZEOLITIC CLAY</p> <p>Sections 2 to 8: Brown to medium dark grey (5YR 4/1) massive, sticky zeolitic clays (Sections 2 to 8) which contain moderate bioturbation in form of variously shaded mottles. The marks are largely subrounded in shape.</p>

1179C-24H 257.8-266.8 mbsf

METERS	GRAPHIC LITH.	BIOTURB.	STRUCTURE	ACCESSORIES	DISTURB.	SAMPLE	DESCRIPTION
258 260 262 264 266						SS SS SS XRD SS XRD PAL	FERRUGINOUS ZEOLITIC CLAY Dusky yellow brown (10YR 2/2) to chocolate gray, massive, and mottled ferruginous zeolitic clays. Iron oxide content varies from 15% to 20%. Mottles contain largely Fe-oxide-rich subrounded bioturbation marks. These mottles resemble to nodules in many ways.


1179C-25X 266.8-273.7 mbsf

METERS	GRAPHIC LITH.	BIOTURB.	STRUCTURE	ACCESSORIES	DISTURB.	SAMPLE	DESCRIPTION
<p>268</p> <p>270</p> <p>272</p>					<p>~</p> <p>~</p> <p>~</p>	<p>SS XRD</p> <p>PAL</p>	<p>FERRUGINOUS AND ZEOLITIC CLAY</p> <p>Dusky yellow brown (10YR 2/2) clay; ferruginous and zeolitic. Stiff, massive, and with rare mottles.</p>

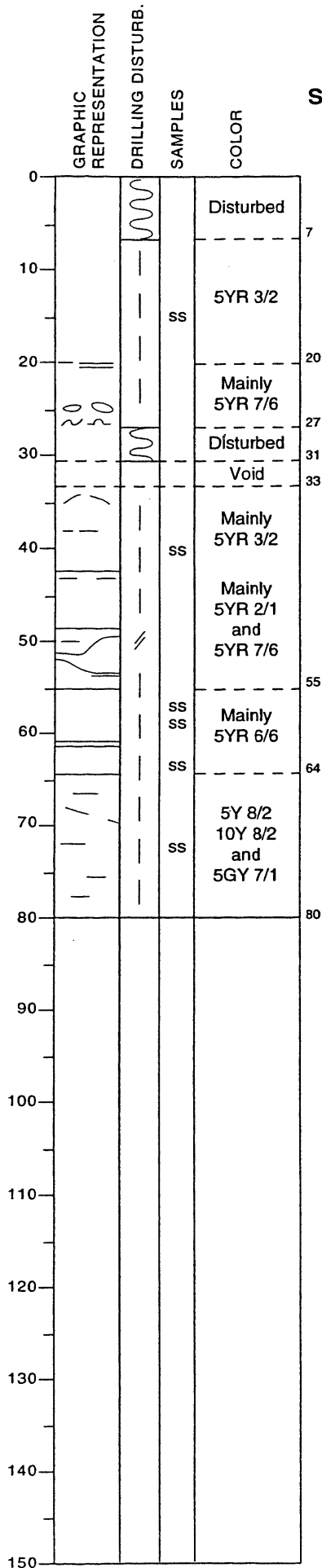
1179C-26X 273.7-283.3 mbsf

METERS	GRAPHIC LITH.	BIOTURB.	STRUCTURE	ACCESSORIES	DISTURB.	SAMPLE	DESCRIPTION
274 276 278 280 282						<p>XRD SS XRD SS</p> <p>WH HS</p> <p>SS PAL</p>	<p>FERRUGINOUS AND ZEOLITIC CLAY</p> <p>Grayish brown (5YR 3/2) clay; ferruginous and zeolitic. Stiff, massive, and with rare mottles.</p>

1179C-27X 283.3-292.9 mbsf

METERS	GRAPHIC LITH.	BIOTURB.	STRUCTURE	ACCESSORIES	DISTURB.	SAMPLE	DESCRIPTION
							<p>PAL CHERT</p> <p>Angular fragments of chert; vitreous to waxy and hard (no porcelanite). Brown tints and shades (10YR 8/2, 4/2, and 2/1) Maximum size 5 cm; most 1 cm.</p>

VISUAL CORE DESCRIPTION SEDIMENTS/SEDIMENTARY ROCKS



191-1179D-1R-1

This section is cuttings recovered from the drilled/washed interval.

Please note that although the section was described, there maybe no true stratigraphic order or structure to this section.

CLAY (slightly to moderately zeolitic)

Sharp color contrasts may represent recovery rather than initial positions.

0-7 Disturbed.

7-20 Grayish brown (5YR 3/2) zeolitic clay similar to lithology near base of Hole 1179C.

20-27 Reddish yellow (5YR 7/6) and adjacent tints zeolitic clay. Two pieces of porcellanite are present in this interval.

27-31 Disturbed.



31-33 Void

33-55 Layered (pseudo-layers(?) from drilling?) clay. Mainly grayish brown (5YR 3/2), some brownish black (5YR 2/1) 0.5 cm layers. Two distinct and 3 or 4 indistinct reddish yellow (5YR 7/6) layers.

55-64 Reddish yellow (5YR 6/6) zeolitic clay with gray and orange layers.

64-80 Zeolite-bearing clays with approximately 0.5 cm thick gray and pale green layers. Colors include pale yellow (5Y 8/2), pale greenish yellow (10Y 8/2), light greenish gray (5GY 7/1) and similar tints.

**VISUAL CORE DESCRIPTION
SEDIMENTS/SEDIMENTARY ROCKS**

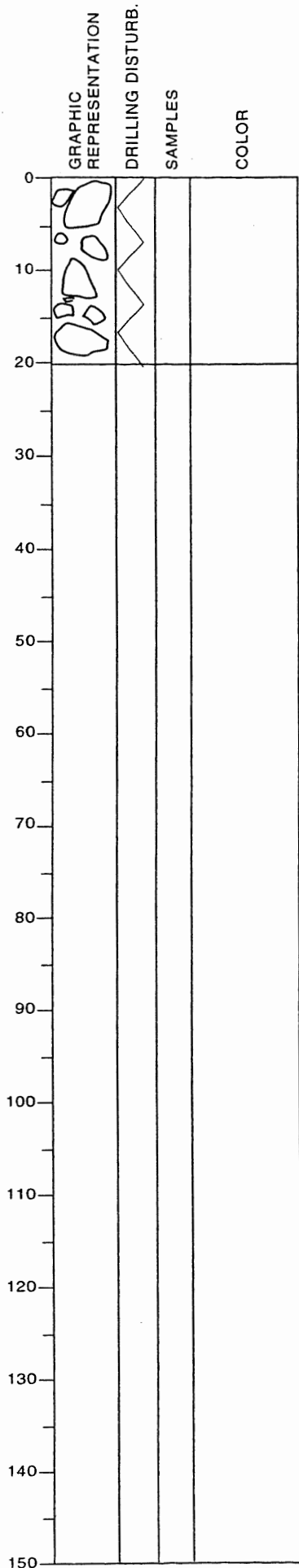
	GRAPHIC REPRESENTATION	DRILLING DISTURB.	SAMPLES	COLOR
0	Clay			5GY 7/1
10			PAL	5GY 7/1
20				5YR 5/6
30				
40				
50				
60				
70				
80				
90				
100				
110				
120				
130				
140				
150				

191-1179D-1R-CC

CLAYS (0-4.5 cm)
Very light olive gray (5GY 7/1), soft, apparently massive clays.

CHERT (4.5-18 cm)
Very light olive gray and medium brown (5GY 7/1 and 5YR 5/6), very hard, compact with sub-conchoidal fractures.

VISUAL CORE DESCRIPTION SEDIMENTS/SEDIMENTARY ROCKS



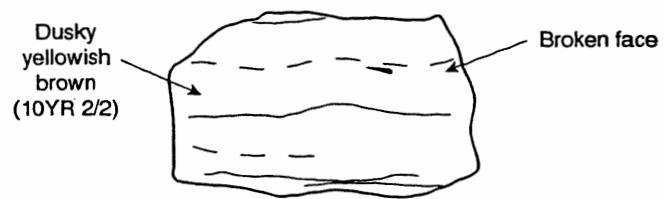
191-1179D-2R-CC

CHERT

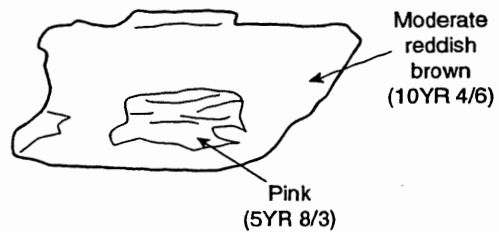
Several pieces of waxy to vitreous, hard chert.
Three largest pieces are approximately 3 x 3 x 5 cm in size.
Others are smaller pieces.

Colors are dusky yellowish brown (10YR 2/2), with faint lighter laminae. (lithology is in deeper cores of 3R and especially in 4R.)

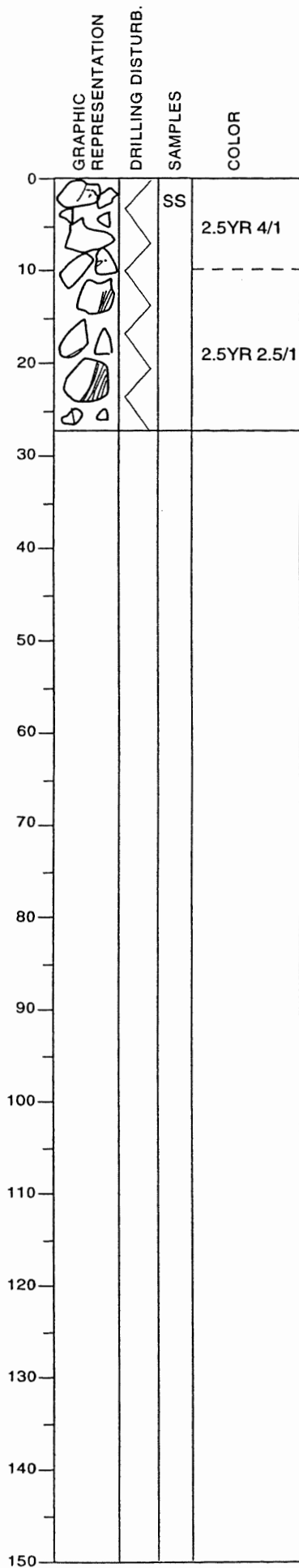
Example:



Some other colors are reddish yellow (5YR 6/6), dark yellowish orange (10YR 6/6), moderate reddish brown (10YR 4/6), and pink (5YR 8/3).



**VISUAL CORE DESCRIPTION
SEDIMENTS/SEDIMENTARY ROCKS**



191-1179D-3R-CC

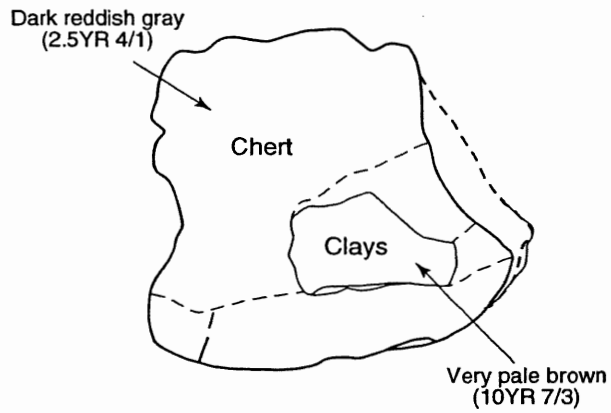
CHERT

Highly fragmented, deep dark brown color, hard and compact with sub-conchoidal fractures.

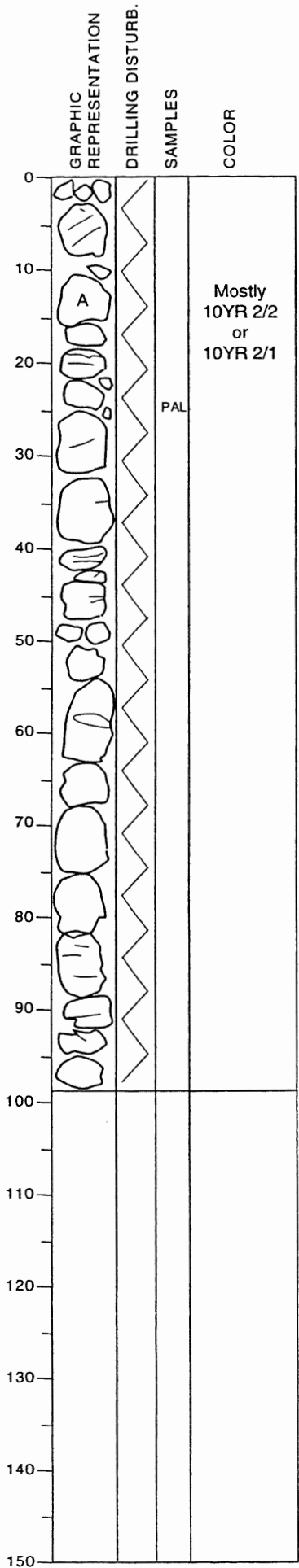
Thin bands are present in some pieces.

A smear slide was made from brownish gray, soft sediment attached to the first piece at about the top (sketch below). It is composed of clays with chert fragments.

Enlarged view of the piece at 0-2.5 cm



VISUAL CORE DESCRIPTION SEDIMENTS/SEDIMENTARY ROCKS



191-1179D-4R-1

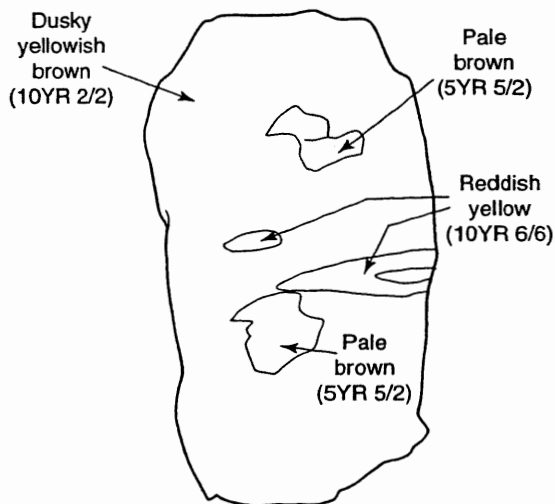
CHERT

18 pieces of 2-cm minimum dimension and 9 smaller pieces.

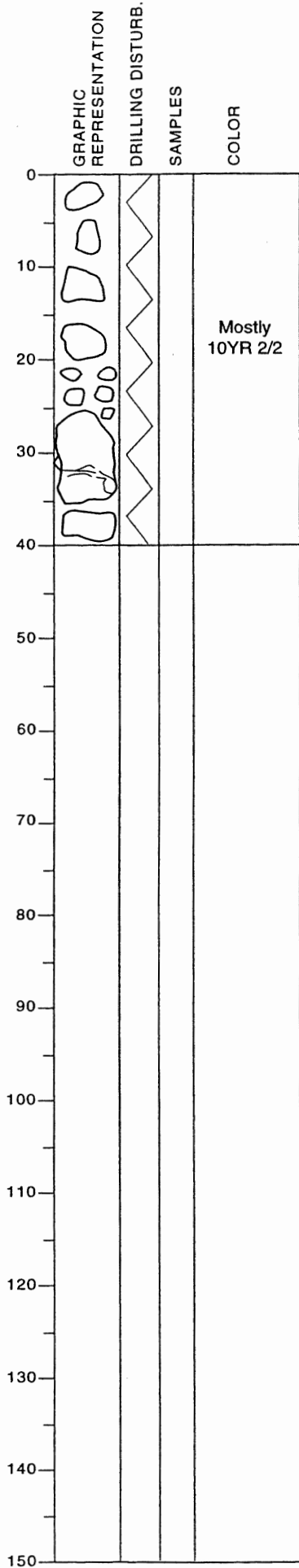
Some show layers (or former horizontal burrows?)

Most pieces are dusky yellowish brown (10YR 2/2) or brownish black (10YR 2/1) except Piece A (11-17 cm), which is lighter brown (5YR 5/6).

Piece at 57-64 cm show mottle(?) and brecciation as below.



VISUAL CORE DESCRIPTION SEDIMENTS/SEDIMENTARY ROCKS

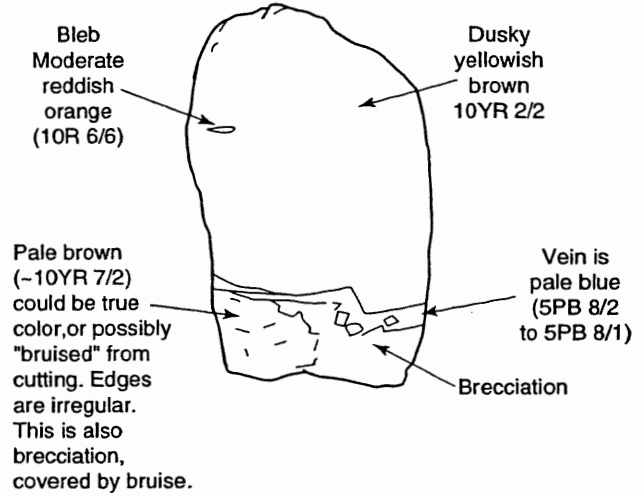


191-1179D-5R-1

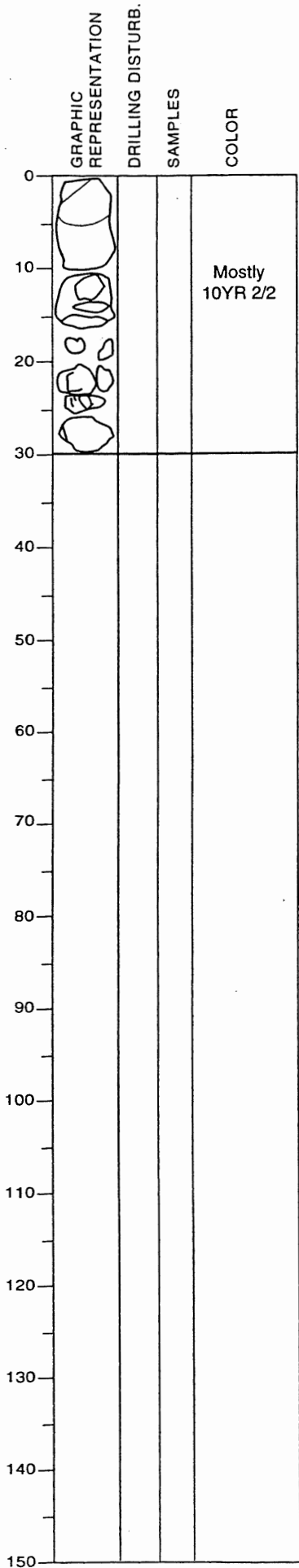
CHERT

One large (see sketch), five >3 cm, and five small pieces.
Color is mostly dusky yellowish brown (10YR 2/2).

Detailed features of the large piece at 27-36 cm is shown below.



VISUAL CORE DESCRIPTION SEDIMENTS/SEDIMENTARY ROCKS

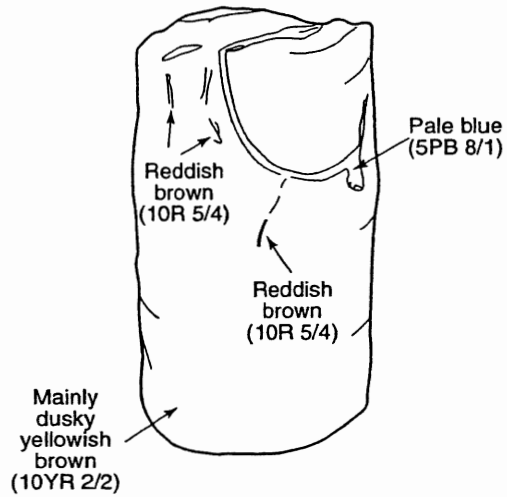


191-1179D-5R-CC

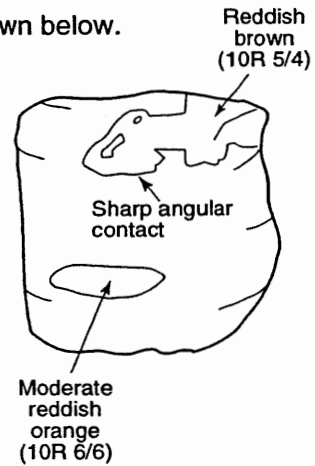
CHERT

Main dusky yellow brown (10YR 2/2). Some moderate yellowish brown (10YR 5/4) in angular contact, some 1-cm thick elliptical areas of moderate reddish orange (10R 6/6).

Largest piece at 0-10 cm is shown below.



Piece at 10-16 cm is shown below.



VISUAL CORE DESCRIPTION SEDIMENTS/SEDIMENTARY ROCKS

GRAPHIC REPRESENTATION	DRILLING DISTURB.	SAMPLES	COLOR
0 10 20 30 40 50 60 70 80 90 100 110 120 130 140 150	PAL	2.5YR 4/1	dark reddish gray
		7.5YR 5/4	brown
		7.5YR 5/2	brown
		7.5YR 5/4	brown
		5YR 5/6	yellowish red
		2.5YR 5/4	light olive brown
		5G 4/1	dark greenish gray
		5BG 7/1	light greenish gray
		2.5Y 4/4	olive brown
		N/6	gray
		N/7	light gray
		7.5YR 4/6	strong brown gray
		N/6	gray
		N/7	light gray
		N/5	gray
		5G 7/1	light greenish gray
		2.5Y 4/4	olive brown
		7.5Y 5/6	strong brown
		5G 7/1	light greenish gray
		5B 5/1	bluish gray
		10YR 5/6	yellowish brown
		5G 7/1	light greenish gray
		10YR 5/4	yellowish brown
		2.5Y 4/4	olive brown
		10YR 4/6	dark yellowish brown
		10YR 4/4	dark yellowish brown
		2.5YR 3/6	dark red
		2.5YR 3/3	dusky red
2.5YR 2.5/2	very dusky red		

191-1179D-6R-1

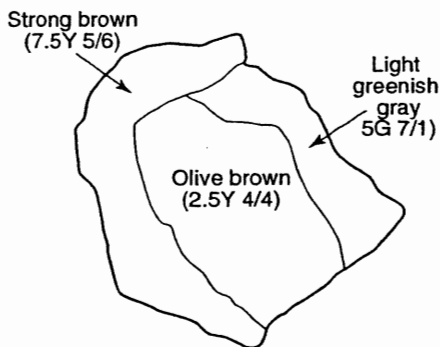
CHERT

Highly fragmented/brecciated, very hard and compact. Remarkable range of colors as shown. The color variations can be a range of chemical environments.

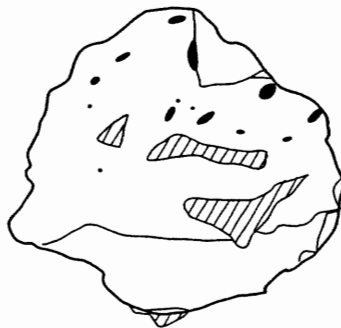
Some pieces have bands/vein of mineralization and/or diagenetic alteration, which are unique in color, luster, and pattern.

Some pieces contain mottles representing bioturbation. Both laterally and vertically oriented mottles range from mm to 4 cm in size and are subrounded, elongated, or tubular. The ichnogenera include Planolites, Zoophycos, and teichichnus.

Enlarged view of the piece at 66-70 cm



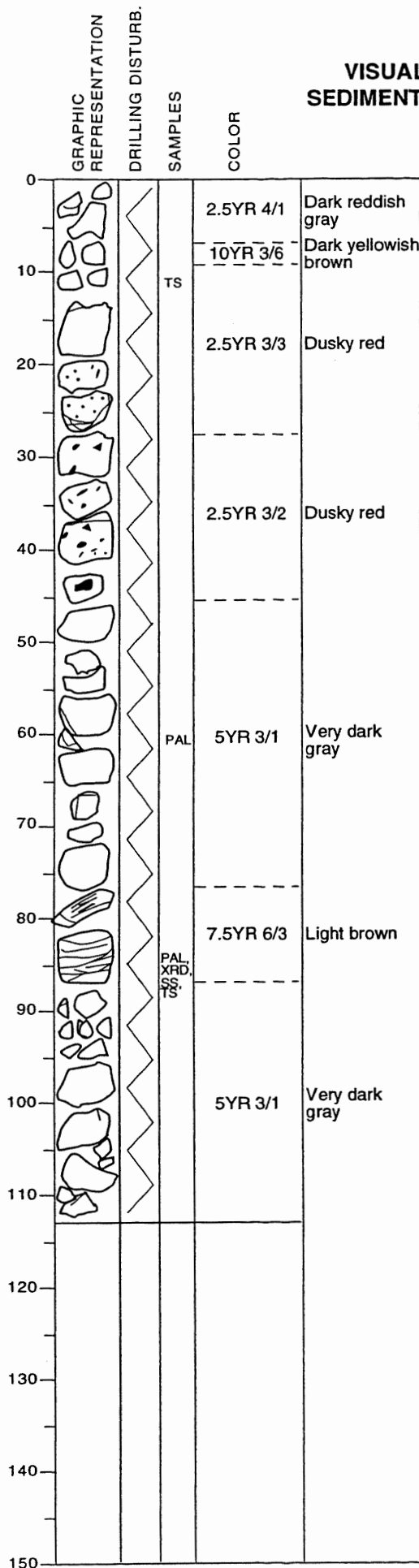
Mottles in the piece at 95-99 cm



Yellowish red (5YR 5/6) mottles represent bioturbation

Brown (7.5YR 5/4) mottles represent bioturbation

VISUAL CORE DESCRIPTION SEDIMENTS/SEDIMENTARY ROCKS



191-1179D-7R-1

CHERT

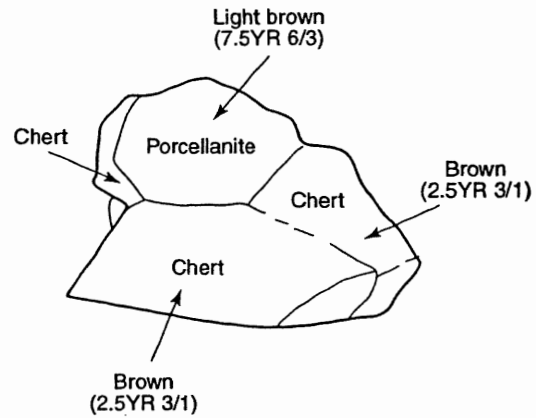
Highly fragmented or brecciated, hard and compact, with sub-conchoidal fractures.

Color variations may reflect various chemical environments. A few mineralized bands or veins are present, which vary in color from the host chert and the sediments.



Two pieces of light brownish gray (7.5YR 4/3) porcellanite with dark gray bands/laminae) are present at around 78-86 cm.

Mottles that represent ichnofossils are present between 21 and 45 cm. Most mottles are subrounded and mm to 1 cm in size. The ichnogenera include Planolites, Granularia, and Phycosiphon(?).

Enlarged view of the piece at 78-81 cm



**VISUAL CORE DESCRIPTION
SEDIMENTS/SEDIMENTARY ROCKS**

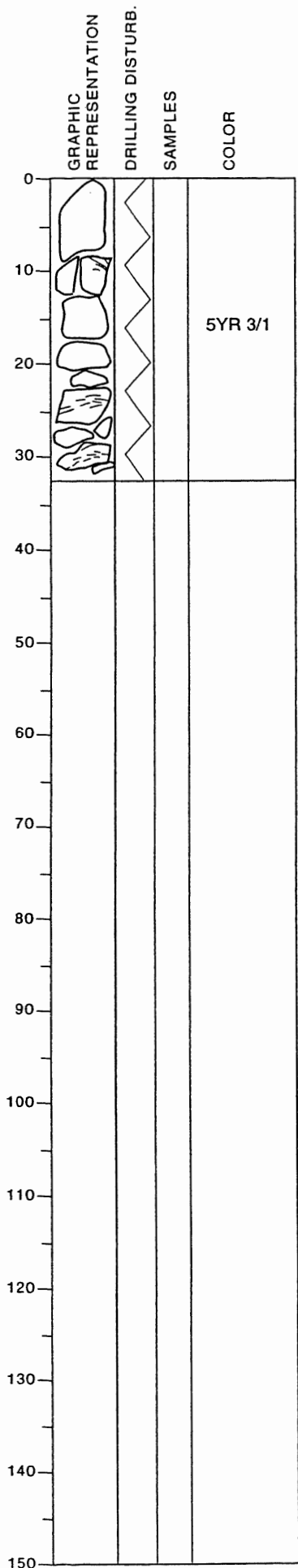
	GRAPHIC REPRESENTATION	DRILLING DISTURB.	SAMPLES	COLOR
0				
10				5YR 3/1
20				
30				
40				
50				
60				
70				
80				
90				
100				
110				
120				
130				
140				
150				

191-1179D-7R-CC

CHERT

Five dark gray (5YR 3/1), highly fragmented/brecciated, very hard and compact pieces with conchoidal fractures.

VISUAL CORE DESCRIPTION SEDIMENTS/SEDIMENTARY ROCKS



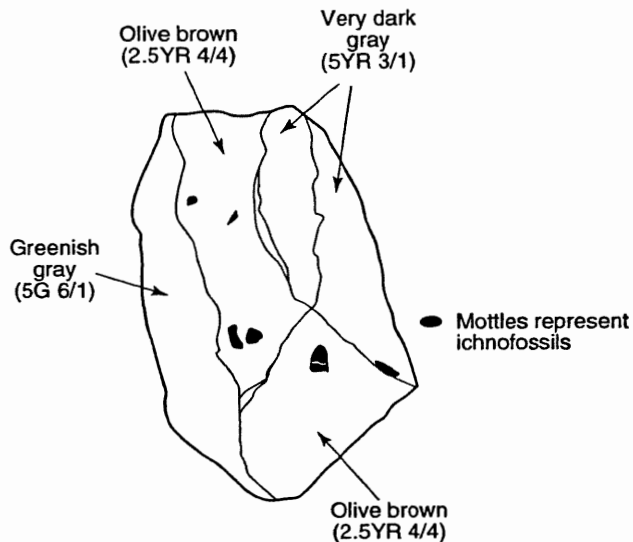
191-1179D-8R-CC

CHERT

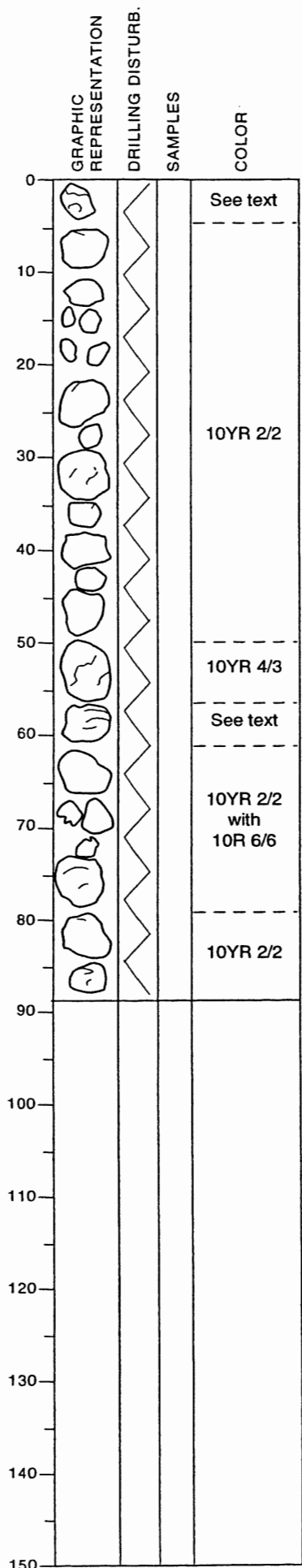
Eleven highly fragmented/brecciated, very hard, and compact pieces with unique sub-conchoidal fractures. Most pieces are very dark gray (5YR 3/1) except left side of the piece at around 8-12 cm. This piece includes a few mottles which represent ichnofossils (see sketch below).

The bottom part of the two large pieces show very thin white (2.5Y 8/0) bands.

Enlarged view of the piece at 8-12 cm



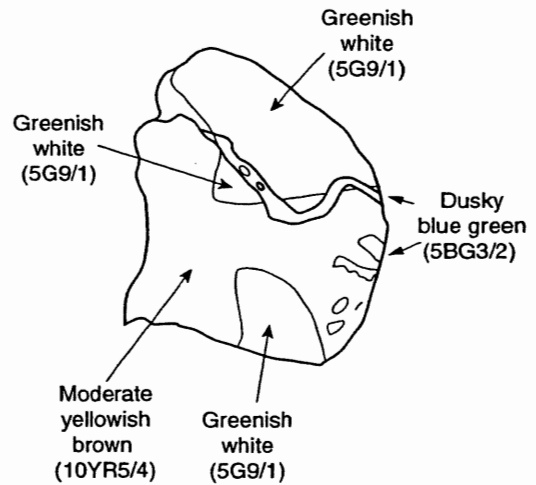
**VISUAL CORE DESCRIPTION
SEDIMENTS/SEDIMENTARY ROCKS**



191-1179D-9R-1

CHERT

Several 5- to 6-cm diameter pieces and several smaller pieces. Color is mainly dusky yellowish brown (10YR 2/2) except the top piece (0-4 cm) which is brownish green and green similar to Core 6R at about 110 cm. This piece is dull greenish white masses in waxy yellowish brown color, both of which are cut by 2 mm blue green veinlet and irregular areas as shown below.



Piece at 50-56 cm is moderate to dark yellowish brown (10YR 4/3) with white veinlets.

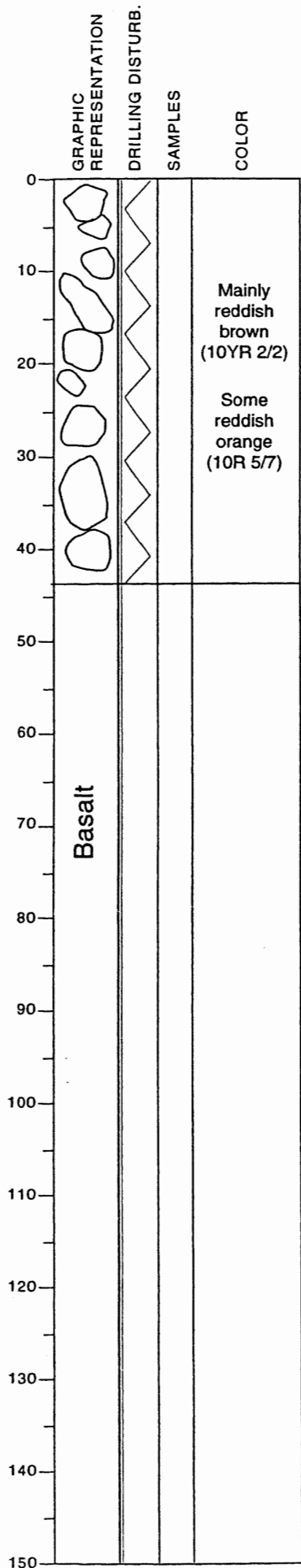
Piece at 56-61 cm has quartz(?) -lined vugs in breccia

Scale: x2



Pieces between 61 and 78 cm have moderate reddish orange (10R 6/6) veinlets, blebs, and layers(?).

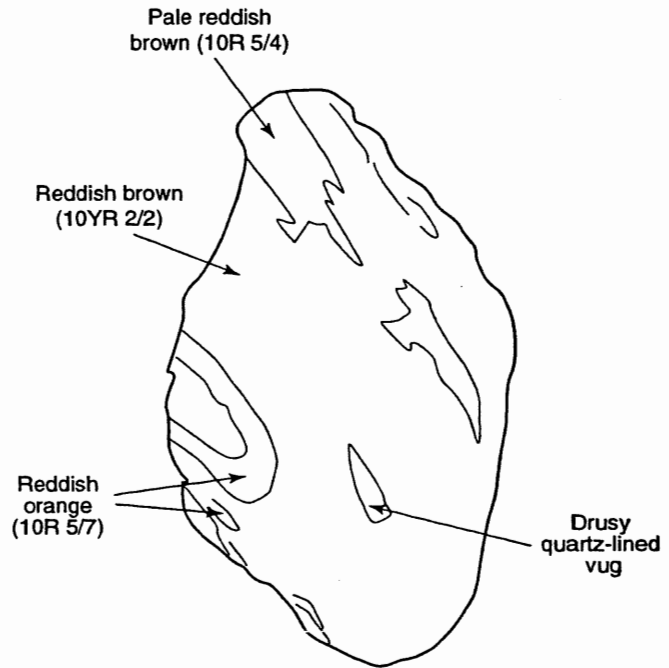
**VISUAL CORE DESCRIPTION
SEDIMENTS/SEDIMENTARY ROCKS**



191-1179D-10R-1

CHERT

Nine pieces of mainly reddish brown (10YR2/2) and yellowish brown (10R 5/7) shards. The reddish orange bands and ovals are especially prominent in a piece at 10-17 cm as shown below.



No evidence of baking at base of chert.